Physics – Uspekhi **38** (4) 347 – 385 (1995)

REVIEWS OF TOPICAL PROBLEMS

PACS numbers: 47.35+i; 47.52.+j; 47.53.+n; 61.43.Hv

Fractals in wave processes

V V Zosimov, L M Lyamshev

Contents

Abstract. A review of fundamental results on fractal structure manifestation in wave processes is presented. Elastic properties and dispersion of fractal materials are discussed; their distribution density, and the shape of wave functions of their localised elastic oscillations, fractons. Examples of their application for the explanation of amorphic properties of solids are presented. Patterns of wave scattering and emission by fractal structures are examined. Principal methods of random signal analysis employed to reveal different fractal structures associated with these signals are described. Data on fractal properties of wave fields are discussed.

1. Introduction

Progress in physics and its applications is to a large extent dependent on the elucidation of the relationship between the microscopic structure and the macroscopic behaviour of complex systems. Major problems pertaining to this issue are those to be solved in the framework of the statistical theory of matter, physics of disordered media, and the theory of turbulence and diffusion.

Notwithstanding considerable efforts by researchers, many of these problems have not until now been completely solved using the traditional approaches of statistical physics. The assumption of either absolute chaos (ideal gas and the classical theory of Brownian motion) or fairly ordered features (the theory of crystalline solids) in examining various media and processes turned out to be a major prerequisite for the successful solution of the problems. Specifically, the microscopic description of disordered media and processes lacking in both crystal-like regularity and absolute chaos was found to be in the main beyond the scope of the canonical statistical theory.

There are several ways to account for the situation. To begin with, a statistical description can be successful if it is based on a limited number of macroscopic variables for which the condition of macroscopic causality is fulfilled [1]. This means that variables of this small set must be related to one another through dynamical interactions which makes it unnecessary to average over microscopic dynamics every time their changes in different processes need to be evaluated.

An exhaustive explanation of requisites for microscopic causality to be fulfilled has never been provided. However, it is clear that the scale of changes in macroscopic variables satisfying this condition must be significantly greater than the scale of correlation between microscopic variables. It is this condition that fails to be fulfilled in disordered media and

V V Zosimov Research Institute of Applied Acoustics, 141980 Dubna-1, Moscow Region, Russia
Tel. (7-09621) 4-5577
E-mail: root@niipa.cntc.dubna.su
L M Lyamshev N N Andreev Acoustic Institute, ul. Shvernika 4, 117036 Moscow, Russia
Tel. (7-095) 126-9014
E-mail: lyamshev@wpd.jpi.msk.su

Received 4 March 1994
Uspekhi Fizicheskikh Nauk **165** (4) 361 – 402 (1995)
Translated by Yu V Morozov; edited by H Milligan

processes with the microscopic structure coordinated in a broad range of scales. A most illustrative example of such a situation is provided by a substance near the type two phase transition point. Amorphous solids are characterised by scales of molecular order within macroscopic zones comprising thousands of molecules [2]. The processes of this sort include hydrodynamic turbulence in which correlation of fluctuation rates is apparent throughout the entire range of flow scales.

For all that, the natural microscopic structure of many irregular objects has the property of scale invariance (scaling). In this case, the problem of the description of disordered media may be solved by introducing macroscopic values dependent on the chosen scale of averaging. The scale invariance allows the theory of such media to be constructed taking advantage of renormalisation groups [3]. However, this obviously universal approach requires complicated and tiresome calculations.

Mandelbrot was the first to elaborate the mathematical notion of fractals in his books [4–6]† and suggest its applications to the description of the shape of various objects. This greatly promoted modelling a broad spectrum of nontrivial scale-invariant structures. The use of such models constitutes a novel technique for the description of disordered structures in physics.

Fractal models are not always amenable to analytical evaluation, but they are constructed following very simple rules and it is not difficult to model them by computer. Experiments on such computerised models are now widely used to obtain deeper insight into the mechanisms of irregular processes. It should be emphasised that this approach is essentially different from the traditional methods employed in theoretical physics. The distinction is utterly irreducible to the simple difference between the numerical solution of differential equations and their analytical examination.

It is perhaps for this reason that fractal models have been used extensively and with an increasing success in physical research during the last 10–15 years. Fractal models are not only applicable to exploring in more detail previously described processes and structures (e.g. random walks, linear polymeric molecules) but they also provide a deeper insight into phenomena which it would be impossible to comprehend and quantify using traditional methods.

Mathematically, a fractal is a set of points in a metric space for which it is impossible to estimate any conventional measure with integer dimension, i.e. length, area or volume (their dimensions are defined by the first, second, and third powers of the length respectively). For example, measurement of the fractal curve length and the area under the curve may yield an infinite value for the former and zero for the latter parameter. This problem can be solved by introducing the Hausdorff measures of any dimension (including non-integer ones). The maximum dimension of a Hausdorff measure which yields a nonzero value on the evaluation of a set is referred to as the Hausdorff–Besicovitch dimension (HBD) of this set‡.

†The term 'fractal' was coined by Mandelbrot by fusing the words 'fraction' and 'fracture'. Therefore, a fractal is a fractured object with fractional dimensionality.

‡A Besicovitch has proved the existence of such dimension. Its exact definition is given in Section 2 of the present review.

At first, Mandelbrot defined the fractal as a scale invariant, i.e. self-similar, object with the HBD in excess of the topological dimension (1 for a line, 2 for a surface, etc.). Later, he described self-affine fractals with intrinsically diverse dimensions [7]. In physics, fractals are characterised not only by HBD but also by a number of other dimensions which are easy to find in experiments and permit a versatile description of the object's properties [7–9].

Advances in application of fractal models in physics are in the first place attributable to the fact that fractal patterns are inherent in a great number of processes and structures. This is not a mere chance. Many models designed to simulate the formation and the development of disordered objects of different nature can actually be reduced either to the percolation transition model [10] or to the model of diffusion-limited aggregation (DLA) [11]. In the former case, the final result is a fractal percolation cluster whereas in the latter a fractal aggregate is formed. Models of many disordered processes are based on different variants of random walk [9] and dynamic chaos [12, 13] and also exhibit fractal properties. As a matter of fact, Mandelbrot discovered a mathematical expression for a general rule pertaining to geometric properties of the physical world.

Numerous published sources concerned with fractals and their applications are currently available including a few books and reviews in the Russian language. Basic information for students is best presented in Ref. [8], one of the first reviews of the subject in this country, and also in an interesting book by Feder [9]. Another book, Ref. [14], written by an expert in speech acoustics and the use of computers in acoustics may be equally helpful. General properties of fractals and methods of their computer simulation are thoroughly examined in Ref. [15]. A detailed introduction to the theory of fractals and examples of its specific application in physics can be found in Refs [10, 11, 16–23]. A concise description of different models of fractal structures is provided in Section 2 of the present review.

The objective of this review is to appraise available information about wave processes in fractal structures on the one hand and results of the studies on fractal structures inherent in wave fields of different nature on the other hand.

Wave processes may be arbitrarily categorised into two classes. The first one includes wave propagation in fractal structures when they serve as a medium in which propagation occurs. The other class of events covers wave scattering and emission by fractal structures when waves propagate in a uniform medium containing fractal inhomogeneities.

Fractal properties of wave fields and signals are apparent in different situations which may also be divided into two groups. In both homogeneous or regularly inhomogeneous media, fractal properties of wave fields are manifested due to nonlinear wave interactions and nonlinear ray dynamics. In statistical wave problems, fractality is preconditioned by diffuse and kinetic processes.

Studies of wave phenomena in fractal materials date from the work of Alexander et al. [24] and are largely based on the notion of fractons introduced by Alexander and Orbach in 1982 [25]: localised oscillations on fractals which replace ordinary phonon states at frequencies greater than a certain transition frequency (crossover). The density of fracton frequency distribution obeys a power law by virtue

of scale invariance. The exponent is determined by the so-called fracton (spectral) dimensionality which, in the case of fractons, plays the role of the space dimension in the low-frequency asymptote of the density of states. Further development of the ideas first put forward in Ref. [24] eventually culminated with the closed microscopic theory of temperature dependences of thermal conductivity, sound velocity and absorption in amorphous solids [26–28].

The principles of the theory of thermal properties of amorphous solids proposed in Ref. [26] proved applicable not only to fractal materials but also to any other material with oscillation states localised in a certain range of scales [29]. Nevertheless, investigations into fractal structure oscillations appear to have provided a major contribution to the understanding of the mechanisms underlying the thermal characteristics of such media.

The theory of fractons along with experimental studies and numerical evaluation of fractons in real and model fractal structures is considered in Section 3 of this review. The section focuses on the description of elastic oscillations in real materials which accounts for the prominence given to the theory of elastic properties of fractal materials. Fracton characteristics evaluated in early studies of materials with fractal structure at smaller scales (less than a few micrometers) can be apparent in both natural and artificial fractal structures at a much greater scale. For this reason, this portion of the review should not be regarded as the only possible way to describe fractal models of oscillation properties of amorphous solids. There are other (nonfractal) approaches in this field [2, 30–32], but their analysis is beyond the scope of the present communication.

The theory of fractons appears to provide a comprehensive solution to the problem of determining the spectrum of mechanical oscillations and conditions of wave localisation in fractal materials. The structure of the fractal oscillation spectrum depends on spectral dimension and scales that restrict manifestations of fractal properties of a given material. At greater scales, oscillations are characterised by a normal phonon spectrum. In the range of fractal structure scales, oscillations occur in the form of localised states, i.e. fractons, with the power-law density of frequency distribution dependent on spectral dimension. At smaller scales, the oscillation spectrum depends on the properties of constituent particles of a fractal structure. The assessment of spectral dimension is a major problem arising in connection with practical application of the theory of fractons. The early hypothesis of the universal value 4/3 for spectral dimension as suggested by Alexander and Orbach was not confirmed in later studies. The spectral dimension turned out to be related to specific features of the fractal structure and the nature of interactions between its constituent elements. This review examines principal models simulating elastic properties of fractals which have many applications and give different values for fractal dimensionality.

There are very few methods currently used in studies on the shape of the fracton wave function. A universally accepted tool is the superlocalised wave function model. At the same time, results of numerical analysis of wave function shapes indicate that this approach may not be sufficient to elucidate their complicated structure. Hence, there is a need for further extensive studies.

Section 4 of this review discusses wave scattering and emission by fractals. One of the first reports devoted to this issue, Ref. [33], considered wave scattering by a random fractal surface. Such a surface cannot be differentiated, and (at variance with the case of a smooth surface) the angular distribution of the dispersed field intensity is not related to the surface slope distribution but instead has the form of a power law with the exponent determined by the fractal dimension of the surface. A similar shape of angular dependence was reported for small-angle scattering of visible light, x rays or neutrons by real materials having fractal structure. Measurement of angular scattering dependences is virtually the sole method for the assessment of fractal dimension in real materials. The relationship between the angular dependence index and the fractal dimension is ambiguous and depends on the fractal structure model being used. The examples include porous materials with a well-developed internal fractal surface [34] as well as materials with the structure of a fractal aggregate [35].

Examples of wave dissipation listed in the previous paragraph illustrate a single-scattering regime. Whenever multiple scattering occurs, the fractal structure of the scatterer is much more prominent because correlation of fractal structures in a wide range of scales results in a spectrum of collective excitations of scatterers that resemble fractons [36, 37]. This accounts for a marked difference between scattering patterns on fractals and those generated by isolated scatterers independently distributed in space. In the case of resonant scatterers, the shape of the resonance absorption curve is dramatically changed in that absorption decreases slower with tuning away from the resonance. Both the absorption coefficient and the section of wave scattered by a fractal structure, calculated per particle, increase. When the fractal dimension is sufficiently low, the increase in the scattering section is so large that the visibility/invisibility transition may be involved [37]. The mathematical problem of collective excitation states is very similar to that of fractons. In the presence of scatterers, the structure of the excitation spectrum is also determined by a certain factor referred to in Ref. [36] as optical spectral dimension.

Peculiar features of wave emission by fractal structures arise even in the simplest case of isolated emitters showing fractal distribution in space, due to the unusual distance dependence of the intensity of emission by fractal structures. This fact was used in an attempt to explain the well-known Olbers paradox of the brightness of the night sky [38]. More subtle signs of emitters' fractality are apparent in association with the aforementioned effects of collective excitation. They have been reported to be responsible for the enhanced efficacy of heat emission by fractal structures per particle [39]. There is another aspect to the problem: fluctuations of emission by fractal structures with intrinsic correlation in a wide range of scales which account for the markedly altered noise characteristics, including level and correlation. Fractal models of rock structure and disintegration are widely adopted in seismology where fluctuations of seismoacoustic emission may perhaps be used to predict earthquakes [40].

Section 5 deals with fractal structures in wave fields. The wave field structure has a distinguishing scale, i.e. wavelength. The fractal structure implying scale invariance may be apparent either on scales greater than the wav-

elength or in the presence of a self-similar wave spectrum, e.g. stationary wave turbulence spectra. No general concept (by analogy with the theory of fractons) has so far been developed in this field although certain pertinent problems evidently require in-depth basic studies.

Primarily, the problems concern fractal structures associated with nonlinear dynamics including spatial dynamic chaos in nonlinear wave interactions [17] and ray fractal dynamics in inhomogeneous media [41]. These issues have recently been discussed in several review articles [17, 41], which is why this section contains only casual references to them. In fact, it alludes only to a few works that describe conditions under which the effects of ray fractal dynamics may occur in the real ocean and those necessary for dynamic chaos to form in capillary waves on a fluid surface.

Another class of problems pertaining to the manifestation of fractal properties is that of statistical problems of wave distribution. In this area, fractal concepts have never been applied to experimental studies, but they may be introduced to highlight novel aspects of certain phenomena due to the scale invariance of many processes, e.g. excitation transfer in resonant media [42, 43] or wave beam trajectories in an inhomogeneous medium [44]. Such processes are known to be associated with anomalous diffusion in which trajectories display nontrivial fractal characteristics.

Section 5 contains a detailed discussion of fractal properties of sea waves. The sea surface (along with mountainous terrain, trees, and coastline) provides an example of fractal forms available for day-to-day observation. The fractal character of this surface is closely related to nonlinear wave dynamics. The spectrum of wind waves contains a self-similar interval characterised by flow from short to long waves. The fractal shape of the sea surface is ultimately also associated with the presence of a self-similar interval [45]. There are more signs of fractal structures in wind-generated waves even though they are less conspicuous. These fractal properties are apparent on scales which greatly exceed the wavelength [46, 47]. Theoretical explanation for such fractal structures remains to be found.

An important topic of Section 5 in the present review is multifractal analysis. This issue has been extensively discussed in numerous books and review articles [9, 17, 22, 48, 49]. Our purpose was to emphasise the usefulness of this approach for the analysis of wave processes. Application of multifractal analysis to the large-scale structure of turbulent pressure pulses has recently been described in Ref. [50]. Another example is provided in Ref. [51] which is dedicated to the structure of fracton wave functions on a percolation cluster.

A variety of fractal approaches to signal analysis are currently available in seismology. Scale invariance is intrinsic in many seismic events which can be accounted for by the scale-invariant nature of disintegration processes in general. But this should be the matter of a special review. The present one examines fractal properties of signals generated by seismoacoustic emission and the possibility of using them for predicting earthquakes [52].

Some aspects of the present communication have already been discussed in the literature. Elastic properties and oscillations of fractal clusters as well as scattering on fractals have been reviewed in several papers included in Ref. [21], a special issue of *Physics D* [53], and Ref. [10]. Data on light emission by fractal structures are available from Ref. [38]. The aforementioned review [41] presents detailed information about fractal structures in light dynamics. Spatial chaos in nonlinear wave dynamics is described in Ref. [17] in the framework of a general approach. A large number of papers on emittance of acoustic waves by fractal structures are thoroughly and consistently reviewed in Ref. [52] which also contains useful information about fractal processing of acoustic signals in seismology. Fractal studies as applied to acoustic problems have been discussed in Refs [23, 54].

2. Fractal structures in physics

Fractal forms available for visual observation are surprisingly widespread in nature. Classical examples of fractal phenomena (a tree, a coastline or mountainous relief) [3–6] pass from one popular book to another. Other fractal forms are not so widely known, e.g. the fracture surface of metal [55] and the surface of rough water [45]. However, the fractal forms most interesting as objects of physical research can be observed and analysed only with special instruments and techniques. They include fractal structures of different materials and those of random processes and fields. In the latter case, fractal analysis is applied to the geometric objects that are constructed during experimentation rather than to the shape of physical bodies, that is to plots describing processes, diagrams illustrating distribution of values in space, sets of meaningful points, and trajectories of movement.

2.1 Structures of matter

It would hardly be a gross exaggeration to argue that a substance has fractal structure in a certain range of scales if it is not in gaseous or crystallised state. The first evidence of fractal structure was obtained for aggregates of microscopic particles formed from the solid phase in air [56]. The authors generated particles by evaporation of iron, zinc, and silicon dioxide from the surface of a heated filament followed by vapour condensation on cooling in the gas medium. Mean particle size was 35 Å. These particles diffused in air and formed aggregates by adhesion. The aggregates were then precipitated on a collecting element and were assayed for fractal properties by direct analysis of electron micrographs. Later studies revealed the fractal structure in polymers [57] and colloid aggregates formed by particles sticking together in colloid solutions [35].

The fractal structure of matter is most readily apparent in unusual mass distribution patterns in space. Mass M of a fractal aggregate is related to its size R by

$$M = m_0 \left(\frac{R}{a_0}\right)^D , \tag{1}$$

where D is the mass fractal dimension smaller than the space dimension d while m_0 and a_0 are the mass and the size of constituent particles respectively. Density of matter ρ is equally dependent on the size:

$$\rho = \rho_0 \left(\frac{R}{a_0}\right)^{D-d} , \tag{2}$$

where ρ_0 is the density of particles which form the aggregate. When the particles are packed in a compacted structure, mass dimension is equivalent to space dimension

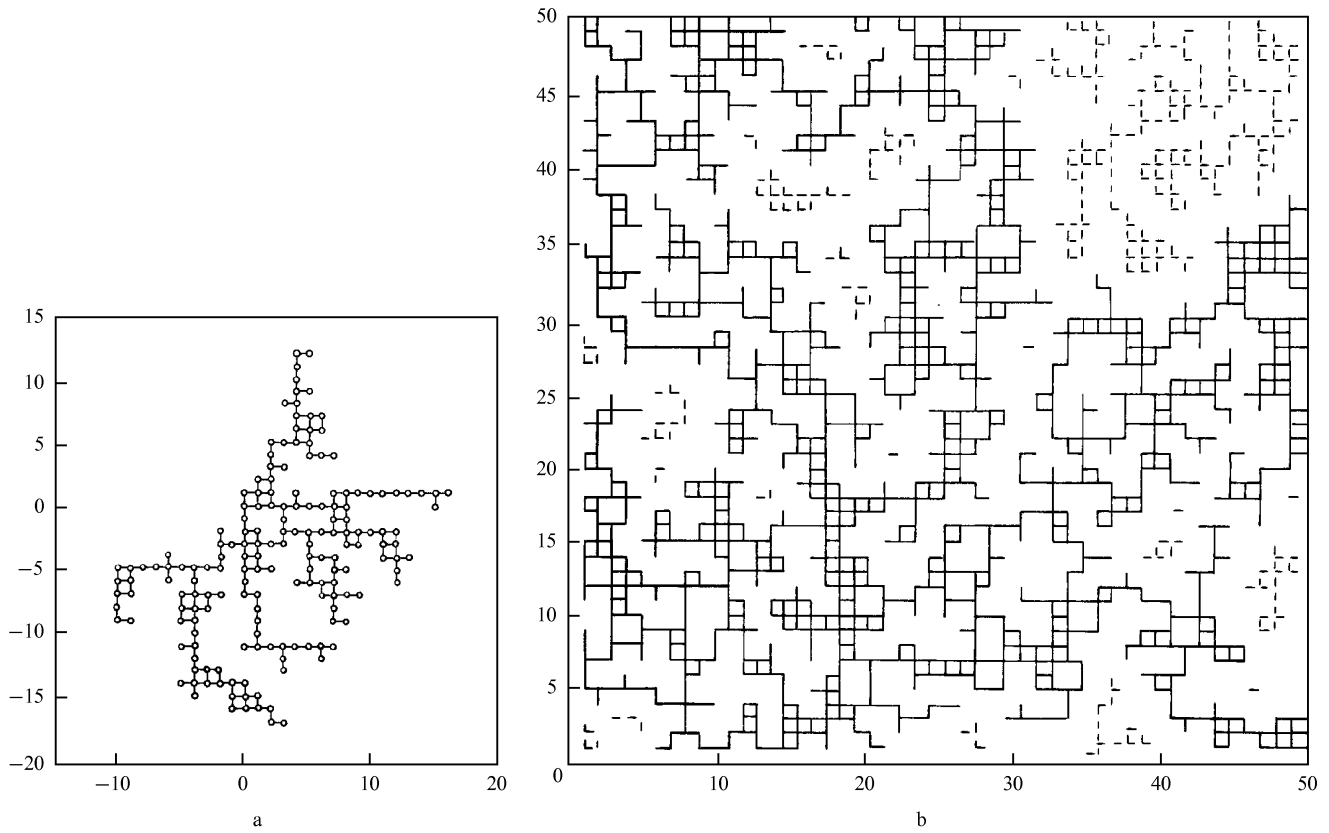

Figure 1. (a) Fractal cluster obtained by computer simulation of diffusion-limited aggregation (DLA) on a plane. The cluster contains 200 particles. (b) Connecting cluster (dashed line) during percolation on a 50×50 square lattice. The node problem; concentration $p = 0.6$, critical concentration for the node problem $p = 0.5927$. Shaded areas represent clusters that did not join the connecting cluster. Their size appears to vary from that of a single bond to the order of the entire lattice. More precisely, the maximum size of the final cluster is the largest size of cavities in the connecting cluster which in turn has scale ξ [see Eqn (15)]. According to Eqn (15), scale ξ increases to infinity near the percolation threshold and attains the lattice size on a lattice of the finite size L.

$D = d$ and the density is constant. Fractal aggregates have irregular structure (Fig. 1) with long-range correlations between particle positions. It is unlikely that random particle distribution at $R \gg a_0$ and density (2) might result in their binding together to form an aggregate.

According to the generally accepted definition, fractals are sets of points whose Hausdorff–Besicovitch dimension (HBD) does not coincide with topological dimension. The exact definition of HBD is given below. Suppose that a set is covered with a countable collection of sets A_i such that their diameter $\operatorname{diam} A_i$ (i.e. the largest distance between two points) does not exceed certain ε. Define m_ε^p as the exact lower border of sums $\sum_i (\operatorname{diam} A_i)^p$ over all possible coverings. Assume m_p to be the exact upper limit of m_ε^p for all $\varepsilon > 0$. Then, by definition, HBD is the exact upper boundary of such p for which $m_p > 0$. This definition is applicable to sets in any metric spaces since it requires only specification of the distance between points. Definitions of fractal dimensions actually used in physics refer to objects in the Euclidean space R^d. Fractal dimension of a structure may be evaluated in different ways. Apart from the aforementioned mass dimension, there is box dimension, i.e. the exponent which describes how the number of boxes (cubes) covering the fractal depends on their size. Take, then, a fractal covered with boxes of size ε. Take a sum over such a cover by analogy with the sum in the definition of HBD. This yields

$$\sum \varepsilon^p \sim \varepsilon^{-D} \varepsilon^p ,$$

where D is the box dimension. If $p > D$, the sum tends to zero as $\varepsilon \to 0$. The finite sum is obtained at $p = D$. When $p < D$, the sum is infinite. $p = D$ is the highest p value at which the sum exceeds zero. This line of reasoning establishes the relationship between HBD and box dimension and also provides the basis for HBD evaluation in physical measurements.

It is worthwhile to note that the definition of the Hausdorff dimension proper is impossible to use in physical measurements as it requires taking the limit to infinitely small volumes. Therefore, taking the limit is substituted by measuring the slopes of straight curves which define the above exponents, i.e. mass and box dimensions. For this reason, the physically meaningful definition of fractals includes the property of self-similarity. In mathematics, the Hausdorff dimension can also be evaluated for sets lacking in self-similarity. Naturally, the property of self-similarity has a statistical sense for real objects: statistical characteristics of the fractal structure are conserved during similarity transformation.

In regular fractals (their most widely known examples are the Sierpinski gasket and the Koch curve), a fragment of a certain size is composed of a number of similar but smaller fragments. The self-similarity dimension is an exponent in the dependence of the number of similar structural elements (the large element components) on

their size ratio. On the one hand, the obvious analogue of the self-similarity dimension for random fractals is mass dimension. On the other hand, the number of boxes of a certain size covering the fractal is equivalent to the number of structural elements of a similar size. Therefore, box dimension is equal to self-similarity dimension. It may be concluded that all introduced dimensions for self-similar fractals are identical. Different dimensions may not coincide in the case of self-affine fractals (which turn into themselves on affinity transformation, i.e. on axial extension with different coefficients) [7].

One of the most striking manifestations of fractal structure is the existence of solid states of very low density. Under certain conditions, fractal aggregates can join together upon contact to form gels and aerogels [11]. In this situation, fractal properties of the structure are typically apparent in a scale range limited from below by the size of particles a_0 forming the aggregate and from above by the size of initial fractal clusters ξ. Such structures are termed uniform clusters. Particles a_0 are normally sized 1–10 nm whereas the aggregate size varies from 10 to 1000 nm. As a rule, fractal dimension lies in the range of $D = 2-2.9$ depending on the regime of aggregate formation. Evidently, the density of such material is defined by

$$\rho = \rho_0 \left(\frac{\xi}{a_0}\right)^{D-d} . \tag{3}$$

Therefore, the density of a material at sufficiently large ξ values and $D < d$ may be significantly lower than the density of each constituent particle taken alone. Such materials are known to be formed by sintering metal powders.

Another class of materials with uniform fractal structure is the amorphous polymers. Their fractal properties are apparent on scales exceeding the size of monomeric molecules, and are limited from above by a scale of several tens of Angstroms. The shape of the fractal curve is intrinsic even in a single linear polymer molecule subject to accidental link displacements whereas ramified polymeric molecules give rise to lattices resembling those which underlie fractal aggregates of gels composed of macroscopic particles.

For almost all real fractal materials, it is possible to evaluate the correlation density function $C(\boldsymbol{R}) \sim \langle \rho(\boldsymbol{r}+\boldsymbol{R})\, \rho(\boldsymbol{r}) \rangle$, i.e. the possibility (averaged over all particles and dimensions) of finding a particle at a distance R from the given one. Clearly, for fractal materials

$$C(\boldsymbol{R}) \sim R^{D-d} . \tag{4}$$

The principal method for the evaluation of the correlation density function is to measure the angular dependence of scattering for waves of an appropriate length. Almost all currently known fractal structures are apparent on scales below one micrometer. Therefore, sufficiently short waves beyond the visible wavelength spectrum are suitable for the evaluation. Usually analysis of x-ray or neutron scattering is used for the purpose. The expression for density correlation leads directly to the following expression for the angular dependence of scattering intensity:

$$I(q) \sim q^{-D} , \tag{5}$$

where the absolute value of the wave scattering vector is $q = 2k \sin(\theta/2)$. Fig. 2 shows results of determination of the angular dependence of light or x-ray scattering for a

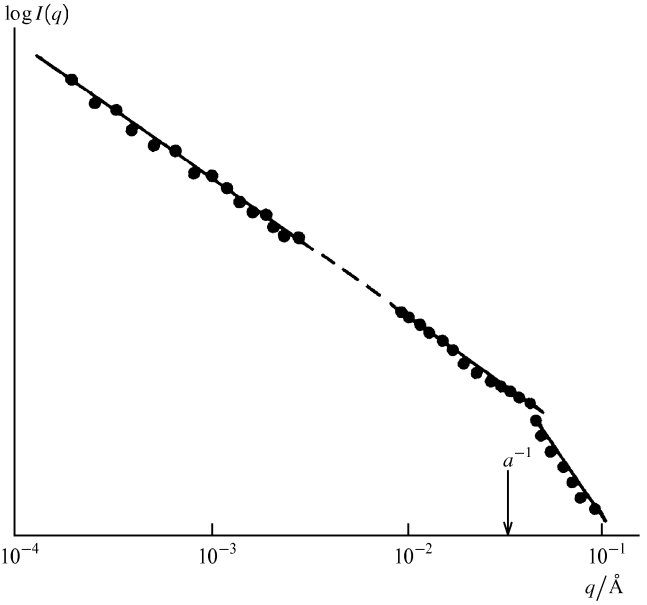

Figure 2. Angular dependence (dependence on scattering wave number q) of scattering intensity of light (for wave numbers in the range of 0.0001 – 0.001 1/Å) and X-rays (for wave numbers 0.01 – 0.1 1/Å) in SiO_2 colloid aggregates [35]. The entire range of wave numbers is overlapped on scattering for two samples of solutions with different solvent composition. Crossover from scattering on a fractal structure with dimension $D = 2.12$ to that on particles with smooth surfaces ($I \sim q^{-4}$) occurs when the scattering wave number is $1/a$, where $a = 27$ Å is the particle size.

fractal structure formed by SiO_2 particles in a colloid solution [35]. According to these data, the fractal dimension of the system is $D = 2.12$.

For all that, interpretation of scattering data is somewhat ambiguous and involves additional assumptions concerning the structure of matter. It is necessary to distinguish between substances with the mass fractal structure similar to that of the above aggregates and porous substances with inner fractal surfaces. Such substances differ in terms of the relationship between the exponents of angular dependence of scattering and fractal dimensions [58] (this issue is discussed at greater length in Section 4). The angular dependence was also reported to have a power-like form in the case of power-law distribution of both pores and particles by size.

The volume–density relationship accounts for the impossibility of using continuous medium models in which density for physically infinitesimal volumes can be unambiguously determined. The same is true of many other parameters normally evaluated to describe media in continuous medium models, e.g. elastic moduli, electrical conductivity, etc. Therefore, both scattering data and scale dependences of these parameters are needed to confirm the validity of structural models of fractal matter. Properties of fractal aggregates appear to be fairly well explained by rather a simple aggregation model referred to as diffusion-limited aggregation (DLA) which was suggested in 1981 [59]. Formation of gels and polymers may be described by the percolation transition model (see Sections 2.3.2 and 2.3.3). The use of these simple models to study generation and further growth of structures that in turn give rise to new ones of appropriate fractal dimension allowed quantitative characterisation of various properties of real fractal materials.

The problem of fractal aggregates of microscopic particles appears to have direct bearing on the properties of ball lightning, one of the most enigmatic objects of the microscopic world [60–62]. The most adequate model of ball lightning currently available is the fractal ball model which assumes that the ball is an aggregate of fractal filaments [62]. Fractal filaments are formed of nanometer particles in a strong electric field with a distinguishing direction in the space. This accounts for the difference between fractal filaments and aggregates formed under isotropic conditions. In the absence of the electric field, this is a nonequilibrium system with high surface energy which may be released during a thermal blow up [62, 63].

Fractal properties of model structures are directly related to the mode of their generation. Unexpected results have been obtained in Ref. [64] where rapid experimental freezing was used to study the geometrical structure of a composite emulsion obtained by simple vigorous mixing of two liquids. Fractal droplet distribution in the dispersed phase has been shown to occur in a certain scale range. The scale of fractal behaviour is dependent on the fraction of occupied volume of the dispersed phase. This dependence is easy to explain on the assumption that droplets in the dispersed phase join together to form a percolation cluster. Interestingly, this structure is likely to be preserved in the case of casual motion of the droplets.

The property of scale invariance of fluctuations of the order parameter during second order phase transitions known from statistical physics can also be formulated in terms of fractal structure. Nevertheless, a consistent statistical approach to the problem does not necessarily require fractal concepts to be used. The relationship between fluctuation structure and fractality have recently been revealed in Ref. [65].

2.2 Structures of processes

Fractal approaches to the analysis of processes are diverse because fractal analysis is applicable to a variety of geometrical objects associated with the process. In a specific case, the plot for a parameter of the process may be regarded as fractal. Also, a set of interception points where a variable takes a given value may be fractal. The square of the amplitude of the process may be considered to be the point density with fractal structure on the time axis. Generally speaking, densities of different parameters which characterise the process can show fractal distribution in space and time.

One of the most efficient approaches to fractal analysis of processes is based on the assumption that the process originates from a dynamic system of finite dimension exhibiting chaotic behaviour. The trajectory of such a system in phase space is a fractal set termed the strange attractor. Analysis of the process initiated by such a system is based on the Takens algorithm [66] which allows the trail of the system in phase space to be reconstructed from the time-dependence of a single variable associated with the system. The theoretical and practical aspects of the analysis of processes which are due to finite-dimensional chaotic dynamics are described in detail in numerous text-books and reviews (see for instance Refs [16, 20]). The following is a brief discussion of this methodology.

In accordance with the Takens algorithm, a point in phase space is identified by a sequence of readings at n times separated by a fixed interval. The trajectory in phase space is formed when the original point moves along the time axis. The reconstruction algorithm is easy to understand bearing in mind that for the process originating from a system described by an ordinary differential equation of the nth order, coordinates in phase space are defined by a set of amplitudes and their derivatives of up to the $(n-1)$th order. In the case of discrete time-readings, a set of amplitudes and their $(n-1)$th derivatives is related to a set of n successive readings of the amplitude through simple nondegenerate transformation.

Evaluation of the fractal dimension of the trajectory in phase space reconstructed according to the Takens algorithm allows characteristics of the process to be found. In the first place, it makes possible the determination of the dimension of the dynamic system. If the number of successive readings n is below a certain value, then the measured fractal dimension equals n. At higher n, the dimension no longer changes with increasing n. This is the case when n exceeds $2d+1$, where d is the true dimension of the trajectory. By constructing the dependence of fractal dimension on number n, it is possible to obtain the lowest value for the dimension of the dynamic system. A fractional fractal dimension suggests the presence of a strange attractor in its phase space.

Fractal properties of wave processes are likely to emerge if the emitting system is governed by chaotic dynamics. The wave amplitude may be regarded as one of the dynamic variables, and fractal analysis may be applied to either time or space-dependent variability using the above algorithms. Examples of dynamic systems with chaotic dynamics which emit waves (sound) are cavitation bubbles generated by a strong sound in water [67, 68] and an electrodynamic loudspeaker functioning in the nonlinear regime [69].

It should be noted that the evaluation of the fractal dimension of a trajectory in phase space reconstructed in compliance with the Takens algorithm is strictly speaking insufficient for an unambiguous conclusion about the finite dimensionality of the system giving rise to the process. It is the case that the fractal dimension of the trajectory remains constant even in the case of a truly chaotic process with a power-law power spectrum, provided the number of readings n exceeds a critical value [70]. To distinguish such a case, one needs to know that the signal is generated by a dynamic system of finite dimension or have additional measurements made, e.g. the Lyapunov numbers [16], which characterise the divergence rate of trajectories starting from the nearby points in phase space. The finiteness of the Lyapunov numbers indicates the dynamic origin of the trajectories. For truly random signals, these exponents are infinite. In the well-known works [12, 13], fractal properties of the phase trajectory were first unambiguously associated with the presence of a set of positive Lyapunov's exponents (the Kaplan–Yorke hypothesis). Results reported later in Ref. [70] indicate that this condition is not always satisfied.

More general implications of fractal analysis are apparent in the examination of random processes of nondynamic origin. The traditional approach to the analysis of random processes is based on the measurement of correlation functions or of power spectra (reciprocal spectra), which is virtually the same. The fundamental principles of this approach, i.e. the correlation theory of random processes, are strictly mathematical. Correlative measurements allow determination of the second moments

of one and two-point probability distributions. Beyond the Gaussian processes, the complete statistical description requires evaluation of probability distributions or moments of higher order if there are any, with an ensuing increase in the volume of measurements. Taking into account the third moments demands that three-point correlations (bi-spectra), be determined. If the fourth moments are considered, it is necessary to determine four-point correlations (tri-spectra), etc. Evidently, as the order of moments taken into account grows, there are more doubts regarding simplification of the description of random processes by the use of averaged values. Moreover, high moments do not always have explicit physical meaning, unlike correlation functions or power spectra. In this context, it is important to evaluate a small number of variables to which it is possible to assign certain sense. Such parameters include fractal dimensions of various geometric objects associated with the signal. This is not a universal approach, but it may be applied to a broad class of processes showing the property of scale invariance in a certain range of parameters. Besides, dispersion and even the very first moment of a process may be nonexistent in some cases of practical importance when the process is a sum of smaller contributions and its probability distribution is in fact the limit distribution of the sum of random values. In this sense, the Gaussian processes represent a specific case for which the finite dispersion exists.

Fractal analysis is equally applicable to Gaussian processes. Even the simplest of the random processes, i.e. Brownian motion, simulated by a normal process with independent increments (the Wiener process) has fractal characteristics. It is a self-transforming process provided time and space scales simultaneously undergo a b-fold and $b^{1/2}$-fold change respectively. The fractal dimension of the plot for the Wiener process is $D = 3/2$, while the trajectory of the Brownian motion on the surface and in space has dimension $D = 2$. Mandelbrot was the first to point out a broad class of Gaussian processes exhibiting fractal properties. They show the following dependence of increment dispersions on the time interval:

$$\left\langle \left[X(0) - X(t)\right]^2 \right\rangle \sim t^{2H} , \tag{6}$$

where $H \neq 1/2$ and lies in the interval $0 < H < 1$. Long before the discovery of fractals, processes with property (6) were recorded by Hurst in a study of annual fluctuations of river flow (see for instance Ref. [9]). The latter author found that exponent H is the same for different rivers and equals 0.73. Exponent H is termed the Hurst exponent. Gaussian processes with the increment dispersion (6) are referred to as processes of generalised Brownian motion.

The local dimensionality of the plot for process (6) is $D = 2 - H$ whereas the fractal dimension of the trajectory of motion in space of dimension N, with the coordinates described by independent processes (6), is given by

$$D = \min(N, 1/H) . \tag{7}$$

This is precisely the case when the trajectory in phase space has finite dimension for an infinitely-dimensional system.

Fractal properties of the trajectory for a dynamic system exhibiting chaotic behaviour are unrelated to the properties of scale invariance of the signal. Locally self-similar domains of the attractor may include temporally remote readings. This is the key difference between dynamic chaos and true random signals. Fractal properties of the trajectory for a purely random process are manifested when the process exhibits self-similarity properties. As a rule, they occur concurrently with a small inner scale t_0 and a higher outer scale T. In the range of $t_0 < t < T$, scaling properties of process increments are apparent on the time interval τ:

$$\left\langle \left[X(t+\tau) - X(t)\right]^2 \right\rangle \sim \tau^{\beta} . \tag{8}$$

An example of such processes is provided by random walks (obeying the stable distribution law) on time and distance scales exceeding the time step and the elementary step of the walk respectively. There is a great variety of such processes with exponent β differing from $\beta = 1$ and even exceeding 2 (these processes are referred to as anomalous diffusion processes). One of the first wave problems pertaining to anomalous diffusion was examined in Refs [43, 44]. It concerns excitation transfer in a resonant medium with a uniformly widened line. The probability distribution of photon absorption by an atom after it has been emitted by another (excited) atom has no finite dispersion. Accordingly, there is no dispersion of the length of the photon's free path. In the limit of large distances, random walks governed by the law of stable distribution are described by Eqn (8) with $\beta > 1$.

Various fractal structures are inherent in hydrodynamic turbulence. In the first place, this is true of the structure of energy dissipation fields. Marked intermittency of an energy dissipation field eventually results in the concentration of dissipation in a negligibly small volume occupied by turbulent motion. It has been shown that the correlation function of dissipation density has the power-law form [71, 72]; hence, dissipation concentrates on a fractal set [73]. The dimension of this set is 2.6–2.8. Later, more accurate measurements demonstrated that the dissipation energy field cannot be described by a single fractal dimension, and is in fact a multifractal [48] (see Section 5 for more details about multifractals). The impurity concentration in a turbulent flow has been reported to have a similar structure [74]. Also, fractality is inherent in the interface separating turbulent and nonturbulent regions of the stream [75] and the trajectory of particles in a random flow [76]. The large-scale structure of turbulent currents in the ocean and atmosphere (in excess of the inertial interval) appears to have fractal properties [18].

2.3 Fractal structure models in physics

It should be borne in mind that the fractal structure of matter is virtually unamenable to theoretical investigation by conventional methods employed in statistical physics. An exception is probably fractals in random walk models and in the structure of polymeric chains (the Flory theory, see for instance Ref. [21]). Many basic studies on fractal structures are performed using computer models. From this viewpoint, a fractal description of structures may be considered supplementary to the results obtained by standard statistical methods. On the other hand, advanced statistical characteristics of fractal structures are unknown. This problem can in principle be solved by introducing a number of Renyi dimensions or by the description of fractal structures in terms of multifractals, which is virtually the same. The most popular models of fractal structures in physics are the percolation cluster model, the model of clusters formed by diffusion-limited aggregation, and random walks without intersection. Fractal properties of fields and signals are described using random walk

models, e.g. summarised Brownian motion and 'Levi flight', leading to processes with fractal time and to superdiffusion processes.

2.3.1 Random walks. Random walk is a mathematical model to simulate particle displacements under the effect of random forces. It is perhaps the simplest and most advanced model in statistical physics leading to fractal structures. Plots of particle shifts versus time and trajectories are fractal curves.

Major applications of the random walk model include the analysis of fractal properties of random signals and waves. Also, its application to the description of fractal forms of material bodies has been reported, in the first place, to characterise random surface reliefs and shapes of polymeric molecules. In the latter case, the model of random self-avoiding walks proved especially useful for interpreting experimental data.

The broadest class of models currently in use for random processes showing fractal behaviour is related to the classical Wiener model of Brownian motion. This model describes processes for which all parameters are derived from two postulates: (a) increment of the process during a given time interval has a normal distribution of probabilities with average zero, (b) increments on nonoverlapping time intervals are statistically independent. In this case, the mean square of the displacement x for time t has the form

$$\langle x^2 \rangle = K_D t \ , \tag{9}$$

where K_D is the diffusion coefficient. It is only for this process out of all the ones with independent displacements that the trajectory is continuous with unit probability. At the same time, neither the trajectory nor the plot for the Wiener process is subject to differentiation. Expression (9) implies self-similarity of the process and the fractal properties as described above.

Generalisation of the Wiener process leading to other fractal events implies cancellation of either the condition of independent increments on nonintersecting time intervals or their normal distribution. In the former case, processes with memory arise, e.g. so-called generalised Brownian motion and self-avoiding walks. In the latter case, there are the 'Levy flight' and superdiffusion processes.

The normal distribution of the increments on the assumption that an increment of the process on the time interval t satisfies condition (6) (with exponent H differing from 1/2) leads to random walks with memory.

A simple model displaying such behaviour does not lead beyond the Gaussian processes. This is the generalised Brownian motion model $X_H(t)$ obtained by linear transformation of the Wiener process $X_{1/2}(t)$ of the form [9]:

$$X_H(t) - X_H(0) = \int_{-\infty}^{t} K(t-t')\,\mathrm{d}X_{1/2}(t') \ , \tag{10}$$

where the kernel has the following power dependence on the interval $t - t'$:

$$K(t-t') \sim (t-t')^{H-1/2} \tag{11}$$

(with the condition that measures are taken to ensure convergence of integral (10), for example by restricting the lower bound). It is clear that the contribution of different temporally separated portions of the initial process to the generalised Brownian motion may be either great or small depending on the H value. On the assumption that $X_H(0) = 0$, it immediately follows from expression (6) that for the long-term correlation of the process [9]

$$\frac{\langle -X_H(-t)X_H(t)\rangle}{\langle X_H^2(t)\rangle} = 2^{2H-1} - 1 \ . \tag{12}$$

At $H = 1/2$ (the Wiener process), correlation is absent. There is positive correlation at $H > 1/2$ and negative at $H < 1/2$. Therefore, the aim of generalisation is to neglect the assumption of independent increments on self-avoiding intervals; in such a case, the process has memory. At $H > 1/2$, the process is persistent whereas at $H < 1/2$, it is antipersistent.

The property of memory for a generalised Brownian process has another useful formulation [77]. This study examined correlation between the sums of signal levels on a sequence of two adjacent time intervals in relation to the number of separating intervals. At $H < 1/2$, the correlation was low even for neighbouring intervals whereas at $H > 1/2$, it was $r_1 = 2^{2H-1} - 1$ for the adjacent intervals and slowly lowered according to the power law with an increase in the number of separating intervals. It should be emphasised that this property showed no dependence whatever on the summation interval. Such a behaviour of the sums suggests the possibility of a situation in which it is impossible to obtain reliable data on average parameters of the process within a limited period of measurements. In such a case, determination of exponent H is an indispensable element of the evaluation in the statistical properties of the process.

Random self-avoiding walks retain property (6) with $H < 1$, but they are not Gaussian processes. Such walks have memory of a more complex structure as compared with (10), and their increments are not independent. However, their fractal characteristics are the same as in generalised Brownian motion. The fractal dimension of the trajectory is $1/H$, and the plot dimension is $2 - H$. Numerical values of H depend on the dimension of space d in which the process occurs. Accordingly, for $d < 4$ $H = 3/(d+2)$, the fractal dimension of the trajectory is $D = (d+2)/3$. The most meaningful physical interpretation of such a process is long polymeric molecule randomly located in the medium. The dependence of the molecular size on the number of links with due regard for their repulsion (absence of intersection) was first derived by Flory (see Ref. [21]) by the methods of statistical physics using free energy minimisation which included the energy of link interaction. A similar result was obtained using the random self-avoiding walk model. This is one of few cases where statistical physics explicitly leads to fractal structures.

Anomalous diffusion processes with increments satisfying Eqn (8), with $\beta > 1$ (superdiffusion processes), cannot be described using the Gaussian model (10). Formally, such processes are subject to the diffusion equation with the displacement-dependent diffusion coefficient. However, this leads to smooth non-fractal trajectories. On the other hand, observations of turbulent diffusion revealed fractal properties of the particles' trajectory [76] which is in conflict with the traditional description of diffusion. Ref. [76] contains numerical analysis of the model of particle motion in a stream with the fractal flow function which leads to fractality of the particles' trajectory. Another approach using anomalous diffusion models has been developed in Ref. [78]; it is based on the theory of processes with stationary independent but non-Gaussian increments.

It has already been mentioned that the Wiener process is distinguished from processes with independent increments. The plot (and the trajectory) of this process is continuous with unit probability. This condition is fulfilled if and only if the process is normal [79]. Neglect of normality of increments inevitably results in broken trajectories. Nevertheless, processes with non-Gaussian increments may have useful applications. Generally speaking, the assumption of the Gaussian nature of the processes under investigation is normally based on the use of the central limiting theorem. A random process is considered to be a sum of contributions of a number of random items. Owing to this, the Gaussian nature of the process follows from the central limiting theorem. However, this is true when random items are distributed with finite dispersion.

Otherwise, the resulting process is not necessarily a Gaussian one. Levy-type stable distributions [79] constitute a generic class of limiting distributions (i.e. distributions of sums of a large number of independent random items) showing self-similar properties. Such distributions possess the following similarity property:

$$t^{1/\alpha}X_1 + s^{1/\alpha}X_2 \stackrel{d}{=} (t+s)^{1/\alpha}X \,, \tag{13}$$

where X, X_1, X_2 are independent variables with similar stable distribution, t, s are any positive numbers, and the label $\stackrel{d}{=}$ means that random values have similar distributions.

Exponent α lies in the range $0 < \alpha \leqslant 2$. At $\alpha = 2$, the normal Gaussian process with finite dispersion occurs; then, property (13) states the dispersion summation rule and is equivalent to Eqn (9). At $\alpha < 2$, there is a variable with infinite dispersion, and only moments of the order of less than α exist. A random walk process with independent displacements subject to the Levy distribution law with exponent $\alpha < 2$ is called the 'Levy flight' [78, 80]. Due to the infinite displacement dispersion, measurement of this variable during a finite time interval may give any result (an analogue is the sum of a divergent series on permutation of its terms) and is therefore unsuitable to characterise the process. In this situation, measurement of fractal dimension is crucial. The trail of the Levy flight may be represented as a set of turning points connected by rectilinear jumps. In two-dimensional phase space, the trajectory of a particle with the coordinates described by stable processes with exponent α has fractal dimension of the turning points $\alpha < 2$. When $\alpha = 2$, the usual Brownian process takes place in which all the points are turning points since the process is continuous and the derivative is absent.

The Levy flight may give rise to a model of anomalous diffusion processes with finite dispersions of increments for a given time interval. Fractal properties of the trajectories of these processes coincide with those of the Levy flight trails [78, 80]. Suppose for example that a process is built up of independent jumps, with the jump length having Levy-type distribution, with jump duration dependent on the jump length and growing with it. Then, the increment dispersion within a given time interval becomes finite [78], the trajectory in phase space preserves its shape, and a new fractal object appears: temporal break-points of the derivative of the process. This provides an example of a process with fractal time [80]. For processes of this type, the exponent in Eqn (8) may exceed unity.

2.3.2 Percolation clusters. The term percolation (permeation, leakage, filtering) is currently adopted in physics to denote a certain class of phenomena investigated by the theory of percolation.

The theory of percolation is actually a mathematical theory pertaining to stochastic geometry. Major problems of the theory of percolation are lattice problems of bonds and nodes. Consider a regular (periodic, with symmetry) spatial or flat lattice of nodes each bound to its immediate neighbours. A typical physical model is a lattice of resistors [81]. When all the resistors are intact, each node is electrically connected with an infinite number of other nodes, and the lattice possesses finite conductance. Suppose that a fraction (concentration) $1-p$ of random bonds are broken and the intact bond fraction is small. Then, lattice conductivity is zero, that is the probability for a node to be connected with an infinite number of other nodes (i.e. to belong to an infinite cluster) is vanishing. This probability will remain zero until the fraction of intact bonds $1-p$ amounts to a critical value p_c referred to as the percolation threshold. At $p > p_c$, there is the nonvanishing probability that a node belongs to the infinite cluster associated with the finite conductance of the lattice. The problem of determining the threshold number of intact bonds is the problem of bonding. In the node problem, all the bonds are considered intact while the nodes are 'damaged', that is a number of randomly located nodes are nonfunctioning (i.e. bonds arising from such nodes are disconnected). Percolation thresholds in the problems of bonds and nodes are different. Also, the percolation threshold depends on lattice dimension, the number of nearest neighbour elements, and, in a broader context, the structure of elementary cells in the lattice.

Nevertheless, different values approaching the percolation threshold exhibit surprisingly universal patterns of behaviour. To begin with, a fraction of nodes p_∞ belonging to an infinite cluster above the percolation threshold shows a universal dependence on the difference between the intact bond (node) concentration and the threshold concentration:

$$p_\infty \sim (p - p_c)^\beta \,, \tag{14}$$

or, after introduction of $\tau = (p - p_c)/p_c$, it is possible to write down $p_\infty \sim \tau^\beta$. Exponent β does not depend on the lattice structure and is determined by the space dimension alone. For two-dimensional lattices $\beta = 5/36$ and for three-dimensional ones $\beta = 0.4$.

It turns out that the infinite cluster above the percolation threshold has fractal structure on scales not greater than a certain value ξ. This scale shows a universal dependence on the difference between the concentration of intact bonds (nodes) p and the threshold value p_c:

$$\xi \sim |\tau|^{-\nu} \,, \tag{15}$$

where exponent ν, similar to β, depends only on lattice dimension: $\nu = 4/3$ for a two-dimensional lattice and $\nu = 0.88$ for three-dimensional one. Expression (15) is equally meaningful for concentrations below the threshold value. In such cases, ξ is the characteristic size of finite clusters. Scale ξ is infinite on precisely the percolation threshold, where the concentration of bonds (nodes) belonging to the infinite cluster is vanishing. In other words, the infinite cluster density is zero as should be expected for fractal clusters in agreement with formula (2). Above the percolation threshold, scale ξ is finite, and

infinite cluster density is determined by the density of constituent fractal fragments of this cluster on scale ξ:

$$\rho \sim \xi^{D-d} , \tag{16}$$

where D is the fractal dimension of the cluster on scales below ξ. On the other hand, expression of τ from Eqn (15) through ξ and substitution into Eqn (14) yields

$$\rho \sim p_\infty \sim \xi^{-\beta/\nu} ,$$

while comparison of the last expression with Eqn (16) allows the equation for fractal dimension of cluster D to be found in terms of the universal exponents ν and β:

$$D = d - \frac{\beta}{\nu} . \tag{17}$$

Therefore, fractal dimension is also determined by lattice dimension alone and equals 1.89 and 2.54 for two-dimensional and three-dimensional lattices respectively. Fig. 1b presents an example of the computer model for a percolation cluster obtained for the problem of nodes on a square lattice.

Applications of the percolation cluster model for the description of fractal structures of matter are diverse. The first application was suggested by De Gennes [82].

De Gennes proposed a simple lattice model of polymerisation in solutions. He considered monomers randomly located in the nodes of a lattice. The reaction between monomers in the adjacent nodes resulted in bond formation. Polymer synthesis was exactly analogous to percolation transition in the problem of nodes and occurred when the concentration of monomers reached a certain threshold value. Monomers that did not react during the preparation of the polymer were washed out. Therefore, the resulting polymer molecule had fractal structure. This model has provided the basis for the development of further lattice models simulating properties of fractal materials.

The percolation cluster model is universal owing to the fact that a percolation cluster inevitably arises from randomly distributed particles provided their concentration is sufficiently high. However, the relative number of particles that stick together to form the cluster, which can be found from expression (14), is not very large at threshold concentration or near it. Removal of particles that do not adhere to the cluster results in a true fractal structure. Another outcome of percolation transition in a nonpercolation situation is percolation in a concentration gradient. The agent level in the diffusion front changes from zero at a distance from the source to unity close to it. At a certain site in the front, the concentration of the diffusing agent equals the threshold concentration of percolation. Near this site, the agent gives rise to fractal clusters [83].

2.3.3 Fractal aggregates. Aggregation is one more mechanism for generating fractals in matter which involves all available particles in the formation of a fractal structure.

Real fractal aggregates are formed by adhesion of solid particles which arise under appropriate conditions in solutions and vapours of certain substances. The most illustrative examples are gel formation in silicon dioxide solutions and formation of particulate soot in a flame [11].

The simplest model of fractal aggregate growth is diffusion-limited aggregation (DLA) [59]. The model is as follows. Suppose that a primer cluster (or even an isolated particle) is placed in a certain volume and that other particles are injected into the same volume one after another to move randomly along the Brownian trajectories. Particles which collide with the cluster adhere to it, and in this way the cluster grows. Fig. 1a shows a cluster thus grown on a surface in a computer model.

Another model, i.e. cluster-cluster aggregation, postulates simultaneous diffusion of many particles in a volume. The particles stick together upon touch to form numerous clusters. The clusters thus formed are also involved in diffusion and give rise to bigger structures by adhesion. Generally speaking, there are a lot of aggregation models differing in the motion patterns, the likelihood of adhesion, and the interaction radius. These models have been reviewed in Refs [11, 84]. The common feature of all such models is that the resulting clusters are fractals, that is statistically self-similar aggregates with noninteger fractal dimension. Mass $M(R)$ of a fractal aggregate in a volume with radius R is defined by Eqn (1).

Aggregation models are categorised on two criteria: the shape of trajectories of travelling particles and the number of clusters involved in the process [11].

Using the first criterion, aggregation is classified as arising from rectilinear motion of particles and from their random walks. Also, it is possible to introduce many trajectories with different fractal dimensions in the range 1–2. Dimension 1 corresponds to straight trajectories and dimension 2 to Brownian trajectories.

Based on the second criterion, two extreme cases can be distinguished: particle-cluster aggregation and cluster-cluster aggregation. In the former case, an isolated growing cluster is surrounded by a number of travelling particles that adhere to it on collision. In the latter case, the volume contains many clusters that stick together to form bigger ones.

Apart from these differences, the probability of adhesion on touch in all the above processes may also differ. Unlike percolation models, aggregation models do not imply universal dimensionality. Fractal dimensions of clusters in different types of aggregation are variable. Moreover, in particle-cluster aggregation with rectilinear motion of particles, the resulting clusters are not fractal, and fractal dimensions in two-dimensional and three-dimensional spaces are 2 and 3. The smallest fractal dimensions occur in cluster-cluster aggregation with Brownian motion of the resulting clusters: 1.44 in the two-dimensional and 1.77 in the three-dimensional case [11].

3. Waves in fractal structures. Fractons

In the case of real fractal materials, dispersion relations and expressions for elastic oscillation density in the fracton region ensue from scale dependences of elastic moduli and density of the materials. Both early studies of the fracton region of the spectrum and many ongoing numerical analyses are based on the examination of the model equation for oscillations on fractal node lattices.

A simple model expression for the wave amplitude on the nodes of a fractal lattice has the form:

$$\alpha \ddot{u}_i = \sum_j K_{ij}(u_j - u_i) , \tag{18}$$

where $K_{ij} = 1$ if internode bonds in the lattice remain intact (otherwise $K_{ij} = 0$) and α is a dimensional constant with the

sense of the inverted square of resonant frequency for a single bond. Eqn (18) has been used in many wave studies of fractal clusters (using lattice models).

In a one-dimensional case, Eqn (18) corresponds to the known equation for longitudinal chain oscillations

$$\alpha\ddot{u}_i = u_{i+1} - 2u_i + u_{i-1} ,$$

where the right-hand side is the finite-difference expression for the Laplacian. Certainly, in two-dimensional and three-dimensional cases, the scalar equation (18) cannot describe lattice oscillations for the general model of elastic forces. Discussed below is a model of isotropic elastic forces that allows Eqn (18) to be used for the description of elastic oscillations for the Cartesian components of node displacements.

In the two-dimensional case, physical meaning may be assigned to Eqn (18) by assuming that masses m are located in the nodes of a lattice and each bond is a stretched spring (string) of length l_0 and tensile stress T. If u_i is the normal mass displacement with respect to the plane, then Eqn (18) describes transverse oscillations and the constant is $\alpha = l_0 m/T$. Such a situation may become real when all the bonds are intact, but it is not so for fractal clusters. Nevertheless, model (18) is widely used to study the structure of fractal oscillation states and appears to provide qualitatively relevant results.

3.1 Oscillations and diffusion on fractals

The very first data to characterise eigenoscillations of fractals were obtained by Alexander and Orbach in 1982 [24]. Their study was based on the analogy between Eqn (18) for elastic oscillations of fractals and the equation for random walks, and on the fact that diffusion of fractals is subject to condition (8) with the exponent $\beta < 1$.

Suppose that $p_i(t)$ is the probability of finding a randomly walking particle in node i at time t. V_{ij} is the likelihood of transition from node i to j for a given time interval ($V = \text{const}$, if the bond is intact and $V = 0$, if it is broken). Then, the following equation can be deduced for $p_i(t)$:

$$\dot{p}_i = \sum_j V_{ij}(p_j - p_i) . \tag{19}$$

Eigenvalues and eigenvectors of operators acting on p_i and u_i in the right-hand sides of Eqns (18) and (19) coincide. In the case of oscillations, the eigenvalues correspond to the squares of fractal oscillation. The distribution of the eigenvalues yields the frequency distribution of oscillation states, and the above analogy with diffusion allows this distribution to be found without solving the problem of eigenvalues. This approach has long been known regardless of fractal studies [85].

Let us express the solution of Eqn (19) for a walk starting from the ith node (with initial condition $p_k(0) = \delta_{ik}$) in terms of the eigenvalues λ_n and eigenvectors $\varphi^n = (\varphi_1^n \ldots \varphi_i^n \ldots)$ of the operator in the right-hand part. Let us further represent the probability of returning back to the original node after time t in the following form:

$$p_{ii} = \sum_{n=1}^{\infty} \exp(-\lambda_n t)\, a_n^i \varphi_i^n = \sum_{n=1}^{\infty} \exp(-\lambda_n t)\, (\varphi_i^n)^2 , \tag{20}$$

where $a_n^i = \sum \delta_{ik}\varphi_k^n = \varphi_i^n$ are coefficients of expansion of the initial condition over eigenvectors. On the other hand, it is known (see for instance Ref. [10]) that walking on a fractal is associated with a mean displacement from the original node $r \sim t^{1/(2+\Theta)}$ where $\Theta > 0$ is the anomalous diffusion exponent (in the case of an ordinary lattice, $\Theta = 0$ and $r \sim t^{1/2}$). A fractal cluster of radius r contains $\sim r^D$ nodes. At any r after sufficiently long time t, the probability for a particle to occur in any node at a distance r from the original one becomes the same. Hence,

$$p_{ii}(t) \sim r^{-D} \sim t^{-D/(2+\Theta)} . \tag{21}$$

Summation of Eqn (20) over all nodes of the cluster and comparison with Eqn (21) yields (φ^n are normalised):

$$\sum_{n=1}^{\infty} \exp(-\lambda_n t) \sim N t^{-D/(2+\Theta)} . \tag{22}$$

With the use of one of the Tauber theorems [79], it immediately follows from expression (22) for the distribution density of eigenvalues at $\lambda \to 0$ that $\nu(\lambda) \sim \lambda^{D/(2+\Theta)-1}$.

For oscillations, $\lambda = \omega^2$ and $\mathrm{d}\lambda = 2\omega\,\mathrm{d}\omega$. Then, the distribution density of oscillation modes versus frequency is

$$\nu(\omega) \sim \omega^{2D/(2+\Theta)-1} . \tag{23}$$

Alexander and Orbach found the fractal dimension to equal

$$d_f = \frac{2D}{2+\Theta} . \tag{24}$$

Fractal dimension plays the role of space dimensionality in a low-frequency asymptote of the density of oscillation states. Indeed, from Eqn (24) a known equality $\Theta = 0$ for the density of normal phonon states on a d-dimensional lattice follows:

$$d_f = d .$$

As regards real fractal materials, there is a maximum scale ξ which limits the region of fractal behaviour. On scales exceeding ξ, hence at low frequencies [below a certain crossover frequency $\omega_c(\xi)$], there is the usual phonon spectrum. At higher frequencies, transition (crossover) to the fracton spectrum occurs. Taking into account the fact that the number of oscillation modes must be equal to the number of particles in the material, the following expressions can be written for the density of states ν_{ph} and ν_{fr} of the phonon and fracton spectra respectively, in a unit volume [24]:

$$\nu_{ph} = N_F\, d\, \frac{\omega^{d-1}}{\omega_c^d} , \tag{25}$$

$$\nu_{fr}(\omega) = N_F\, d_f N_{at}\, \frac{\omega^{d_f-1}}{\omega_d^{d_f}} = N_F\, d_f\, \frac{\omega^{d_f-1}}{\omega_c^{d_f}} , \tag{26}$$

where $N_F = (1/\xi)^d$ is the number of fractal fragments in a volume unit participating, without deformation, in oscillations of the phonon spectrum in the capacity of rigid particles, ω_c is the crossover frequency, $N_{at} = (\xi/a)^D$ is the number of atoms (particles) of size a in a fractal fragment of size ξ, and $\omega_d = (\xi/a)^{D/d_f}\omega_c$ is the fracton Debye frequency, by definition. The latter equation in (26) explicitly follows from expressions for N_{at} and ω_d.

As with the usual Debye frequency for the phonon spectrum, the choice of the fracton Debye frequency as the integration limit ensures that the number of oscillations coincides with the number of particles. Integration of densities (25) and (26) from 0 to ω_c and from ω_c to ω_d respectively yields $N_{ph} = N_F$ for the total number of

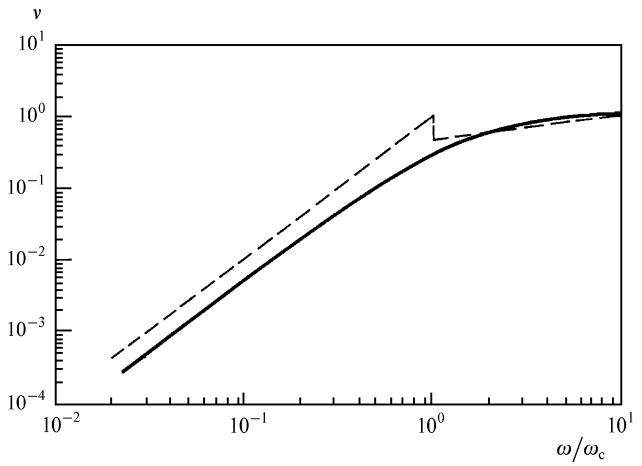

Figure 3. Density of oscillation states deduced from formulas (25), (26) (dashed line) and from the formula which approximates smooth curve transition (solid line). Density is given in arbitrary units, but the full number of states is the same for both curves. Frequencies are normalised with respect to crossover frequency.

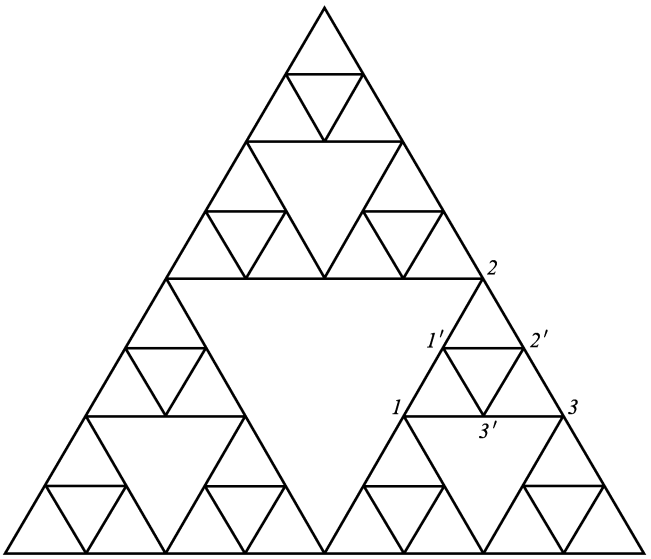

Figure 4. Triangular Sierpinski gasket. Figures denote nodes used in the decimation procedure.

phonon states and $N_{\rm fr} = N_{\rm F}(N_{\rm at} - 1)$ for fractons. The number of all oscillation states $N = N_{\rm ph} + N_{\rm fr} = N_{\rm F} N_{\rm at}$, i.e. it is the same as the total number of atoms, as anticipated. It should be borne in mind that according to expressions (25) and (26), the density of phonon states at crossover frequency $\omega_{\rm c}$ exceeds the fracton density of states:

$$\nu_{\rm ph} = N_{\rm F}\, d > \nu_{\rm fr} = N_{\rm F}\, d_{\rm f} ,$$

because $d > d_{\rm f}$. This may result in a peak in the density of states near the crossover frequency as shown in Fig. 3. The presence of such a peak is not always possible to confirm in experiment, nor does it appear in numerical calculations of the state density using Eqn (18). However, analysis of experimental findings based on the temperature dependence of aerogel thermal capacity [86] indicates that the peak must be present.

The absence of the peak suggests smooth transition from phonon density (25) to fracton density (26) within a certain frequency range. The transition approximation commonly used has the form

$$\nu(\omega) = \frac{\omega^2}{(\omega_{\rm c}^2 + \omega^2)^{(3-d_{\rm f})/2}} .$$

The approximate behaviour of the density of states unevenly replacing one another at the crossover frequency as deduced from this formula and formulas (25) and (26) is shown in Fig. 3. It appears that both possibilities are attained for different materials.

3.2 Fractons on regular fractals. Localisation

Further progress in the understanding of eigenstates of Eqn (18) on fractals is ensured by the analysis of the solutions of this equation on a regular fractal, the triangular 'Sierpinski gasket' (Fig. 4) [87, 88]. The authors used a kind of decimation procedure† which enabled them to find analytically the solution of Eqn (18) for the case of self-similar fractal lattices.

†Decimation in old Rome was the punishment of each tenth soldier in a cohort that betrayed cowardice in the battle.

Consider Eqn (18) for oscillations with frequency ω:

$$\alpha\omega^2 u_i = \sum_j K_{ij}(u_i - u_j) . \tag{27}$$

Assume that $u_{i'}'$, u_i, $i = 1, 2, 3$ are the oscillation amplitudes in the nodes labelled 1, 2, 3, 1′, 2′, 3′ in Fig. 4. Based on a portion of Eqn (27), the amplitudes $u_{1', 2', 3'}'$ may be expressed in terms of amplitudes $u_{1, 2, 3}$. Substitution of the solution into the remaining Eqn (27) leads to a system of equations containing only amplitudes $u_{1, 2, 3}$ with the renormalised frequency value $\alpha\omega'^2 = 5\alpha\omega^2 - \alpha^2\omega^4$. Due to self-similarity, equations for amplitudes $u_{1, 2, 3}$ describe oscillations on precisely the same lattice as the original one. For an analogue of the Sierpinski gasket in a space of d-dimensions (such a figure is composed of d-dimensional tetrahedrons), it is possible to obtain a general expression for renormalised frequency

$$\alpha\omega'^2 = (d+3)\alpha\omega^2 - \alpha^2\omega^4 . \tag{28}$$

Evidently, the decimation procedure may be repeated on larger scales. In the end, one comes to the following conclusion: if there is eigenoscillation with frequency ω, there must be eigenoscillation with frequency ω'. Concurrently, the number of cluster elements involved in oscillations undergoes a $(d+1)$-fold change, and the following expression [88] is available for spectral dimension:

$$d_{\rm f} = \frac{2\ln(d+1)}{\ln(d+3)} . \tag{29}$$

The spectrum structure defined by the parametrisation equation (28) is very complicated in itself and shows scaling properties on the frequency axis. The spectrum consists of δ-like peaks which give rise to a complex self-similar structure on the frequency axis [87]. Expression (29) is fulfilled only for the density of states averaged over frequency bands.

Structural analysis of eigenmodes of Eqn (27) on the Sierpinski carpet accomplished in Ref. [88] demonstrated that all eigenstates are localised. There are two classes of localised states. One includes molecular states with a strictly limited small number of structural elements. The other

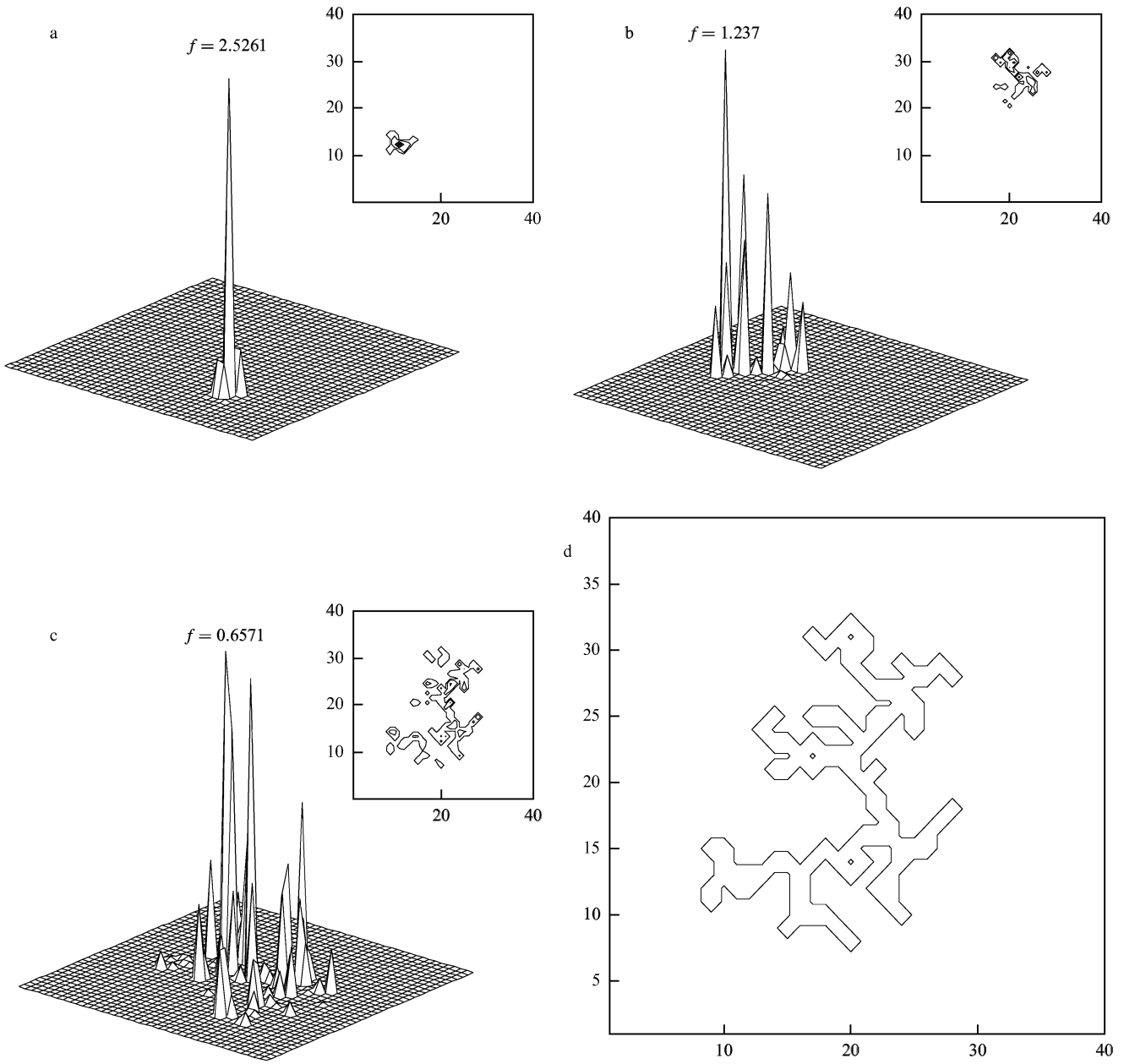

Figure 5. (a, b) Eigenfunctions of Eqn (27) for the cluster shown in Fig. 5d. Three-dimensional plot: the square of amplitude modulus. Top right: eigenfunction level lines on a cluster to be compared with the cluster contour. (a–c) Different frequencies of eigenoscillations: (a) 2.5261 (b) 1.237 (c) 0.6571. (d) Contours of the cluster obtained by computer simulation of DLA on a plane and used to calculate eigenoscillations.

comprises states with the amplitudes differing from zero on all the scales and the well-defined localisation length. The relative numbers of states belonging to the two classes for a d-dimensional Sierpinski gasket are $d/(d+1)$ and $1/(d+1)$ respectively.

Qualitatively, such a situation takes place in the case of irregular fractals as well. Figs 5–7 show results of numerical evaluation of eigenmodes on a fractal cluster obtained by computer simulation of DLA. Figs 5a–5c are diagrammatic representations of the shape of eigenoscillations for different frequencies. It can be seen that the size of the region of localised oscillations increases with decreasing frequency. At the same time, there is marked variability of the localisation size for close frequencies. Fig. 6 shows states with similar frequencies which are strikingly different in terms of the localisation region size and appear to belong to the above two classes of states. Two classes of states in numerically determined eigenoscillations of a percolation cluster have also been distinguished in [89]. Fig. 7 shows the frequency distribution function of cluster eigenoscillations and the corresponding distribution density for the case in question. Broken and irregular density is typical of any specific example of the cluster, and expression (24) naturally refers to averaged density.

3.3 Elastic properties of fractal materials

In the general case, elastic oscillations of fractal clusters cannot be described by Eqn (18). However, the properties of the fracton region of the spectrum defined by spectral dimension may be preserved although the fracton dimen-

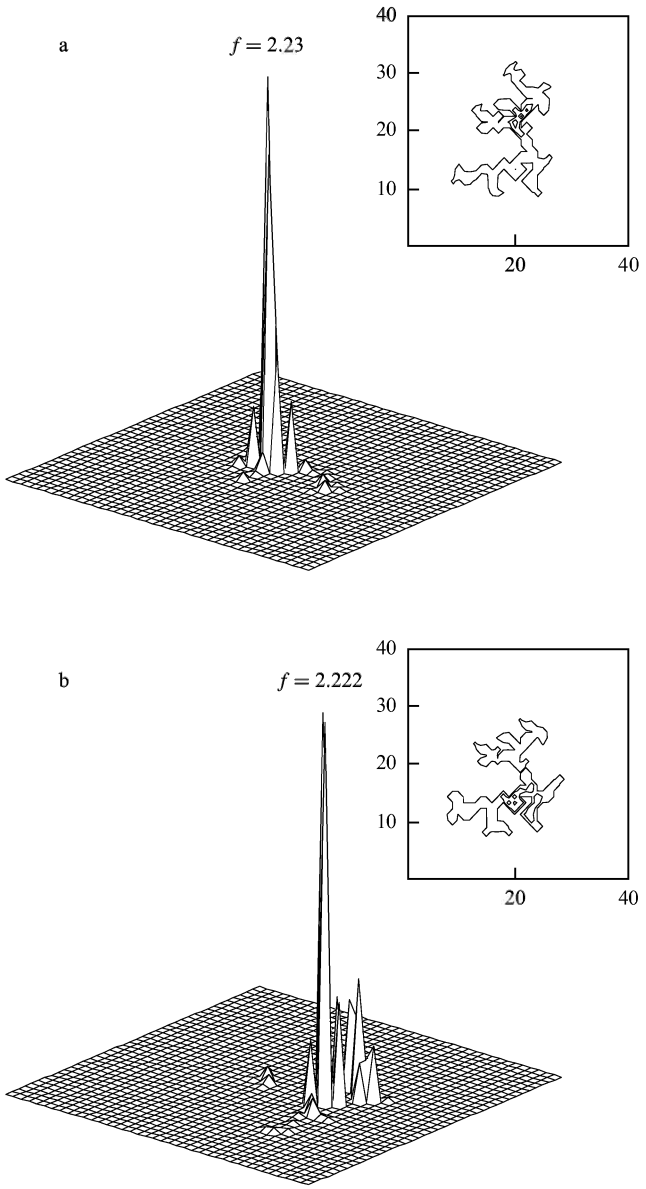

Figure 6. Same as in Fig. 5. (a) 'molecular' and (b) 'extensive' oscillation states for very close frequencies. Top right: location of their centres on the cluster.

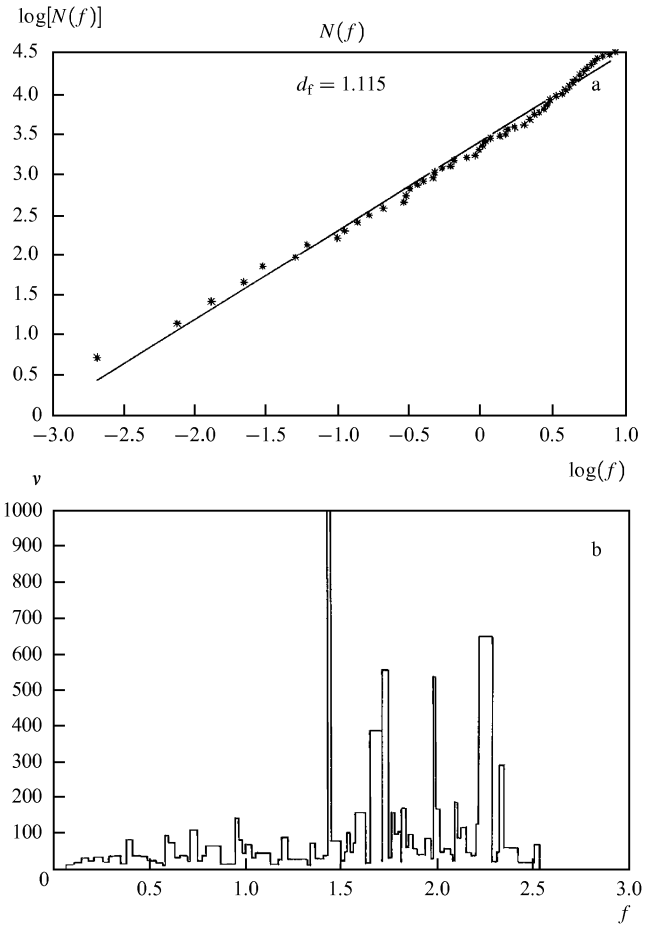

Figure 7. Eigenoscillation distribution function for the cluster in Fig. 5d plotted against frequencies (a) and corresponding distribution density of eigenstates (b).

sion is not specified by expression (24) but is instead derived from various models of fractal elastic properties. The elastic properties of fractals are important by themselves, and the theory provides a good example of the macroscopic description of scale-invariant disordered media.

3.3.1 Scale dependence of elastic models. The principal difference between the elastic behaviour of fractal materials and that described by the theory of continuous elastic media can be accounted for by the dependence of elastic moduli on the deformation scale. Measurements of elastic moduli using fragments of differently-sized fractal structures are likely to produce different results. However, in such a general formulation as this, it may be regarded as a distinctive feature of both fractals proper and a broad class of natural and artificial materials and devices with hierarchical structure [90]. Such a structure is inherent in natural and technological composite materials, open-work metallic constructions like the Eiffel tower or natural constructions (honeycomb). On the whole, a hierarchical structure such as that of composite materials is made up of elements of smaller scale (e.g. layers) which in turn consist of even smaller structures (e.g. fibres), etc. Therefore, different hierarchical levels may have different structure (fibres, layers) while the number of levels is not necessarily very large (three in the case of the Eiffel tower).

Fractal materials differ from the general case by the structural similarity of levels on different scales in a certain scale range. Fragments of a material with sizes lying within this range are made up, according to a certain rule, of elements of a smaller scale which in turn consist, following the same rule, of even smaller fragments, etc. Of course, self-similarity of real materials should be understood in the statistical sense. The statistical characteristics of the location of similarly-sized elements in a fragment of a greater scale are independent of the absolute scale values and determined only by their ratio.

Suppose that $E(l)$ is the elastic modulus for a fragment of a fractal structure with length l in the fractal range of scales. Due to self-similarity of the structure, the ratio of elastic moduli for different scales l, l' is dependent on the scale ratio alone:

$$\frac{E(l)}{E(l')} = f\left(\frac{l}{l'}\right) . \tag{30}$$

For three diffferent scales l, l', and l'', equations $E(l)/E(l') = f(l/l')$, $E(l')/E(l'') = f(l'/l'')$, $E(l)/E(l'') = f(l/l'')$ are fulfilled. Therefore, the scale ratio function $f(x)$ must satisfy the following functional equation: $f(xy) = f(x)f(y)$. The general solution of the latter equation has the form of $f(x) = x^{-\zeta}$, where ζ is an arbitrary number. Hence, the equation for scale dependence of the elastic modulus E is

$$E(\lambda l) = \lambda^{-\zeta} E(l) \,, \tag{31}$$

if scales λl and l belong to the self-similarity interval. The scale dependence of fractal elastic properties is defined by the exponent ζ which is often termed the geometric exponent of elasticity. Exponent ζ characterises the scale dependence of the elastic modulus, i.e. the relative deformation to strain ratio. Rigidity of the fragment (the force to displacement ratio) also has scale dependence of the form of Eqn (31) but with a different exponent ζ_E. It is easy to establish the relationship between exponents ζ and ζ_E for a fractal located (embedded) in a space of dimension d. Consider the rigidity of a d-dimensional cube made up of cubes smaller by a factor of two. At a constant stress, the force increases 2^{d-1}-fold, in proportion to the area of the side faces. The displacement is proportional to the size and increases two-fold while rigidity shows a 2^{d-2}-fold rise. It is evident that

$$\zeta_E = \zeta - d + 2$$

(exponents ζ and ζ_E are identical in a two-dimensional case).

Exponents ζ and ζ_E are determined by the structure of the fractal material and the nature of the interaction forces between their elements. These exponents may differ even for materials with similar fractal dimensions.

The power-law dependence of elasticity on the size has long been known for polymeric chains. This is the so-called entropic elasticity unrelated to the interaction between chain links. Due to the fractal structure of polymer chains, the line of reasoning followed in the previous paragraphs equally applies to the present case. Further discussion does not concern entropic elasticity but is focused on elasticity of fractal lattices resulting from the specified bond elasticity. (See Refs [91, 92] for information on the theory of entropic elasticity of polymer lattices).

Real materials with fractal structure consist of coupled fractal aggregates of size ξ. The scale of ξ depends on the regime of the material formation and the nature of its constituent particles (see Section 2).

Elastic properties of materials on scales exceeding ξ are described in the continuous medium approximation and the corresponding elastic moduli are defined by elastic moduli of constituent fractal aggregates of the maximum size ξ.

Computer simulation of fractal structure formation proved crucial for the development of lattice models for elastic fractal properties [93, 94]. Lattice models examine periodic lattices with nodes of definite symmetry (square, cubic, triangular, etc.). A fractal cluster is obtained as a percolation cluster, i.e. an infinite cluster derived from the theory of percolation on such a lattice (see Section 2, Fig. 1b). Bonds between constituent nodes of the cluster are believed to possess elastic properties. Using the results of the theory of percolation, it is easy to obtain characteristics of the elastic behaviour of fractal clusters. These data may be useful in the analysis of both percolation clusters and fractal clusters of different nature if their fractal dimensions coincide. It is worthy of note that fractal clusters of equal dimension may differ in other characteristics, e.g. ramification or the number of nearest neighbour elements, which sometimes influence their elastic properties.

If elastic forces in a cluster are active only between neighbouring nodes and exhibit linear dependence on their relative displacement, the potential energy of the deformed cluster may be expressed in the form of the quadratic combination of the displacement components for all pairs of adjoining nodes. Elastic properties of fractals were first investigated in Ref. [93] where the following variant of such an expression was used for potential energy:

$$U = \frac{1}{2} \sum_{ij} K_{ij} \left[\alpha (\boldsymbol{u}_i - \boldsymbol{u}_j)_{\parallel}^2 + \beta (\boldsymbol{u}_i - \boldsymbol{u}_j)_{\perp}^2 \right] \,, \tag{32}$$

where $\boldsymbol{u}_i$ is the displacement vector of the ith node in the lattice, α and β are constants, symbols $\parallel$ and $\perp$ denote displacement components along and across the nonperturbed direction of an internode bond, $K_{ij} = 1$ if nodes i and j are connected and $K_{ij} = 0$ if there is no connection between them.

At $\alpha \neq 0$ and $\beta = 0$, expression (32) leads to the model of central forces; if $\alpha = \beta$, it yields an isotropic model used in the theory of elasticity of crystal solids (the so-called Born approximation).

The energy minimum condition (32) gives the system of equations for the evaluation of the displacement. Effects on the system from the outside are taken into account in the boundary conditions, and its solutions allow elastic cluster constants to be determined.

In the case of a percolation cluster, the geometrical exponent ζ introduced in the previous section can be found from the dependence of elastic properties on the relative concentration of intact bonds p near the threshold concentration p_c (in fact, relative concentration p is the likelihood that the bond is intact). Clearly, elastic constants vanish at $p < p_c$. When $\alpha = \beta = 1/2$, elastic constants at $p > p_c$ for model (32) are described by a scaling law of the following form (see Section 2):

$$E(p) \sim (p - p_c)^T \,. \tag{33}$$

Exponent T unambiguously defines the geometric exponent ζ. Consider a percolation cluster above the percolation threshold (a uniform fractal) of size $L > \xi$ where ξ is the earlier deduced size restricting the region of fractal behaviour. Rigidity of a cluster of size L is expressed in terms of that of another cluster of size ξ (see derivation of the relation between exponents ζ and ζ_E):

$$K(L) = K(\xi) \left(\frac{L}{\xi} \right)^{d-2} \,. \tag{34}$$

On the other hand, $K(L) = \tau^T$ where $\tau = p - p_c$; since ξ is expressed through τ in the form of $\xi = \tau^{\nu}$ where ν is the critical component for ξ, it is possible to have

$$K(\xi) = \xi^{d-2} \xi^{-T/\nu} = \xi^{-T/\nu + d - 2} = \xi^{-\zeta_E} \,. \tag{35}$$

The relation between ζ and T following from Eqns (34) and (35) has the form:

$$\zeta_E = \frac{T}{\nu} + 2 - d; \qquad \zeta = \zeta_E + d - 2 = \frac{T}{\nu} \,. \tag{36}$$

In an isotropic model, the equilibrium equations [minimum energy Eqns (32)] are the same for all Cartesian

displacement components and coincide with the system of Kirchhoff equations for electric currents in a lattice provided shift components are understood as node potentials and electrical resistances of bonds are assumed to be equal [82]. It is known that for the resistance of a random resistant lattice near the percolation threshold the following rule holds: $R \sim (p - p_c)^{-t}$, where t is the critical exponent. Therefore, $T = t$. For two-dimensional and three-dimensional lattices t is 1.29 and 1.7 respectively, $\nu = 4/3$ and 0.88, and $\zeta_E = 0.97$ and 0.93.

The isotropic force model is hardly realistic and cannot be verified by the results of experiments on the direct measurement of elastic moduli for many real fractal materials. On the other hand, the data below concerning spectral dimension and obtained in neutron emission experiments indicate the possibility of using this model in selected situations.

The central force model, seemingly a more realistic one, leads to disturbance of the elastic coupling, which causes the rigidity of an infinite cluster near the percolation threshold to vanish [93]. Nonzero elasticity is manifested at $p = p_l$ where the value of $p_l > p_c$ is higher than the threshold concentration. However, even in this case, the dependence of elastic models on intact bond density has a form analogous to Eqn (30), with substitution of p_c by p_l [93]:

$$E(p) \sim (p - p_l)^{T'} , \tag{37}$$

where $T' = 2.4$ and $T' = 4.4$ for two-dimensional and three-dimensional cases respectively. For a triangular flat lattice, $p_l = 0.58$ ($p_c = 0.3473$) while for a face-centred cubic lattice, $p_l = 0.42$ ($p_c = 0.119$). For the case of an ordinary cubic lattice, expression (37) has no sense at all and $p_l = 1$. In qualitative terms, the central force model corresponds to a lattice of connected springs which can pivot freely while zero elasticity at the percolation threshold is possible only due to the relative rotation of bonds, without a change in their length.

The elastic connectivity condition is fulfilled if elasticity is taken into consideration when the angle between bonds is changed (the so-called bond-bending model). Such a model has been suggested in Ref. [94]. The expression for potential energy in this model has the form

$$U = G \sum_i \delta\varphi_{ijk}^2 + \frac{Q}{a^2} \sum_{ij} \delta u_{ij\parallel}^2 , \tag{38}$$

where $\delta\varphi_{ijk}$ is the change of the angle between bonds ji and ki belonging to the common node i, $\delta u_{ij\parallel}$ is the difference between displacements of nodes i and j parallel to bonds (i, j), G, Q are elasticity constants, and a is the lattice constant. In the case of a tortous chain of bonds with a large number of links N but without loops, the contribution of central forces [the second term in expression (38)] becomes negligibly small, and elastic stiffness of the chain is described by a simple expression obtained in Ref. [94]:

$$K = \frac{G}{N S_\perp^2} . \tag{39}$$

Here, $S_\perp$ is the radius of gyration for the chain in the direction perpendicular to the force that acts on it. Its value is derived from expression

$$S_\perp^2 = \frac{1}{N} \sum_{i=1}^{N} (R_N - R_{i-1})_\perp^2 ,$$

where $(R_N - R_{i-1})_\perp$ is the projection of the radius vector connecting the beginning of the ith link of the chain with the end of the last one on the direction perpendicular to the acting force.

The transition from the elastic properties of a one-dimensional chain to those of fractal clusters in Ref. [94] is based on the intuitively explicit suggestion that the cluster's softness is dependent only on the contribution of singly connected channels containing bonds. It is shown that for percolation clusters on lattices in Ref. [94], $T = 3.6$ and $T = 3.55$ for two-dimensional and three-dimensional lattices respectively. Using Eqn (36), the values of ζ_E are found to be 2.75 and 3.13 respectively.

One of the first experiments to measure elasticity of fractal materials in a broad range of scales was reported in Ref. [95]. In this study, the authors used materials obtained by sintering submicron silver powder. The resulting materials differed in terms of the occupied volume fraction of the powder (f) in the range from 0.06 to 0.291. Evaluation of their elasticity E and electric conductance σ gave respective scaling dependencies:

$$\sigma \sim (f - f_c)^t , \quad E \sim (f - f_c)^T ,$$

where $f_c \approx 0.062$ is the critical occupied volume fraction. Exponents $t = 2.15 \pm 0.25$ and $T = 3.8 \pm 0.5$ are significantly different which indicates the inapplicability of the isotropic force model. On the other hand, the threshold equality suggests disparity between the experimental results and those predicted by the model. At the same time, the numerical values of T are in agreement with the model [94].

In Refs [96, 97], elastic properties of two-dimensional percolation clusters were studied using a simple physical model of a perforated metal plate. In Ref. [96], the authors made use of randomly distributed holes in the nodes of a periodic square lattice and their totally random location (continual percolation). In these cases, the exponents T of the scaling dependence of plate rigidity on concentration differed. For lattice percolation, $T = 3.5$, in accordance with the prediction in Ref. [94], while for continual percolation the same exponent was higher than $T = 5$. A similar value of $T = 4.95$ was obtained in Ref. [97] where holes were also randomly distributed. The value of exponent T for continual percolation may be theoretically predicted based on the model (38) [98]. In Ref. [99], the elasticity of a wire lattice with randomly cut bonds was measured from the resonant frequency of torsional oscillations of the cylindrical screen obtained by folding the lattice. Unlike percolation models greatly restricted in terms of the node number as used in Refs [96, 97], the wire lattice model contained several thousands of bonds. The value of $T = 3.6 + 0.2$ measured in Ref. [99] is in excellent agreement with the theoretical value predicted in Ref. [94].

Thus, these models may be in a sense useful for the quantitative description of elastic properties of percolation fractal clusters and serve as a basis for determining the parameters of elastic oscillations, at least for the systems similar to those investigated in the experiment.

Results of the investigations into elastic properties of fractals using percolation models cannot be directly applied to aerogels. In the case of aerogels, density dependence takes the place of the dependence of elastic properties on a rise in concentration above the threshold level. Aerogels are formed by the aggregation of submicron particles of the

solid phase which precipitate from solutions of certain substances (e.g. Al_2O_3, SiO_2) if conditions permit. Aggregation results in fractal clusters whose density ρ is related to the cluster size r by (see Section 2)

$$\rho = \rho_0 \left(\frac{r}{r_0}\right)^{D-3}, \tag{40}$$

where D is the cluster fractal dimension (for the known aerogels, $D = 1.7-2.2$) and ρ_0 and r_0 are the density and the radius of cluster particles respectively. After a certain cluster size R is reached, depending on growth conditions, the clusters join together upon contact to form an aerogel having density $\rho \sim R^{D-3}$. Typical cluster size values in aerogels lie in the range of tens and hundreds of nanometers whereas aerogel density ranges from units to tens of grams per litre [100]. Therefore, an aerogel with density ρ comprises clusters of the size

$$R = r_0 \left(\frac{\rho}{\rho_0}\right)^{1/(D-3)}.$$

Hence, its Young's modulus has the form

$$E(\rho) = E_0 \left(\frac{\rho}{\rho_0}\right)^{-\zeta/(D-3)} = E_0 \left(\frac{\rho}{\rho_0}\right)^{\beta}, \quad \beta = \frac{\zeta}{D-3}. \tag{41}$$

Experimental data on density dependence of Young's modulus for aerogels are reported in Refs [100]. According to these data, $E_0 = 10^{6.58\pm0.18}$ N m^{-1}, $\beta = 2.8 + 0.2$, $\rho_0 = 0.13$ g cm^{-1}. Substitution into Eqn (41) of ζ values obtained in lattice models and fractal dimension measured for aerogels ($D = 1.77$) yields $\beta = 1.57$ in the isotropic model ($\zeta = 1.93$) and $\beta = 3.35$ for the model of one-dimensional chains with energy given by Eqn (38) ($\zeta = 4.13$). The latter value is closer to that obtained in experiment although there are no grounds to believe that the theory in Ref. [77] ensures accurate quantitation of aerogel elastic behaviour.

Evidently, acoustic velocity in aerogels also shows a power-law dependence on density:

$$c(\rho) \sim \left[\frac{E(\rho)}{\rho}\right]^{1/2} \sim \rho^{\beta/2-1}. \tag{42}$$

Fig. 8 presents experimental findings of sound velocity with respect to density dependence in aerogels [100, 101].

The percolation cluster elasticity models discussed above evidently can be generalised. Broken bonds may have non-zero elasticity values differing from those attributed to intact bonds. In the limit, it is possible to consider a lattice with absolutely rigid intact bonds. A more detailed numerical analysis of the elastic properties of percolation clusters in the framework of such models and the comparison of its results with experimental findings have recently been reported in Ref. [102]. This study indicates that physical gels (i.e. gels composed of solid macroparticles) are well-described by the Webman–Kantor model [94] whereas chemical gels (polymers) are better described by the central force model. At the same time, experiments to measure the scaling of the oscillation spectrum of fractal materials by the neutron scattering technique as a rule give the ζ value at variance with that predicted by any of the above models.

It should be emphasised that the theory of elasticity as described in this section may serve as a basis for practical development of artificial materials with unusual oscillation properties.

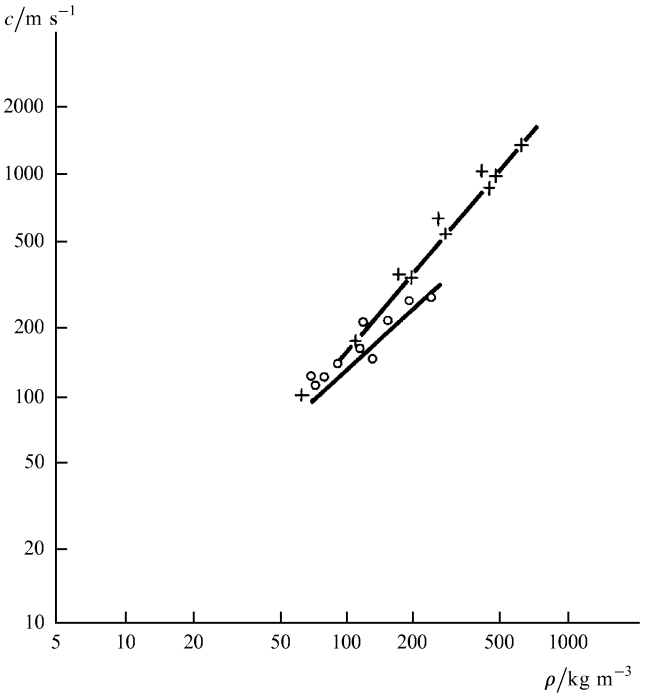

Figure 8. The relationship between sound velocity in aerogel and its density (o from Ref. [83], + from Ref. [84]). Slopes of the straight lines are in the range 0.8–1.3.

3.3.2 Nonlinear-elastic properties of fractal clusters. Nonlinear-elastic properties of fractals are poorly known except where fractal features of collapse are concerned. Extensive studies have recently been devoted to the latter case [103–105]. Nonlinear characteristics at weak deformation are important primarily for the understanding of nonlinear wave effects in fractal materials. It should be emphasised that nonlinear wave effects in fractals are due not only to nonlinear elasticity but also to fractal structure. The fact is that the spatial distribution of fractal oscillation amplitudes is not uniform. Therefore, locally, the square of the oscillation amplitude may significantly exceed the square of the average amplitude used for the evaluation of nonlinear effects in homogeneous models of nonuniform media [106]. The structure factor also influences the static nonlinear elasticity of fractals.

The simplest approach to studying nonlinear-elastic properties of fractals in the framework of lattice models may be based on the introduction of terms with higher powers of δu and $\delta\varphi$ in expressions (32) and (38). For the case of the central force model (neglecting $\delta\varphi$), this approach has recently been employed in Ref. [107] to simulate percolation on a flat triangular lattice. It has been shown in a study on elasticity moduli of the second and the third orders [107] that power-law dependence of the form (37) is also fulfilled, with the exponent $T' \approx 3.3 \pm 0.7$ for the second order modulus and $T' \approx 4.3 \pm 1$ for the third order one.

Nonlinear-elastic properties of fractal clusters may be equally apparent in the absence of nonlinearity. This is purely geometric bond nonlinearity similar to the Hertz nonlinearity of contacts in solid bodies. Webman analysed geometric nonlinearity for a model with elastic energy described by expression (38) on the assumption that the most important contribution was of single chains of bonds

[108]. In this case, geometric nonlinearity can be easily understood from the following example. Suppose that a spring with a large radius R is made of another spring with a smaller radius r rather than of wire. Then, the large spring has low rigidity, but when it is stretched to a straight line, its stiffness is determined by that of the smaller spring, i.e. by the degree of deformation. There is a continuous scale range of 'coils' in random fractal bond chains which results in the power-law dependence of rigidity on extension.

The following expression for the dependence of fractal chain rigidity K on extension F in excess of a threshold level $\tilde{F}$ was obtained in Ref. [108]:

$$K(F) \sim F^{(D+2)/(D+1)} , \tag{43}$$

where D is the lattice fractal dimension. The threshold $\tilde{F}$ depends on the cluster size as

$$\tilde{F} \sim l^{-(D+1)} .$$

For a percolation cluster with scale ξ of fractal behaviour decreasing with the distance from the threshold concentration p_c:

$$\xi \sim |p - p_c|^{-\nu} = \tau^{-\nu} ,$$

the threshold tension appears to grow whereas nonlinearity decreases at a given strain. The nonmonotonic dependence of the second-order relative nonlinear modulus on the intact bond concentration when it is significantly higher than the threshold one (as obtained in Ref. [107]) qualitatively corresponds to such nonlinear behaviour.

Nonlinear elastic properties of aerogels have been experimentally investigated in Ref. [101]. The above example of a spring is equally applicable to this case. This model turned out to be valid not only for spreading but also for compression, i.e. the hardness of undeformed aerogel was greater than that of the compressed one.

3.4 Eigenoscillations of fractal materials

Dispersion properties of oscillation states of fractal materials follow from expression (31) for the scale dependence of elastic moduli and from the power-law relation between the size and the mass of a fractal cluster fragment. Consider a fragment of a fractal cluster with size l. Its rigidity $K(l)$ (the force to displacement ratio) undergoes transformation on a change of scale by analogy with (31):

$$K(\lambda l) = \lambda^{-\zeta_E} K(l) . \tag{44}$$

The cluster mass, by definition of fractal dimension D, behaves as

$$M(\lambda l) = \lambda^D M(l) . \tag{45}$$

For the lowest eigenoscillation frequency of the cluster, it may be regarded as concentrated mass and elasticity. Then, it follows from Eqns (44) and (45) that the scale dependence of the oscillation frequency has the form

$$\omega(\lambda l) = \lambda^{-(\zeta_E+D)/2} \omega(l) . \tag{46}$$

Clearly, oscillation frequencies of a cluster with the characteristic scale (wavelength) l smaller than the cluster size show similar behaviour. Roughly speaking, the dispersion law for fractal oscillations has the form

$$\omega(k) \sim k^{(\zeta_E+D)/2} , \quad k \sim \frac{1}{l} , \tag{47}$$

which makes fractal oscillations significantly different from oscillations of continuous elastic media. Indeed, for ordinary media, the scale dependence of elastic moduli is absent, i.e. $\zeta_E = -d + 2$, and fractal dimension equals space dimension $D = d$ while Eqn (47) gives the known expression for acoustic phonons: $\omega(k) \sim k$. Density ν_{ph} of the phonon mode distribution by frequency below the Debye frequency for the case of a continuous medium is determined by space dimension d in the usual way, i.e. $\nu_{ph} \sim \omega^{d-1}$.

In the case of fractal materials, the situation is quite different. Suppose that $N(\omega)$ is the number of oscillation states with frequencies below ω. It follows from Eqn (46) that fragments of a cluster with size

$$l \sim \omega^{-2/(\zeta_E+D)} \tag{48}$$

participate in such oscillations without deformation; rather they shift as a whole. Then, the number of oscillation modes at frequencies below ω equals the number of such fragments in cluster N_F while the latter is explicitly described by relation

$$N_F \sim l^{-D} . \tag{49}$$

Expression (49) is nothing other than the definition of box fractal dimension. It follows from Eqns (48) and (49) that

$$N(\omega) \sim \omega^{2D/(\zeta_E+D)} . \tag{50}$$

The density of states is

$$\nu(\omega) \sim \omega^{2D/(\zeta_E+D)-1} = \omega^{d_f-1} , \tag{51}$$

where $d_f = 2D/(\zeta_E + D)$ is the spectral or fracton dimension.

It is worth noting that comparison of Eqns (51) and (24) establishes an explicit relationship between anomalous diffusion and geometric exponents for elastic moduli. However, this relation holds only for the isotropic model of elasticity forces and is obscure in a general case. It is in terms of the characteristics of random walks that the definition of fracton dimension is given in many published sources. It should be borne in mind that such a dimension is not always associated with the real fractal oscillation states.

It follows from relation (51) that d_f is totally determined by exponent ζ_E and the fractal cluster dimension. This relation is inherent in all models of fractal elastic behaviour, but different numerical values of d_f tend to characterise qualitatively different behaviour. Indeed, the density of states diverges at $d_f < 1$. This means [108] that a cluster loses stability with respect to thermal fluctuations provided its size is sufficiently large (i.e. the lowest mode frequency is small). At the same time, the density of states tends to zero at $d_f > 1$, precisely as it does in the case of ordinary materials. Exponents ζ_E reported in Refs [94, 108] as derived from the Eqn (38) model correspond to fracton dimensions below unity. In this case, there is divergence in the density of oscillation states in the low frequency range.

It is now well known that all eigenoscillation states of a fractal material in the fracton spectrum region are localised. This agrees with the general effect of wave localisation (frequently referred to as the Anderson localisation) in inhomogeneous media with the sole difference that inhomogeneities associated with the fractal structure are characterised by a wide range of scales and correlation at greater distances. This should probably make the problem of determining localisation conditions and the

spectrum of localised states on fractals much more difficult than the problem of localisation in a medium with non-correlated inhomogeneities. However, the intrinsic property of self-similarity of fractals considerably facilitates the solution of this problem.

Simple behaviour determined by crossover frequency and spectral dimension is inherent in elastic waves not only in fractal lattices but also in continuous inhomogeneous solids containing mixed portions with different elastic properties. Such a situation is the case for instance in solid bodies undergoing percolation phase transitions [109]. In this case, the fractal structure may appear in bound clusters of those portions of the medium which exhibit similar elasticity. Ref. [110] reports the fracton spectrum in an artificial longitudinally nonuniform waveguide for Lamb waves in which inhomogeneities display fractal distribution.

Generally speaking, the shape of localised wave functions in the case of strong localisation is determined by three scales, viz. wavelength, free path of the wave when scattered on inhomogeneities, and the localisation scale itself. Due to scale invariance of fractals for fracton wave functions, all these scales are identical and may be reduced to one for which frequency dependence is described by expression (47) [111]. The following model of the superlocalised wave function ψ is suggested for the wave function shape in Ref. [111]:

$$|\psi(r)| \sim l^{-D/2} \exp\left[-\left(\frac{r}{l}\right)^{d_s}\right], \tag{52}$$

where l is the frequency-dependent localisation length, D is the fractal dimension, and d_s is referred to as the superlocalised exponent. The frequency dependence of the localisation length is defined by expression (47). Taking into account Eqn (51) one obtains

$$l \sim \omega^{-d_f/D}. \tag{53}$$

The expression for the wave function in the form of (52) follows from the supposition of ordinary exponential dependence of the wave function on the internal length l_{in} on a fractal; for one-dimensional chains of bonds, exponent d_s is related to the exponent of anomalous diffusion in the following way:

$$d_s = 2 + \Theta = \frac{2D}{d_f},$$

where d_f is the fracton dimension estimated from the analogy of oscillations and diffusion of fractals. It is evident that in a general case, the last expression is not fulfilled. However, the fracton wave function model (52) is widely used for parametrisation of the results of experimental and numerical studies of localised states of fractals.

3.5 Experimental studies of fractons

It can be inferred from the above that computer models of fractal clusters allowed the solution of the problem of wave localisation in inhomogeneous media with fractal structure of inhomogeneities. The localisation condition is fulfilled if the wave frequency exceeds a certain threshold level, i.e. the frequency of crossover, which depends both on the maximum size of the fractal aggregates of which the medium is composed and the speed of longer waves. The density of localised states is the power-law function of frequency, with the exponent determined by fracton dimension. The spatial scale of localisation always shows power dependence on frequency, with the exponent equivalent to the ratio of spectral dimension to mass fractal dimension.

The objective of experimental studies is to verify these inferences with respect to real materials. First experimental evidence of the existence of a fracton region in the oscillation spectrum with localised states appears to have been obtained in Ref. [24] by the analysis of data on temperature dependence of heat conductivity and thermal capacity of amorphous solids. Specifically, these properties were examined in the temperature range of units to several tens of degrees Kelvin at oscillation frequencies 10^9–10^{12} Hz.

A rise in thermal capacity with temperature was found to be directly related to the frequency dependence of oscillation states. Analysis of the thermal capacity of epoxy resin performed in Ref. [24] demonstrated that the density of states is proportional to ω^2 for frequencies in the range of $h\omega/k_B < 8$ K (this is the normal phonon density of states) and to ω for the 8 K $< h\omega/k_B <$ 50 K range (this corresponds to the fracton spectrum with fracton dimension $d_f = 2$). Estimation of the respective maximal scale of fracton clusters yielded $\xi = 30$ Å. In Ref. [24], this scale was found to be related to the distance between cross-links formed by the hardener to connect the parent molecules of the epoxy resin. Increasing the amount of hardener may be expected to diminish the scale and raise the crossover frequency, in agreement with experimental findings.

Thermal conductance of solid dielectrics is attributable to heat transfer by a stream of phonons and is known to depend on both the thermal capacity of phonon gas and the length of the phonon free path. The length of the free path is restricted by the nonlinear interaction between phonons. In a crystalline solid body, heat conductivity at a temperature below several tens of degrees Kelvin grows due to a rise in thermal capacity of the phonon gas but thereafter drops precipitously as a result of excitation of high-frequency phonons and a decrease in their free path caused by enhanced nonlinear scattering on high-frequency phonons. The temperature dependence of heat conductivity in amorphous solids is strikingly different from that in crystals. Following a temperature rise of a few degrees Kelvin, heat conductivity attains a 'plateau' level and remains practically constant until the temperature rises further to several tens of degrees Kelvin. This causes heat conductivity to grow anew. Fig. 9 presents an example of temperature dependences of heat conductivity in crystalline quartz and quartz glass [112].

The presence of the plateau is easy to explain by the fact that thermal capacity over this temperature range grows due to the involvement of localised modes of the fracton region of the spectrum [24]. In other words, Ref. [24] indicates that data on heat conductivity and thermal capacity of amorphous solids can be understood on the assumption of the presence of a fracton portion of the oscillation spectrum and the localisation of fractons. It should be noted from the very beginning that this is not the sole possible explanation. The fractal structure of gels and polymers is not questioned and it is only natural to apply the theory of fractons to the analysis of their thermal properties. However, structural studies of glasses failed to reveal signs of fractality. A variety of models have been suggested to account for the thermal characteristics of glasses [30]. At present, it is universally accepted [2, 113]

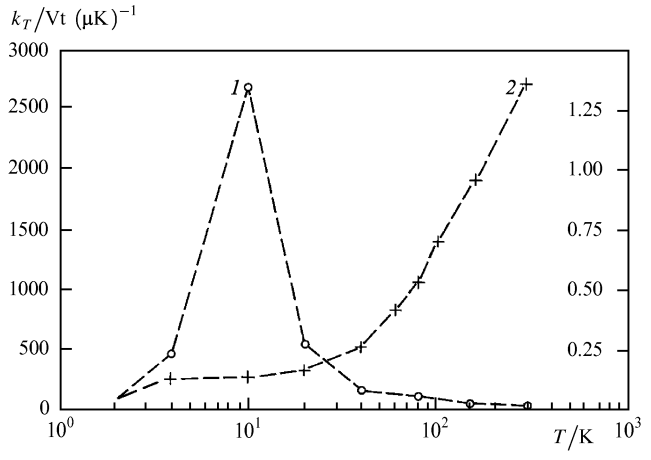

Figure 9. Temperature dependences of heat conductivity for crystalline quartz (curve *1*) and quartz glass (curve *2*). Data from tables of Ref. [112] were used. Experimental points are denoted by labels ∘ and +. The heat conductivity of glass is significantly lower than that of crystals which accounts for the different scales of the curves. Left and right-hand vertical axes give values for crystals and glass respectively.

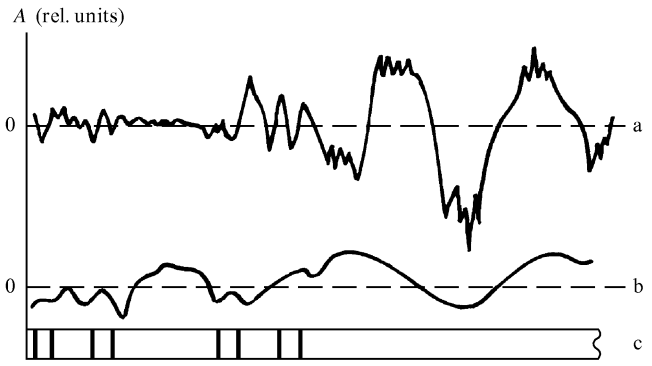

Figure 10. The shape of wave functions for the states of fracton (a) and phonon (b) regions of the eigenoscillation spectrum in a segment of one-dimensional waveguide with fractal distribution of inhomogeneities [110]. Oscillation modes are symmetrical; amplitudes are shown on half a specimen. The waveguide is ceramic with rubber interlayers. (c) Distribution of interlayers along the waveguide (black bars).

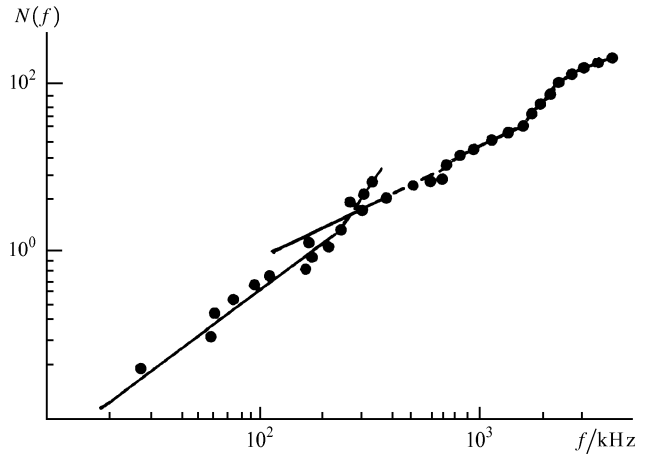

Figure 11. Integral frequency distribution of waveguide eigenoscillations (see Fig. 10) [110]. Points: experimentally determined values; solid lines: theoretical values.

that glasses also have a region in the oscillation spectrum which contains localised oscillations with scales of the order of ten interatomic distances. The appearance of such a region is believed to be due to the presence of the median order in the glass structure. In this context, the fracton model of oscillation spectra may be considered as a specific model of the median order structure of amorphous bodies which uses the fractal approach.

Direct measurements of the shape and the distribution density versus frequency of oscillation states have been made in a recent study on an artificial one-dimensional fractal structure [110]. This structure was a segment of a one-dimensional waveguide for Lamb waves made up of rubber and ceramic layers alternating along the direction of travelling waves. The centres of the rubber layers were located on a straight line as points of a self-similar fractal set, Cantor dust (Fig. 10). This set had fractal dimension 0.63 and was obtained in the following way. The segment was divided into three equal parts, the middle part was removed, and the remaining ones were again each divided into two. This procedure was repeated till the infinite number of steps resulted in a fractal set of points self-similar on all scales smaller than the initial length of the segment. The experiment described in Ref. [110] used the structure which was obtained after the above procedure was repeated 4 times. As a result, self-similarity was observable on scales greater than 3^{-4} of the initial length of the segment. The thickness of the rubber layer was less than this size and chosen in such a way as to ensure equality of distribution times in the thinnest layers of rubber and ceramics [110].

Measurements were performed in a frequency range of 10 kHz to 5 MHz. Oscillation patterns were estimated from the normal displacements of the waveguide surface using a laser vibrometer. Fig. 11 shows estimated and measured integral distribution of eigenoscillations by frequency. Fig. 10 presents measured oscillation forms corresponding to phonon and fracton regions of the spectrum respectively. Normally propagating modes were excited at low frequencies whereas the frequency of 200 kHz was associated with a sharp transition to fracton behaviour. Oscillations in this part of the spectrum became localised, and the measured spectral dimension was $d_f = 0.67$. A further rise in frequency (to circa 1.5 MHz) was accompanied by backward transition to the phonon density of states until in the end (at 2 MHz) it again conformed to the initial spectral dimension of 0.67. The occurrence of two crossover frequencies may be accounted for by the fact that artificial nonrandom structures do not exhibit self-similarity at any coefficient of scale transformation; rather, they possess the property of self-similarity only in case of a set of discrete coefficient values.

The very first experimental study of crossover from the phonon spectrum to the fracton one was reported in Ref. [114]. In this study, ultrasound propagation experiments were performed in the 1–20 MHz frequency range on sintered copper powder samples with powder diameters of 0.5 to 10 μm and occupied volume fraction from 0.3 to 0.6. Measurements were made of the variation with frequency of the ultrasonic attenuation in copper powder sinters. There was a rapid increase in attenuation at a certain frequency ω_c depending on the occupied volume

fraction f_c. The length of attenuation at the transition (crossover) frequency satisfied the scaling relation

$$l \sim (f - f_c)^{-\nu} ,$$

where exponent $\nu = 0.88$, similar to that for the correlation length in a percolation cluster, and f_c is the critical occupied volume fraction in the model based on percolation through a three-dimensional lattice of adjoining spheres [81]. The velocity of ultrasound also showed scaling dependence on the occupied volume fraction:

$$v \sim (f - f_c)^{T/2} ,$$

where exponent $T = 3.6$, in excellent agreement with the Webman model for elastic properties of fractals [94].

The maximum scale ξ in gels, polymers, and related materials which restricts the fractal behaviour region does not exceed the length of visible light waves. For this reason, the analysis of fracton spectra is most effectively performed by measuring Raman light scattering (RLS) spectra and inelastic incoherent neutron scattering (IINS) spectra.

With the IINS technique, the scattered neutron spectra obtained by either 'time-of-flight' spectrometry or the 'neutron spin echo' method provide information about the density of oscillation states. Because the neutron wavelength is of the order of interatomic distances, neutrons are independently scattered on nuclei. The differential section of neutron scattering into a single solid angle and a single energy interval $d\sigma$ is related to the density of oscillation states $\nu(\omega)$ by the following expression:

$$d\sigma = \frac{\sigma_{inc}}{4\pi} \frac{k'}{k} \frac{N}{4M} q^2 \exp\left(-\frac{1}{3} q^2 \langle u^2 \rangle\right) \frac{\nu(\omega)}{\omega} n(\omega) , \qquad (54)$$

where σ_{inc} is the section of incoherent neutron scattering on nuclei, k and k' are the wave vectors of incoming and scattered neutrons, $\boldsymbol{q} = \boldsymbol{k} - \boldsymbol{k}'$ is the scattering vector, N and M are the number and the mass of scattering nuclei respectively, $\langle u^2 \rangle$ is the mean quadratic displacement of nuclei, and $n(\omega)$ is the Bose factor

$$n(\omega) = \frac{1}{\exp(\hbar\omega / k_B T)} - 1 .$$

Expression (54) is feasible on the assumption of linearity and low amplitudes of nuclear oscillations compared with those of the neutron wavelength.

At least the scaling properties of oscillation spectra are possible to observe using expression (54) with a minimum number of a priori postulates pertaining to the scattering mechanism.

With RLS, the situation is far more complicated. Light undergoes scattering on polarisability fluctuations where its interference becomes of greater importance. Although a formula similar to (54) is fulfilled

$$I(\omega) \sim C(\omega)\, n(\omega)\, \nu(\omega) ,$$

the frequency dependence for factor $C(\omega)$ is largely determined by the shape of wave functions of oscillatory excitation and the mechanism of Raman scattering. In all likelihood, this dependence is of scaling nature for fractal materials even though more reliable data are needed to support this inference and the problem remains a matter of ongoing studies [115].

Generally speaking, the main outcome of experimental studies is that oscillation spectra of amorphous materials show singularities at frequencies corresponding to scale oscillations of the order of several intermolecular distances, in conflict with the postulate of totally chaotic distribution of molecules. The appearance of such singularities can be accounted for by the localisation of oscillations leading to the redistribution of the density of states and its shift to the low frequency region. In the case of amorphous materials with nonfractal structure of the nearest order, this results in the so-called boson peak in the density of oscillation states [2, 31, 113, 116]. This peak reflects the distribution of localisation scales near a certain mean scale. Such localised states have no self-similar structure and may be found in glasses and molecular amorphics.

Localisation for materials with the structure of 'mass fractals' coincides with the self-similarity interval of the structure. In this case, the boson peak is replaced by the power-law density of states with the exponent determined by spectral dimension. (True, experiments have been reported which indicate a similar structure in glasses [117] and the amorphous phase of liquid crystals [31]).

Early studies on the structure of oscillatory states in fractal materials dealt with silica gels [118, 119]. A direct analysis of the spectrum of multiple scattering was reported in Ref. [118] for the fracton frequency range of 600 to 5400 GHz. The authors used hard gel (1.7 g cm^{-3}) with the properties of a polymer rather than composed of macroscopic particles. They obtained the following form of the power-like spectrum:

$$I(\omega) \sim \omega^{\mu} .$$

The frequency dependence of factor $C(\omega)$ is assessed in Ref. [118] on the assumption of incoherent summation of waves scattered in each point of the medium. For scattering with frequency shift ω, intensities of scattered waves are summed over volume $l(\omega) = \omega^{-\tilde{d}/D}$ filled by the superlocalised fracton wave function. Finally, expression $C(\omega) \sim \omega^{\alpha}$ for the factor $C(\omega)$ is obtained where the exponent $\alpha = 2\tilde{d}d_f/D - \tilde{d}$. This expression is most probably invalid because summation over volume for each fracton must be performed for the dissipation amplitude and followed by the summation of light intensities scattered by different fractons [120] This and the assumption of the superlocalised form (52) for the fracton wave function gives exponent $\alpha = 2\tilde{d}d_f/D - 1$ [120]. For this reason, estimates of spectral dimension as reported in Ref. [118] may be questioned†. Nevertheless, the presence of the scaling component in the scattering spectrum was reported on the frequency interval of about a decade [101].

The Mandelstamm–Brillouin dissipation spectra in aerogels with the density of 103 to 407 kg m^{-3} were analysed in Ref. [119]. The dependence of the frequency shift of scattered light on the dispersion angle leads to the dispersion relation for phonons. Experimental findings reported in Ref. [119] are fairly well described by the following formula:

$$\omega = \frac{2v_l}{\pi l} \sin \frac{\pi k l}{2} ,$$

†The use of incoherent summation in Ref. [118] allowed experimental findings to be used to estimate spectral dimension which proved coincident with the value of 4/3, in agreement with the hypothesis of the universal character of spectral dimension widely accepted at that time.

Table. Results of experimental fracton studies

Object	Method	D	Frequency range/Hz	ω_c/GHz	ξ/nm	ω/GHz‡	d_f	ζ_E	Reference
Smoke SiO_2 particles	IINS time-of-flight	2.5	$2.4\times10^{10}-2.4\times10^{12}$	48	30 (4 nm particles)	480	1.8 2.1	0.27 −0.11	[122]
Epoxy resin	IINS	—	$3\times10^{11}-1.9\times10^{12}$	600	2	—	1.5	—	[121]
SiO_2 aerogel	IINS	2.4	$<10^9-2.5\times10^{11}$	1	11	250	1.3	1.29	[124]
	time-of-flight	2.2		10			2.1	−0.1	
				0.8	7		0.9	2.68	
	spin echo			3			1.7	0.51	
SiO_2 in different chemical structures	IINS	2.4	$10^{11}-10^{13}$	600	0.16†	—	1.54	0.72	[125]
	spin echo	2.9		240	0.15	—	1.7	0.51	
		2.5		1300	0.19	—	1.22	1.6	
SiO_2 aerogel	IINS	2.2	$>2\times10^{10}$	5.0 ± 1.2	0.12†	—	1.45	0.83	[126]
		1.9		10.7 ± 2	0.16	—	1.69	0.35	
		2.2		>17	0.25	—	—		
PMMA film	IINS	2–2.2	$2.4\times10^{11}-2.4\times10^{12}$	~480	3	2400	1.8 —	0.23 —	[120]
massive deuterated							1.65	0.45	

†Density values (g cm^{-3}).
‡The upper limit of the scaling part of fracton density.

where length l and sound velocity v_l are related to density ρ through the scaling relation

$$l\sim\rho^{-z},\qquad v_l\sim\rho^{x}$$

with exponents $z\approx1.57$ and $x=1.397$. This result may be interpreted in terms of localised oscillations with scales smaller than l. Independent estimates of aerogel fractal dimension $D=2.364$ yield the z value coincident with the measured one whereas the use of relations like (41) and (51) enabled the authors of Ref. [119] to determine spectral dimension $d_f=1.252$. Here, the exponent ζ_E was found to be 2.41, an intermediate value between the isotropic force model and the model in Ref. [94].

More direct estimates of the fracton region of oscillation spectrum were obtained by different methods using aerogels and polymers in Refs [120–126]. The IINS technique was employed in Refs [121, 122, 125, 126], RLS in Ref. [123], and both methods together in Refs [120, 124]. All these sources report the power-law component of oscillation states about a decade wide. The exponent differs (being smaller) from the phonon density spectrum and there is a transition (crossover) from one type of behaviour to another at a certain frequency. Fractons in polymers were studied in Refs [120, 121, 125]. The crossover frequency was found to be around 100 GHz and corresponded to scale $\xi\approx20-30$ Å. Other authors used SiO_2 aerogels and revealed a crossover frequency of 1 to 10 GHz corresponding to scale $\xi\approx100-1000$ Å. The upper frequency in the fracton region of aerogels was shown to be dependent on the size of constituent particles in the aggregate and approximately equivalent to the first longitudinal resonance of elastic oscillations of equally-sized quartz particles.

Thus, the structure of the oscillation spectrum of fractal materials is qualitatively confirmed in experiments on light scattering and IINS. Spectral dimensions and the corresponding exponents ζ_E obtained by the IINS method in different studies are listed in the table above. It is clear that as a rule the results fail to show quantitative correspondence to any model of fractal elastic properties. The discrepancy arises for several reasons. First, according to Ref. [122], it may be anticipated that expression (54) is inapplicable to the IINS section because of pronounced anharmonicity of oscillations in the fracton region. Different values of spectral dimension (see the Table) have been obtained in Ref. [122] for different temperatures, i.e. $d_f=1.8$ at 136 K and $d_f=2.1$ at 265 K. The authors of the study reported in Ref. [124] failed to notice a temperature dependence of spectral dimension but revealed its dependence on the wave scattering vector q. Based on the analysis of data obtained with significantly different scattering vectors, the authors of Ref. [124] postulated the presence of oscillations in aerogels governed by different types of elastic forces. At low frequencies associated with smaller spectral dimensions and higher amplitides of oscillation displacements, a major contribution to the IINS spectrum was provided by oscillations with elastic forces, described by the Webman model [94]. At high frequencies where displacements were smaller and spectral dimensions higher, the greatest contribution was made by oscillations with central elastic forces. On the whole, the IINS spectrum must be described by the sum of contributions of the form of Eqn (54) with different average quadratic displacements and form of density of states. It is also worth noting that according to Ref. [124], the products of wave scattering vectors and the displacements are not very small (a few tenths) and, strictly speaking, formula (54) cannot be satisfied because it does not take into account terms of the second order in nuclear oscillation displacements.

To sum up, the fracton spectrum data obtained by the IINS method only qualitatively support the theory of elasticity for fractal materials. It was shown above that the same refers to the RLS method.

3.6 Numerical fracton studies

As a rule, numerical studies consider equations in the form of Eqn (18) on a percolation cluster [51, 89, 127–130]. It is worthwhile to note that in spite of the simple structure of Eqn (18), numerical study of it is by no means a simple task because an investigation into fracton properties, especially fracton density of states, on random fractal lattices requires a large number of lattice nodes to be considered. At the same time, the dimension of the problem of eigenvalues is equivalent to the number of particles. The problem of eigenvalues with a dimension of several tens of thousands is very difficult to solve even if up-to-date computers are used. For this reason, a roundabout approach is normally used [128, 129] notwithstanding several works reporting direct diagonalisation of the operator matrix in Eqn (18) [130, 51].

Numerical studies confirm the crossover from of the phonon spectrum to the fracton one. The power-law form of the density of states has been verified in a frequency range of at least two decades and the spectral dimension proved to be 4/3, in agreement with the prediction in Ref. [25] for Eqn (18) on a percolation cluster. State localisation of the fracton spectrum in the form of Eqn (52) may be just as well obtained in numerical studies although concrete values of the superlocalised exponent vary in different papers. For example, a high value of the superlocalised exponent $d_s = 2.3$ has been obtained in Ref. [127] whereas superlocalisation was altogether absent in Refs [128, 129]; herein $d_s = 1$. The reason for this is most likely to be that the amplitude of localised wave functions on random fractals is characterised by a highly nonuniform and random distribution within the localisation radius (see Figs 5 and 6). Therefore, different methods used in Refs [128–130] to evaluate its mean distribution in space might give different results. Form (52) for the wave function appears to have the sense of a certain averaged quantity. This problem was partly clarified in Ref. [51] where intermittency of the wave function amplitude in space was investigated. This work demonstrated that the square of the fracton wave function amplitude on a percolation cluster had a multifractal distribution. Therefore, evaluation of the moments of different order may yield different values of the superlocalisation exponent. Also, Ref. [72] reports the presence of molecular states on both percolation clusters and regular fractals (see Section 3.2).

3.7 Nonlinear phonon interactions with fractons and thermal conductivity of amorphous bodies

It has already been mentioned that the temperature dependence of heat conductivity of amorphous bodies is strikingly different from that of crystals. This difference can be accounted for by the presence of the plateau several tens of kelvins wide and the growth of thermal conductivity above the plateau with a rise of temperature (see Fig. 9). The plateau temperature range precisely corresponds to excitation of a region of the localised oscillation spectrum. This is equally true of both fractal materials and glasses.

The arguments that follow are not restricted to the fracton oscillation spectrum but are also applicable to the explanation of temperature dependence of thermal conductivity of any amorphous material [29]. However, it was the theory of fractons that served as a basis for the better understanding of the heat conductance mechanism in amorphous bodies.

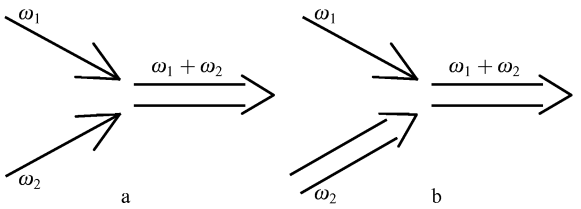

Figure 12. Diagrammatic representation of nonlinear interaction between phonons (→) and fractons (⇒). (a) Two phonons give rise to a fracton of summed frequency. (b) A phonon is absorbed by a fracton which results in fracton formation with summed frequency [26].

The presence of the plateau is easy to explain by taking into account the fact that that localised states (referred to as fractons below) (1) do not participate in heat transfer and (2) effectively restrict the length of the phonons' free path. The fact is that, due to localisation of oscillations, the possibility for nonlinear interactions between fractons and phonons to take place is not limited to the conditions of spatial synchronism. A phonon is scattered on a fracton serving in the capacity of a compact scatterer. In a quadratic approximation, processes of two types are conceivable [26]: those involving two phonons and one fracton (two phonons give rise to a fracton with a generalised frequency) and processes in which only two fractons participate (a phonon is absorbed by a fracton with a change in the former's frequency) (Fig. 12). Both processes restrict the length of the phonon free path, and the latter is responsible for the rise in heat conductivity above the plateau level. The following mechanism for the heat conductivity growth has been suggested in [26]. Interaction with phonons by the second mechanism results in energy dissipation over various localised states accompanied by its transfer in space. Excitation of an increasingly number of fractons with rising temperature leads to a rise in heat conductivity above the plateau. The authors of Ref. [27] made an accurate calculation of the temperature dependence of heat conductivity taking into account interactions between fractons and phonons. Matrix elements of these interactions were estimated in Ref. [27] using the expression for the fracton wave function in the form of Eqn (52). The results of the calculation were expressed in directly measurable variables and found to be in perfect agreement with experimental data. It was demonstrated in Ref. [29] that there is no need to use a specific expression for the wave function of localised states and their spectral density. It proves sufficient to assume localisation of oscillations with the frequency exceeding a certain crossover frequency.

Peculiar features of the nonlinear fracton/phonon interactions can be manifested in a variety of ways not necessarily associated with thermal properties of amorphous bodies. The absence of the requirement for spatial synchronism is in itself unusual in traditional nonlinear acoustics and there may be interesting possibilities for its application. An example of a study in this field may be found in Ref. [131] where the nonlinear interaction between fractons and phonons was investigated in the system previously surveyed in Ref. [110] (see Section 3.5). It was experimentally found in Ref. [131] that the threshold parametric generation in such a system was 5–7 times lower than in either a uniform or a periodically nonuni-

form waveguide. The initial frequency lay in the fracton range, and the oscillation mode was parametrically excited in the phonon region of the spectrum. Wave functions participating in mode interactions are shown in Fig. 10. Analysis made in Ref. [131] demonstrated that a decrease in the threshold parametric generation in a fractal system was attributable to the existence near the half-frequency of modes with overlap integrals between wave functions of interacting modes that are higher than overlap integrals in the case of a homogeneous or periodically inhomogeneous waveguide.

3.8 Fluctuations of elastic properties in a homogeneous fractal

It has been shown in the foregoing review that in such materials as homogeneous fractals, elastic moduli and hence the elastic wave distribution rate on large scales are determined by the scale dependent elastic moduli of the fractal clusters of which the material is composed. Because cluster formation is a random process, it is clear that both the cluster size and the elastic characteristics of the material must undergo random fluctuations in space. To our knowledge, there have been no comprehensive studies on cluster size fluctuations in gels. As for percolation clusters near the percolation threshold, it is known that they possess the so-called *super-lacunarity* property [9]. The number of nodes S in a cluster of size L is defined by expression

$$S \sim L^D ,$$

and its dispersion has the form of $\langle S^2 \rangle - \langle S \rangle^2 \sim L^{2D}$, i.e. relative fluctuations near the transition point do not decrease with increasing cluster size.

This property plays an important role in seismoacoustics. A model has been suggested in which the growth of strain in rocks leading to earthquakes is assumed to be analogous to percolation transition. Increased concentration of isolated consolidation foci in the rock leads to the formation of clusters of increasing size which eventually results in percolation transition and a subsequent growth of the scale of a strain focus [52]. Sound velocity fluctuations in inhomogeneous media with such percolation transition have been investigated in Ref. [132]. It has been shown using the model of quasidimensional chains that fluctuations of sound velocity c display critical behaviour and unlimited growth near the transition point:

$$\frac{\langle \delta c^2 \rangle}{\langle c \rangle^2} \sim (p - p_c)^{-x} .$$

Exponent x is expressed in terms of the lattice dimension d and the critical index ν of the transition as

$$x = d\nu - 1 .$$

On the whole, the nature of fluctuations of elastic properties of fractal materials is poorly understood, and we did not find another study dedicated to this problem.

4. Wave emission and scattering by fractal-like structures

The properties of the fracton region in the elastic oscillation spectrum pertain either to small scales (several tens of Angstroms) in real materials or to artificial fractal structures. Peculiar features of wave emission or scattering by fractal objects can become manifest under natural conditions and in the macroscopic scale region. The fractal structure is intrinsic in the distribution of eddies and impurities in a turbulent flow [18, 74], the sea surface [45], front percolation through a random porous fluid medium [83], and regions of concentrated strain in geologic rocks [52]. The fractal properties of soot particles have a marked effect on both absorption and scattering of light in the atmosphere. One and the same particulate mass causes low-level scattering and absorption in a compact cluster and much greater scattering and absorption sections in a fractal one [133]. The most conspicuous manifestations of fractality during wave scattering have been reported in the case of multiple scattering [36, 37] although its selected features are apparent even in a single scattering episode.

4.1 Wave scattering by fractal surfaces

Angular distribution of wave intensity during scattering by a large-scale smooth irregular surface is determined by the surface slope distribution. The fractal surface is not subject to differentiation and has no well-defined slope. Moreover, fractality suggests the existence of irregularities on all scales including some that exceed the length of the wave being scattered. Therefore, neither the tangential plane approximation nor the low excitation method is applicable to the evaluation of the scattered field. There is no acceptable rationale for a general solution of the problem. The very first work in this field, Ref. [33], used the phase screen approximation; in other words, it examined diffraction of a wave that passed through a thin phase screen with the optical width distribution $kh(x)$ rather than undertook to solve the problem of wave scattering on a rough surface $h(x)$.

In the Fresnel approximation, the applicability of which is confirmed by computation, the expression for the wave amplitude ψ at distance z from the phase screen has the form

$$\psi(x, z) = \exp\left[i\left(kz - \frac{\pi}{4}\right)\right]\left(\frac{k}{2\pi z}\right)^{1/2} \times \int_{-\infty}^{\infty} dx' \exp\left\{\frac{ik}{2z}\left[2h(x')z - (x - x')^2\right]\right\} . \quad (55)$$

Here, k is the wave number and x is the coordinate directed along the surface.

The study in Ref. [33] considered a surface with one-dimensional irregularity having the structure of a Gaussian fractal (the plot of generalised Brownian motion) with the structure function in the form of Eqn (6). Because such a surface is self-affine rather than self-similar, it is possible to derive a characteristic scale as follows:

$$\left\langle \left[h(x + L) - h(x)\right]^2 \right\rangle = L^2 . \quad (56)$$

Loosely speaking, scale L (sometimes called topothesy) is the distance at which surface slopes $(\Delta h/\Delta x)$ tend to unity. In terms of topothesy, the structure function (6) may be rewritten as

$$\left\langle \left[h(\xi + x) - h(\xi)\right]^2 \right\rangle = L^{2(1-H)} x^{2H} . \quad (57)$$

It follows from expression (57) that at $L < x$ the slopes are smaller than unity $(0 < H < 1)$ whereas at $L > x$, they exceed unity.

The Gaussian distribution $h(x)$ permits simple calculation of the amplitude correlation function [33]:

$$R(x) = \langle \psi(\xi, z)\, \psi^*(x+\xi, z) \rangle = \exp\left[-\frac{1}{2} k^2 L^{2(1-H)} |x|^{2H} \right] . \quad (58)$$

Angular distribution of wave intensity is defined by the Fourier transformation of the correlation function (58):

$$I(\sin\theta) = \int R(x) \exp(\mathrm{i}\kappa x)\, \mathrm{d}x = \frac{1}{k} \int \mathrm{d}x' \exp\left[-\frac{1}{2} (kL)^{2(1-H)} x'^{2H} - \mathrm{i}x' \sin\theta \right] , \quad (59)$$

where $\kappa = k \sin\theta$. The last equation in (59) is obtained by the substitution $x' = kx$. It is worthwhile to note that the angular distribution of intensity as a function of $\sin\theta$ formally coincides with the density of the Levy-type stable distribution with parameter $\alpha = 2H$ [79] (see Section 2.3.1). At large angles, distribution (59) decreases with increasing angle as $(\sin\theta)^{-2H-1}$; at smaller angles, the intensity is relatively stable. The exponent in the angular dependence can be expressed through the fractal surface dimension $-2H - 1 = 2D - 5$. The angle separating these extreme cases is easy to determine from Eqn (59). It is specified by an explicit condition

$$(kL)^{-(1-H)/H} \sin\theta \sim 1 . \quad (60)$$

Interpretation of the latter condition is simple. Since exponent H does not exceed unity, the angle that limits the region of constancy of angular distribution increases with growing kL, i.e. as the wavelength decreases with respect to topothesy. Such behaviour corresponds, according to Eqn (57), to an increase in the surface slope with decreasing scale of the surface under examination, which corresponds to a decrease in the incident wavelength.

The fractal surface is intermediate between an ordinary smooth surface and a distribution of mass in a volume. Therefore, another feasible approach to the evaluation of scattering characteristics on the fractal surface is based on the theory of volume wave scattering [34].

4.2 Single scattering on fractals and the Fourier transformation of fractals

The angular dependence of the intensity of single scattering on inhomogeneities of the refractive index is defined by the known expression

$$I(q) \sim \int \langle \varepsilon(\boldsymbol{r})\, \varepsilon(\boldsymbol{r}+\boldsymbol{r}') \rangle \exp(-\mathrm{i}\boldsymbol{q}\cdot\boldsymbol{r}')\, \mathrm{d}V , \quad (61)$$

where the scattering vector $|\boldsymbol{q}|$ is determined by the scattering angle θ and the incident wavelength λ

$$|\boldsymbol{q}| = \frac{4\pi}{\lambda} \sin\frac{\theta}{2} ,$$

while the correlation function of the refractive index fluctuations is proportional to that of the cluster density:

$$\langle \varepsilon(\boldsymbol{r})\, \varepsilon(\boldsymbol{r}+\boldsymbol{r}') \rangle \sim \langle \rho(\boldsymbol{r})\, \rho(\boldsymbol{r}+\boldsymbol{r}') \rangle ,$$

which, in the case of fractal clusters, is directly defined by its fractal dimension D:

$$\langle \rho(\boldsymbol{r})\, \rho(\boldsymbol{r}+\boldsymbol{r}') \rangle \sim |r'|^{D-d} , \quad (62)$$

where d is the embedding space dimension. It follows from expressions (61) and (62) that for the angular dependence of scattering intensity

$$I(q) \sim q^{-D} ; \quad (63)$$

$I(q)$ is the scattering intensity into a single solid angle at an angle θ to the direction of the incident wave.

Naturally, for real fractals, relation (62) is fulfilled in a limited scale range $a_0 < r' < \xi$; accordingly, relation (63) is fulfilled for $1/\xi < q < 1/a_0$. The angular dependence $I(q)$ is more exactly expressed as the product of form factor $F(q)$ and structure factor $S(q)$: $I = FS$ [134]. The form factor corresponds to angular dependence of the intensity in scattering on individual elements, i.e. particles which produce a fractal cluster when they stick together upon contact. The form factor turns to zero at $q \to 1/a_0$ whereas the structure factor has the form $S(q) \sim q^{-D}$. At $q \ll 1/a_0$, the form factor is approximately constant, and expression (63) is obtained for scattering intensity.

Generally speaking, the angular dependence characterised by expression (63) is not a specific property of scattering on fractal objects. A similar angular dependence may be associated with singularities of dielectric permittivity randomly and independently located in points r_i in the form [135]:

$$\varepsilon(\boldsymbol{r} - \boldsymbol{r}_i) = \varepsilon_0 (\boldsymbol{r} - \boldsymbol{r}_i)^{\alpha} . \quad (64)$$

The angular dependence of scattering intensity on each diffusor has the form

$$I_i(q) \sim q^{-2(\alpha+d)} .$$

This expression also holds for the envelope of angular dependence of scattering intensity on a randomly located set of scatterers. It is clear that such a set is not necessarily fractal for the simple reason that the Poisson law of distribution over space implies the presence of a scale that disturbs scale invariance and is determined by the average difference between the scatterers. The angular dependence of each individual member of a set of scatterers is broken as a result of random interference of the fields of isolated scatterers. The same refers to scatterers in the form of Eqn (64) and also to scattering on fractals. In such cases, the differences may be expected to appear in the fine structure of angular dependence relations. A comprehensive formulation of these differences remains to be developed. In Ref. [134], Fourier transformation of regular fractals has been studied. It has been demonstrated that the fine structure of angular dependence is scale-invariant with respect to extension along axis q. In other words, the angular dependence is subject to the relation

$$S(\gamma q) = \gamma^{-D} S(q) ,$$

while expression (63) is satisfied for the angular dependence $\langle S(q) \rangle \sim q^{-D}$ averaged in certain intervals of q values. At the same time, for random scales, the scale invariance of the fine structure is likely to have statistical sense.

It should be emphasised that for a set of scatterers in the form of Eqn (64), there is a power-law form (63) of the angular dependence of scattering for each individual scatterer. In contrast, in the case of scattering on fractals, the dependence (63) occurs as a result of interference of the fields scattered on the particles of which the cluster is composed. The correlation is especially pronounced as

regards characteristics of multiple scattering on fractals and will be discussed in the following section.

Another example of scattering on a nonfractal object with angular dependence of intensity Eqn (63) is provided by the case where the scatterer contains pores or particles with the power-law size distribution [136]. If the pore or particle size distribution $P(r)$ in scale ranges comparable with the scattered wavelength has the form $P(r) \sim r^{-\gamma}$, the angular dependence of intensity I is also described by the power law $I(q) = q^{-x}$ with the exponent $x = 7 - \gamma$.

The relationship between angular dependence and fractal dimension during scattering on a fractal object differs from Eqn (63) when the scatterer has a fractal surface. Suppose that the surface separates bodies with similar refractive indices, unlike the situation considered in the previous section. Then, expressions (61) and (62) may be used to evaluate the angular dependence of scattering. However, the relationship between the density correlation function and the fractal structure in this case will be different from that in the mass fractal case.

Let us estimate the mean probability of finding a filled volume at a distance r from the occupied point for a body with a fractal surface of dimension D. It may be expressed as a sum of a distance-independent part for the points located at a distance larger than r from the surface and a distance-dependent part for the points near the surface. The volume filled up by the latter points can be estimated in terms of the volume V_s of the covering of the r-sized cube surface. It follows from the definition of fractal dimension that $V_s = N_0 r^{3-D}$, where N_0 is a constant. If $p(r, x)$ is the probability of finding a particle at distance r from another particle situated at distance $x < r$ from the surface, averaging this probability over r gives the following expression for the correlation sought [34]:

$$C(r) = \frac{V - V_s}{V} + \frac{V_s}{V}\frac{1}{r}\int_0^r p(r, x)\,\mathrm{d}x \ . \tag{65}$$

The average from $p(r, x)$ must not depend on r. Therefore

$$C(r) = 1 - \text{const} \times r^{3-D} \ .$$

Substitution of this expression into Eqn (61) yields the angular dependence of scattering intensity in the form $I(q) = q^{-(6-D)}$.

For surface fractal dimension lying in the range of 2–3, the angular dependence exponent is in the range 3–4 which does not overlap the range 0–3 of the exponent for mass fractals. Therefore, these situations are easy to distinguish in experiments.

4.3 Multiple scattering on fractals

Specific features of multiple scattering on fractals can be accounted for by a slowly decreasing correlation of particle density and its theoretical analysis is based on the property of self-dependence. Fractal effects in multiple scattering are apparent even when it occurs on fractal clusters with size smaller than the wavelength [36]. This can be accounted for by the effect of correlation of particle positions in the cluster on fields imposed upon isolated particles on rescattering of an incident wave by other cluster particles.

Suppose that a wave with the amplitude φ^0 falls on a set of scatterers situated in a space region which is compact with respect to the wavelength. In this case, for a set of responses of individual scatterers x_i (e.g. dipole moments, amplitude of volume fluctuations for monopoles, etc. depending on the nature of both the waves and the scatterers), the following system of equations may be written which takes into account interactions between scatterers:

$$x_i = \chi_0 \varphi_i^0 + \chi_0 \sum_{i \neq j} f(\boldsymbol{r}_{ij}) x_j \ , \tag{66}$$

where χ_0 is the frequency-dependent coefficient of the scatterer response to the external field, $f(\boldsymbol{r}_{ij})$ is the function of radius vector $\boldsymbol{r}_{ij}$ connecting the ith and the jth scatterers. This function determines the field imposed by one scatterer on another ($f \sim 1/r_{ij}$ for monopoles; in the case of dipoles, x_i are the vectors and f is the tensor function $\sim 1/r_{ij}^3$). Eqn (66) may be written in the matrix form $\boldsymbol{x} = \chi_0 \varphi^0 + \chi_0 \boldsymbol{W}\boldsymbol{x}$. For a compacted cluster, matrix $\boldsymbol{W}$ is really a symmetric matrix diagonalisable by means of orthogonal transformation in the form of

$$\boldsymbol{U}\boldsymbol{W}\boldsymbol{U}^{\mathrm{T}} = \mathrm{diag}(w_n), \quad \boldsymbol{U}\boldsymbol{U}^{\mathrm{T}} = 1 \ .$$

Then, the solution of Eqn (66) has the form

$$\boldsymbol{x} = \boldsymbol{U}^{\mathrm{T}}\,\mathrm{diag}\left(\frac{1}{z - w_n}\right)\boldsymbol{U}\varphi^0 \ , \tag{67}$$

or

$$x_i = \sum_{n,j} u_i^n u_j^n (z - w_n)^{-1} \varphi_j^0 \ ,$$

where u_i^n are the components of eigenvectors corresponding to eigenvalues w_n and $z = \Delta + \mathrm{i}\delta = \chi_0^{-1}$ is the variable inverted with respect to the response of an individual scatterer. For a resonant diffusor, Δ corresponds to withdrawal from the resonant frequency and δ to the inverse resonance quality. If an isolated particle ($\Delta \gg \delta$) is far from the resonance, Eqn (67) gives the following expression for the imaginary component of the averaged response (polarisability) of a particle in a cluster:

$$\mathrm{Im}\,\chi(\Delta) \sim \left\langle \frac{1}{N}\sum_n u_i^n u_j^n \delta(\Delta - w_n) \right\rangle \ . \tag{68}$$

This means that the frequency dependence of the response is determined by the distribution of eigenvalues of matrix $\boldsymbol{W}$. Since functions $f(\boldsymbol{r})$ rapidly decrease with growing distance, the matrix $\boldsymbol{W}$ structure for a fractal cluster resembles the structure of the operator matrix from Eqn (18) for elastic oscillations. The distribution of eigenvalues of this operator has the form of a power law which is determined by spectral dimension. It may be supposed that a similar situation also takes place in the case in question. And this is really true. The study [36] dealt with polarisability and absorption of a fractal cluster composed of monomers with the dipole–dipole interaction on optical frequencies. The authors obtained the power law form of the distribution of eigenvalues $\nu(\omega)$ and of the proportional to imaginary component of the cluster's response to relative tuning Δ of the incident wave frequency away from the resonant frequency of an individual particle:

$$\mathrm{Im}\,\chi(\Delta) = \frac{\pi}{3}\nu(\Delta) \sim \Delta^{d_0 - 1} \ , \tag{69}$$

where d_0 is an analogue of spectral dimension referred to in [36] as optical spectral dimension. Ref. [36] reports the numerical value of d_0 which lies in the range of 0.3–0.6. In

other words, the frequency dependence of the particle's response in a cluster is altogether different from the resonance curve for an isolated particle in that absorption of an incident wave remains high at a large distance from the resonance where it but slowly decreases with further detuning of resonant frequency, in accordance with the power law. In such a case, eigenvectors of u^n correspond to the collective excited states of particles (fracton analogues) in the cluster. Their spatial volume exhibits power-law dependence on the degree of withdrawal $l \sim \Delta^{\alpha}$. However, the exponent α is related to optical spectral dimension in a different way compared with the exponent in the dispersion relation for fractons (53). Ref. [36] reports the following relation: $\alpha = d_0 - 1/(3 - D)$.

The most interesting result of multiple scattering on fractal clusters is the enhanced local field fluctuation observed in Ref. [36]. Eqns (67) and (69) give the following expression for the magnification of the field square averaged over cluster particles:

$$G = \frac{\langle |\varphi_i|^2 \rangle}{|\varphi^0|^2} \sim \frac{1}{\delta} |\Delta|^{d_0+1} . \tag{70}$$

This is a high value for large degrees of relative detuning which may result in a significant increase in nonlinear effects during the interaction between an incoming wave and a cluster. This observation agrees with experimental findings pertinent to photomodification† of fractal clusters at intensities of light falling below the threshold level. In this case, the effect is caused by enhanced local fluctuations of the field. Evidently, this increment is a universal wave effect which is certain to have the most conspicuous manifestation in nonlinear interactions between waves of different nature.

The analogy of collective excitations of particles during multiple wave scattering on a compact fractal cluster can be accounted for by the fact that phase shifts in Eqn (66) are neglected when particle fields affecting a given particle are considered. When the phase is taken into account, matrix $\boldsymbol{W}$ becomes complex and even loses the property of self-coupling which makes the problem far more complicated and difficult to solve. The diagrammatic technique developed in Ref. [137] has been used in Ref. [37] to examine multiple scattering by a fractal cluster of metal particles with dipole surface resonance. Scattering was analysed taking into consideration phase shifts. Calculations were made with due regard for correlation of the particles' positions in the cluster in order to enhance the probability of constructive interference of waves scattered over different channels and the appearance of a similar effect of strong local field fluctuations. The study [37] demonstrated the existence of a critical cluster fractal dimension 3/2, such that clusters of lower dimension underwent a huge increase in the scattering section. In Ref. [37], this effect was termed visibility–invisibility phase transition. However, the authors did not offer any qualitative interpretation of such a sharp transition. Clearly, correlation of the particles' positions grows with falling fractal dimension although this growth is quite smooth. The cause behind the appearance of the transition at fractal dimension $D = 3/2$ can probably be understood from the following considerations. A cluster of size r contains r^D particles and $\sim r^{2D}$ corresponding radius vectors which connect the particles in pairs. These vectors originate from one point and occupy a region of size $\sim r$. At $D > 3/2$, the number of radius vectors grows faster than the cube of the size; actually, they may be considered to occupy the whole region. The situation is qualitatively different at $D < 3/2$ since the number of vectors grows more slowly than the volume, and they occupy zero volume at large r. Assuming multiple scattering to be the ray walking from one particle to another, the case of $D < 3/2$ is reflected in marked restriction of possible walk steps (possible steps occupy a set of zero measure). Obviously, this leads to a sharp increase in the possibility of constructive interference of beams that have covered different distances.

The problem of scattering on fractal particles is solved in Ref. [133] with regard to multiple scattering but in the self-coordinated field approximation. Fractality is taken into consideration by means of the power-law alteration of density with increasing distance from the centre of the aggregate. Even this approximation indicates the growth of the scattering amplification factor with decreasing fractal dimension.

4.4 Wave emission by fractal objects

Radiation fractal effects may take place even in a set of independent point sources of radiation showing fractal distribution in the space. Consider their contribution to the intensity of emission from the sphere of radius R with its centre at the observation point. In the case of fractal distribution with dimension D, the number of such sources on the sphere is described by the expression

$$N \sim R^D , \tag{71}$$

each source contributing to the total intensity in proportion to $1/R^2$. Hence, the total intensity is

$$I \sim R^{D-2} . \tag{72}$$

Given the uniform distribution of sources, $D = 2$ and the total intensity does not depend on the distance whereas in the case of fractal distribution, $D < 2$ and the intensity falls with increasing distance.

Expression (72) under the assumption of fractal distribution of stars and galaxies may be used to find a solution for the well-known Olbers paradox of night-sky luminosity [39]. If the Universe is considered infinite, integration of Eqn (72) over distances yields an infinite result. On the contrary, distribution over spheres with sufficiently small fractal dimension gives a finite result even if the Universe is infinite.

It is worthwhile to note that the presently available data suggest a fractal distribution of galaxies on scales of up to 100 Mpc, with the mass fractal dimension $D = 1.2$ [138]. Corresponding to such patterns is distribution over spheres with dimension $D_s = D - 1$. This results in the following distance dependence for the total intensity: $I \sim R^{-1.8}$; its integral over distances is $\int I \, dR \sim R^{-0.8}$. Therefore, fractality may well be supposed to contribute to the luminosity of the night sky.

There are more aspects as regards fractal effects in wave emission. Heat radiation by fractal aggregates has been investigated in Ref. [38]. Localised collective states discussed in the previous section are responsible for abnormally high absorption if calculated per aggregate

†Photomodification of clusters of small metal particles consists of burning out some of them by means of heat generation induced by absorption of an incident wave.

particle. Hence, anomalous heat emission per unit mass of the aggregate.

This result has been obtained in Ref. [38] based on more trivial considerations. The author suggested that the boundary conditions for the waves emitted from the cluster surface are coincident with the conditions for a continuous particle when its heat radiation is not different from that of the cluster containing $(r/r_0)^{3-D}$ times fewer particles (r, r_0 being the size of the cluster and its constituent elements respectively and D is the fractal dimension). Radiation of the cluster per particle is higher.

Another manifestation of fractal structure participation in radiation is associated with its fluctuations when produced by fractal systems. Such phenomena have been examined in the context of seismology in Refs [40, 52] which are concerned with the role of acoustic emission fluctuations in the processes of rock restructuring. One of the models used in Ref. [40] is related to the percolation model of front diffusion. Concentration of an agent in the diffusion front changes from zero at a distance from the source to unity near it. There is a front region where the diffusing agent concentration is equivalent to the threshold percolation level. In proximity to this site, the diffusing agent tends to form fractal clusters [83]. This results in a change of the coherent volume filled by the agent due to differently sized mature clusters joining the front and leaving it rather than the motion of individual particles. This process is accompanied by the so-called geometric noise general characteristics of which have been investigated in Ref. [83].

It is important that this is an universal effect which does not require special conditions for the formation of fractal objects. It is due solely to diffusion and may be noticed on examining waves of different nature. For example, the authors of Ref [139] studied pressure fluctuations during the slow invasion of a random porous medium by a heavy fluid. This percolation was of a diffusive nature which favoured conditions for the production of fractal geometric noise.

5. Fractal structures in wave fields

There is no well-developed methodology in this area of research. A great variety of geometric objects may be associated with wave fields, viz. spatial distribution of field intensity, wave shape, radiation patterns, etc. A study of fractal structures in wave fields as well as in random processes (see Section 2.2) may be useful for the concise description of fields with the complicated structure necessary to understand nonlinear wave processes or charac-teristics of natural noise.

The presence of the distinguished scale (wavelength) in wave fields is an important limitation on the manifestation of fractal properties. Given a broad wave spectrum, they are apparent as fractal structure of the wave shape in the self-similar region of the spectrum. In the general case, fractality may be observed on scales exceeding the characteristic wavelength, that is in the ray structure or the large-scale distribution of field intensity.

This section presents a description of results obtained in different studies concerning fractal structures in wave fields and discusses a promising general approach to the analysis of signals and waves based on the use of the multifractal model.

5.1 Multifractals and analysis of signals

A multifractal is a union of fractal sets having different dimensions. A detailed description of multifractals and relevant notions is given in Ref. [9] and Ref. [48].

Multifractal analysis may provide nontrivial data applicable to a wide range of objects not restricted to self-similar ones or even to fractals. The most important component of the analysis is the examination of the Renyi D_q dimensions of different orders. For objects regarded as self-similar in the narrow sense of the word, all these dimensions are similar and equivalent to the fractal dimension D_0. Consider moments of point distribution density at an object:

$$M_q = \sum_{N(l)} [p(l)]^{q+1} \tag{73}$$

as related to the breaking scale of object l. Then, it follows from the definition of the Renyi dimensions that

$$M_q(l) \sim l^{\varphi(q)} = l^{qD_{q+1}} = l^{qD_0} , \tag{74}$$

where the last equation is fulfilled for self-similar objects. In other words, function $\varphi(q)$ for self-similar objects is linear. This inference does not hold for a general case. However, an object can be described in terms of the multifractal model provided scaling (74) with a certain function $\varphi(q)$ still exists. Suppose that an object can be broken up into complexes of fractal sets with dimension $f(\alpha)$ near which densities exhibit a power-law dependence on the cell size in the form of $(l) \sim l^{\alpha}$. Then, moments of distribution density may be expressed in the following way:

$$M_{q-1}(l) \sim \int l^{q\alpha - f(\alpha)} \, \mathrm{d}\alpha . \tag{75}$$

The integral at small l may be obtained by the 'pass' method. At the saddle point $\bar{\alpha}$,

$$\left.\frac{\mathrm{d}f}{\mathrm{d}\alpha}\right|_{\alpha=\bar{\alpha}} = q(\bar{\alpha}) , \tag{76}$$

and the integral is given by expression $l^{q\bar{\alpha} - f(\bar{\alpha})}$. Hence, functions $f(\alpha)$ and D_q are related through the Legendre transformation $(q-1)D_q = q\bar{\alpha} - f(\bar{\alpha})$.

The multifractal model has the most explicit sense when applied to the analysis of signals (fields) in the quantitative description of distribution of singularities of signals non-differentiable in an infinite number of points. An example of such a signal is provided by the Wiener process with no derivative at any point. Naturally, the notion of non-differentiability in application to real physical signals may be discussed only with respect to a certain range of scales which exceed a selected minimal scale. For instance, in the case of spatial dependence of turbulent flow velocity, such scales are those in excess of the internal Kolmogorov turbulence scale.

Suppose there is a discontinuous process $x(t)$ with singularities of the derivative. Also suppose that the square of the difference between signal values in adjacent points near the singularities shows power-law behaviour when distances between the points are changed:

$$|x(t) - x(t+\tau)|^2 \sim \tau^{2\alpha} . \tag{77}$$

This relation corresponds to the presence of a point of singularity of the Hoelder derivative of the α order [8]. At the points where the derivative is discontinuous, $\alpha = 1$, while the quantity $\alpha > 1$ corresponds to the points with

zero derivative, although the second derivative may have a break. Specifically, $\alpha = 1/2$ for all points of the Wiener process. Further suppose that the points with a definite exponent α constitute a fractal set with dimension $f(\alpha)$; then, the following expression can be written for the structure function of the process of order q, by analogy with (75):

$$\left\langle \left| x(t) - x(t+\tau) \right|^q \right\rangle = \int \tau^{q\alpha - f(\alpha)} \, \mathrm{d}\alpha \sim \tau^{q\bar{\alpha} - f(\bar{\alpha})} \ ,$$

where

$$\left. \frac{\mathrm{d}f}{\mathrm{d}\alpha} \right|_{\alpha=\bar{\alpha}} = q \ .$$

Therefore, if structure functions of the study process of different orders show power dependence on the interval in the form of $\tau^{\varphi(q)}$, the multifractal model for the distribution of singularities of the signal derivative may be adopted. Function $f(\alpha)$ is obtained in the form of the Legendre transformation of the derivative $\varphi(q)$.

Function $f(\alpha)$, commonly referred to as the singularity spectrum, has recently been used by many authors. Unlike the power spectrum and correlation functions of the process, the singularity spectrum bears information about its local structure useful for distinguishing between signals of different origin. Also, it is worth noting that multifractal analysis gives a meaningful summary of data on different order moments of the two-point distribution of process probabilities.

The multifractal model appears to have been applied first to the description of the structure of turbulent flow velocity in the inertial scale interval [140, 141]. The spectrum of velocity singularities thus obtained permits one more important interpretation. In agreement with the Kolmogorov theory, the velocity difference in points located at distance r is related to energy dissipation $\langle \varepsilon_r \rangle$ averaged over the volume of size r by the following expression:

$$\Delta v_r = \left(\langle \varepsilon_r \rangle r \right)^{1/3} \ .$$

Assuming $\langle \varepsilon_r \rangle$ to be independent of the averaging volume, it is possible to obtain for structure velocity functions

$$\left\langle |\Delta v_r|^p \right\rangle \sim r^{p/3} \ ,$$

with the singularity spectrum being degenerate to a point. Experimental studies indicate that this relation is not fulfilled. Hence, energy dissipation is not uniformly distributed in space; its distribution may be described using the multifractal model, similar to the distribution of velocity singularities. In other words, multifractals may be useful to characterise an intermittency of energy dissipation fields which was previously described in terms of a logonormal distribution. It is clear that the multifractal model is applicable to the analysis of intermittent patterns of any density distribution both in space and time. In this case, the integral of such density is regarded as a multifractal measure. With this measure being taken as a nondifferentiable function, its singularity spectrum coincides with that of the corresponding density. Any signal or its instantaneous power may be viewed as a density on the time axis suitable for multifractal analysis.

Such an approach has been employed in Ref. [50] to analyse periwall pressure pulses that are known to occur in a turbulent flow in a pipe. The analysis of the process in

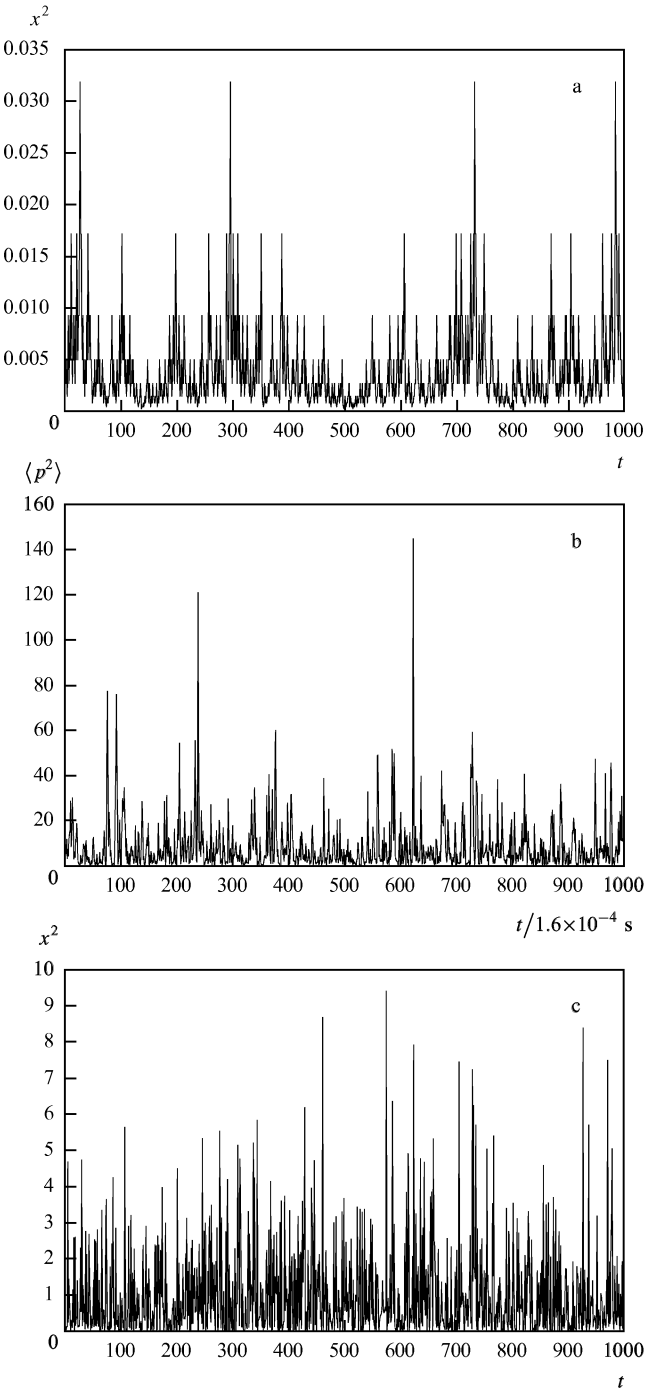

Figure 13. (a) Multifractal process obtained with the model described in Ref. [140]. (b) The square of periwall pressure pulses in a turbulent flow averaged over intervals 1.6×10^{-4} s [50]. Probe size 1 cm, flow velocity 10 m s^{-1}. (c) The square of white noise with normal amplitude distribution. The horizontal axis gives reading numbers, and the vertical axis represents conventional units.

Ref. [50] was performed on times exceeding its correlation scale; it is on such scales that intermittence of the process acquires multifractal structure. It was also essential that direct measurements demonstrated that the energy singularity spectrum of the process was independent of flow velocity. Indeed, the singularity spectrum reflects the structure rather than energy characteristics of the process.

A simple multifractal model has been proposed in Ref. [142]. Suppose that a segment of the amplitude is

initially equal to a. Divide the segment into two new ones and randomly ascribe amplitudes pa and $(1-p)a$ to either half. Repeat the procedure over and over an infinite number of times. The resultant density has the multifractal singularity spectrum. The process simulated by this model is illustrated in Fig. 13a. Fig. 13b shows the change with time of the pressure squared during near-wall turbulent pulsation. For comparison, the square of Gaussian white noise is presented in Fig. 13c. Fig. 14 demonstrates singularity spectra for these processes. It can be seen that the singularity spectrum for the Gaussian noise concentrates near the point $f=1$, $\alpha=1$. Experimentally measured points of the singularity spectrum for pressure pulses were found to fit the curve well for the singularity spectrum of the simulated process with $p=0.7$. Also, similar intermittent patterns of simulated and real processes are directly apparent from the figures (Fig. 13a,b).

The application of multifractal analysis to the amplitude distribution of fracton wave functions on a percolation cluster is described in Ref. [51]. The authors used multifractal analysis to examine the density equivalent to the squared amplitude of the eigenfunction for Eqn (18) on a percolation cluster. The cluster was obtained by simulating percolation at the threshold node concentration on a 64×64 square lattice. Wave functions were derived by means of direct numerical evaluation of eigenvectors of the equation. The study revealed the power-law behaviour of values M_q obtained with formula (73) in the range $q=5-10$. For eigenfunctions on the full square lattice, the exponent $\varphi(q)$ from Eqn (74) had the simple form of $\varphi(q)=2q$. This dependence changed for fractons, first, because wave functions were fixed on a fractal, second, because the wave functions had highly irregular structure. At $q=-1$, $\varphi(q)=-1.9$ was obtained and reported to be equal to the fractal dimension of a percolation cluster, as expected [43]. For other q values, equality $\varphi(q)=qD_0$ is no longer fulfilled which can be accounted for by the marked intermittency of wave functions within a cluster. The distribution of wave function amplitudes is characterised by the nontrivial singularity spectrum $f(\alpha)$. This spectrum displays weak frequency dependence, but its general structure is the same regardless of frequency (Fig. 15). To begin with, $f(\alpha)$ is smaller than the cluster dimension $f(\alpha)=1.5-1.6$ at $\alpha=2$ corresponding to the points on a cluster with the normal smooth amplitude distribution. This means that the points with smooth behaviour of the wave function occupy only a small portion of cluster nodes, the smaller the higher characteristic localisation scale. Nevertheless, spectrum $f(\alpha)$ is rapidly diminished at $\alpha<2$, that is the number of points where the amplitude shows abnormally fast growth undergoes a further decrease. However, the majority of the points occur at $\alpha>2$. In the range of $\alpha=2-5$, the singularity spectrum approaches the constant value $f(\alpha)=1.9$ equal to the cluster dimension D_0. Therefore, the wave function amplitude is subnormally small for almost all points of the cluster. It should be noted that M_q at $q=0$ is directly related to the process of nonlinear excitation of fractons with double frequency. The singularity spectrum indicates that the nonlinear source of fractons with double frequency is largely located in that portion of the cluster where fractal dimension is smaller than that of the whole cluster. This is supposed to have a marked effect on the generation of harmonics by fractons.

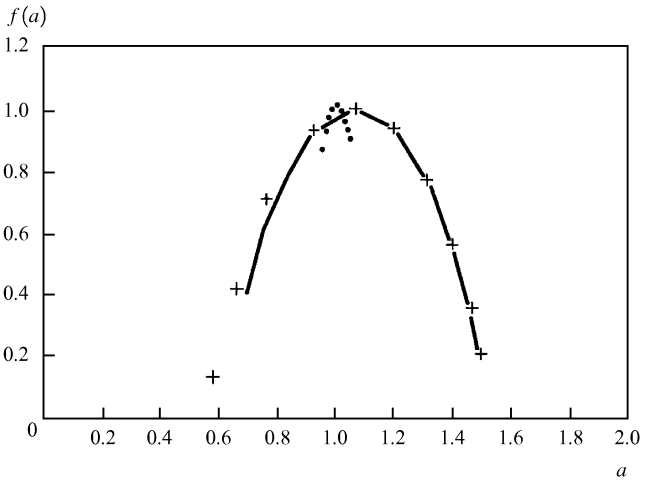

Figure 14. Singularity spectra of processes shown in Figs 13a–13c. The solid line is the singularity spectrum of the model process, crosses show the experimental spectrum of pressure pulsation [50], and the dotted line represents white noise with normal amplitude distribution.

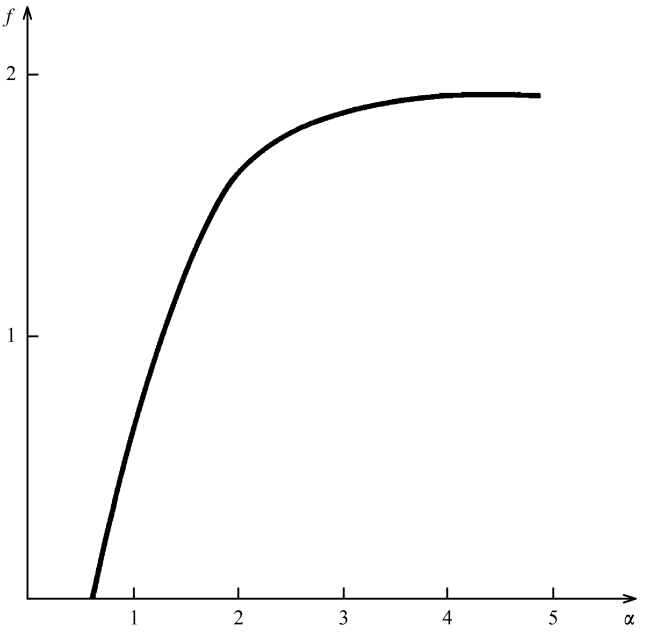

Figure 15. Fracton singularity spectrum on a percolation cluster [51].

5.2 Fractal ray structure

Fractal structures are known to associate with rays which propagate in a longitudinally nonuniform waveguide. Fractal structures arise due to nonlinearity of ray equations. Studies on the effects of nonlinear ray dynamics are based on the representation of ray equations in the Hamiltonian form and the analogy with the results of nonlinear Hamiltonian dynamics [143, 41].

In longitudinally homogeneous waveguides, rays undergo periodic oscillations relative to the axis but do not leave the waveguide. Ray capture is due either to the effect of the reflecting walls or to the nonuniform cross distribution of the refractive index. The length of a ray cycle is determined by the initial angle of slope relative to the waveguide axis. Ray trapping in nonlinear resonances is possible in the presence of longitudinal inhomogeneities

(wall roughness, axial oscillations, changes of refractive index). There are two types of ray behaviour which lead to fractal structures. In the absence of overlapping nonlinear resonances, ray dynamics are not chaotic, and fractality is a property of the resonance structure.

It has been shown using the model of an acoustic waveguide in a shallow sea with a periodically irregular bottom [144] that ray propagation in a longitudinally inhomogeneous waveguide may result in the situation when the dependence of spatial ray frequency (inverse cycle length) on the angle of departure is a fractal measure. This curve has zero derivative almost throughout its length with the exception of the fractal set of points. Fractality is also manifest in the dependence of propagation time on the angle of departure which is obviously responsible for the fractal nature of an impulse signal during its propagation in the waveguide.

A uniformly occupied waveguide with absolutely reflecting walls has been examined in Ref. [144]. One of its walls was flat whereas the other had periodic irregularities of the form

$$f(z) = \frac{4b}{L}\,\xi(1-\xi)\,,$$

where b and L are the amplitude and the irregularity period respectively while $\xi = z/L$ is the fractional part of the longitudinal coordinate z normalised on the period. The depth of the waveguide at $b = 0$ is h. In such a waveguide, travelling rays are alternately reflected from the walls. Ray propagation may be described by a nonlinear representation which defines both the angle and the longitudinal coordinate of ray reflection from the flat wall via the angle and the coordinate of the previous reflection from the flat wall. Assuming that the amplitude of irregularities vanishes, the ray cycle length D, i.e. the distance between two subsequent reflections from the wall, is constant and equals $D = 2h\cot\theta_0$, where θ_0 is the initial outlet angle of the ray. Irregularities have marked effect on the rays in nonlinear resonance with the period of irregularity. For certain integers m and n, this means the fulfillment of equality $2n\pi/D = 2\pi m/L$ or

$$\tan\theta_0^{(m,\,n)} = \frac{m}{n}\,\frac{2h}{L}\,, \tag{78}$$

which maintains resonance between irregularity harmonics and ray trajectory. The rays with angle of departure near one of the resonance angles $\theta_0^{(m,\,n)}$ are involved in the resonance and have similar average periods of reflection and propagation times. Fig. 16a illustrates the dependence of the ray oscillation spatial frequency κ on the angle of departure θ_0 [144]. This curve consists of steps with a constant κ value which are located near the resonant angle of departures. The step distribution with respect to the angle of departure is fractal in that the number of intervals between steps $N(r)$ shows the power-law dependence on resolution r when the resolution over the angle increases. This implies fractal distribution of singularities of a derivative curve (see Section 5.1). Fractality is also illustrated by two inserts in Fig. 16 which represent an enlarged portion of the curve and the plot of $N(r)$ dependence. Fig. 16b shows a similar stepwise dependence of the ray length (time of signal propagation along the ray).

The fractal structure of nonlinear ray resonance follows from Eqn (78). Fig. 17 demonstrates the distribution of

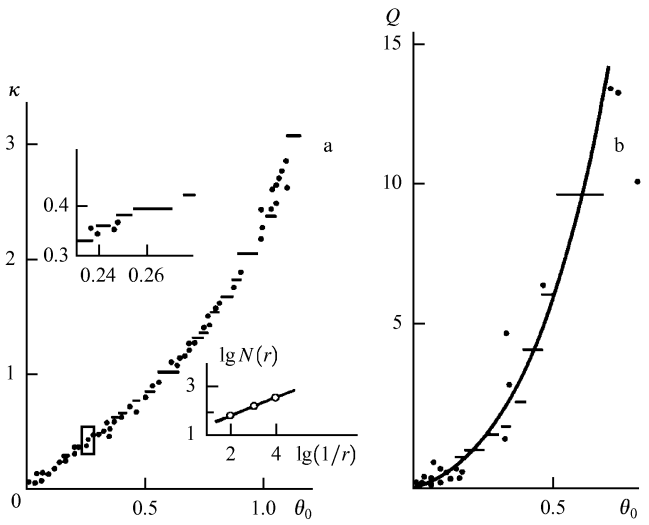

Figure 16. (a) Dependence of ray oscillation spatial frequency on the angle of the ray leaving the source [144]. Angle step 0.01. The insertion shows the enlarged portion of the plot inside the rectangle; angular step 0.001. Characteristics of the waveguide: $h/L = 1/3$, $b/L = 0.001$. (b) Dependence of ray length (excepting the distance along the waveguide z) on the angle of departure [144]. Characteristics of the waveguide: $h/L = 1/3$, $b/L = 0.005$.

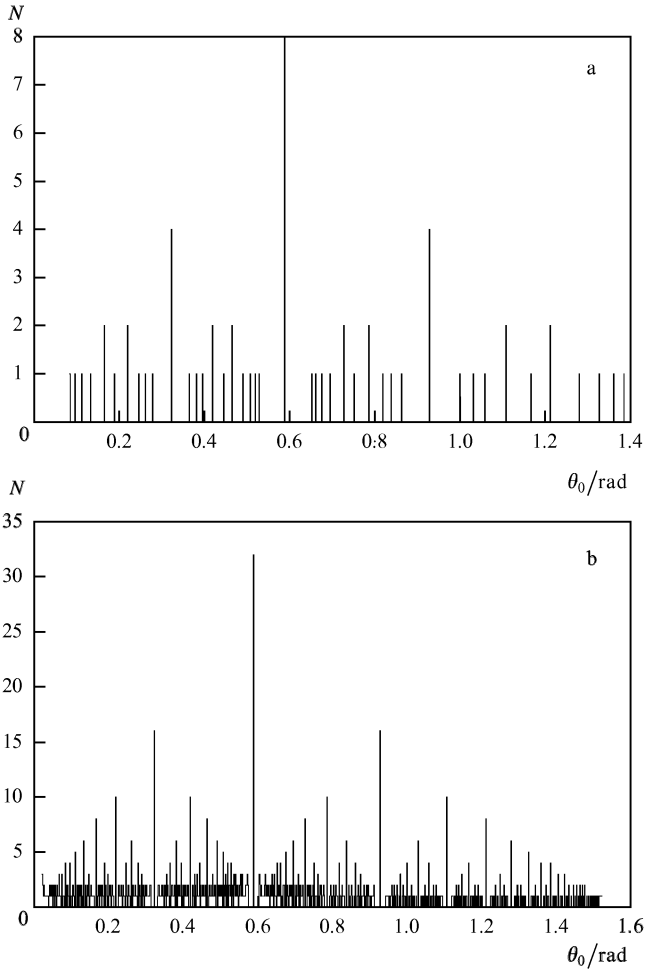

Figure 17. Distribution of resonance angles of departure derived from Eqn (78) taking into consideration the first eight harmonics (a) and the first 32 harmonics (b).

solutions of the second equation in (78) with respect to the angle of departure. Fig. 17a presents solutions with regard for resonances up to the eighth harmonic ($m \leqslant 8$, $n \leqslant 8$). Solutions taking into consideration resonances up to the 32nd harmonic are shown in Fig. 17b. Comparison of Figs 17 and 16a indicates that the broadest ranges of nonlinear resonance capture correspond to the angle of departure in which a few resonances coincide. Comparison of Figs 17a and 17b reveals the self-similar structure of resonances. The number of resonances grows with increasing harmonic number equivalent to increasing resolution over the angle. The distribution of separate resonance groups for a large number of harmonics is similar to the resonance distribution in the entire range of angles for a smaller number of harmonics.

Resonance overlapping results in chaotic ray dynamics with the resulting fractal properties of the phase picture typical of chaos. So far as rays in a waveguide are concerned, this may be reflected in the ray distribution density in the 'angle of slope relative to the axis – transverse coordinate' plane. Chaotic behaviour of rays in an acoustic waveguide in a shallow sea with periodically rough bottom was investigated in Ref. [144]; it was shown to arise at sufficiently small angles of departure of rays. Conditions for the formation of chaotic ray dynamics in deep-water ocean waveguides appear to have been examined first in Ref. [145]. This situation is of special interest from the viewpoint of the theory of wave propagation in natural media, and it seems appropriate to discuss it at greater length proceeding from a recent study [146]. Studies of chaotic ray dynamics are based on eikonal equations in the Hamiltonian form, e.g.

$$\frac{\mathrm{d}z}{\mathrm{d}r} = \frac{\partial H}{\partial p}\ , \qquad \frac{\mathrm{d}p}{\mathrm{d}r} = -\frac{\partial H}{\partial z}\ , \tag{79}$$

where z is the depth, r is the distance, and p is the slip angle tangent

$$H(z, p, r) = 0.5p^2 + V(z, r)\ ;$$

$$V(z, r) = 0.5\left\{1 - \left[\frac{c_0}{c(z)}\right]^2\right\} + g(z, r)\ . \tag{80}$$

Here, c_0 is the basic acoustic velocity at a selected level, $c(z)$ is the unperturbed acoustic speed profile, and $g(z, r)$ is the excitation describing the longitudinal nonuniformity of the wave-guide. A necessary condition for the chaotic ray behaviour is local instability of the solutions of Eqns (79). According to Ref. [146], the criterion of such instability has the form

$$\frac{c_0^2}{[c(z)]^4}\left[c(z)\frac{\partial^2 c(z)}{\partial z^2} - 3\left(\frac{\partial c(z)}{\partial z}\right)^2\right] + \frac{\partial^2 g(z, r)}{\partial z^2} < 0\ . \tag{81}$$

Analysis of condition (81) as performed in Ref. [146] indicates that it is readily fulfilled in the case of a small longitudinal perturbation (caused, for instance, by inner waves in the ocean) provided the underwater acoustic channel has two axes. This inference is confirmed by the numerical solution of Eqns (79) for a typical acoustic channel in the North Atlantic. Therefore, both ray chaos and fractal signal properties may prove typical of sea acoustics at least.

The above results characterise two-dimensional waveguides with one-dimensional longitudinal inhomogeneity. The situation is strikingly different in three-dimensional problems if two-dimensional inhomogeneities are taken into consideration. Specifically, diffusion in the phase space becomes possible, i.e. the so-called Arnold diffusion. Three-dimensional effects have recently been examined in Ref. [147] based on the model of the near-bottom ocean waveguide on a rough bottom. Ray diffusion is qualitatively reflected in random changes of ray propagation directed along the trail in the horizontal plane, any direction being possible including the reverse one.

It should be emphasised that fractal ray dynamics (including chaos) do not arise in randomly inhomogeneous media. Longitudinal perturbations may have a quite regular character. The following section reviews selected statistical wave problems in which fractal structures may appear.

5.3 Wave superdiffusion

It should in the first place be noted that the diffusion approximation for the description of ray propagation in a random medium obtainable from Eqn (79) with the short-range correlated random index of refraction $V(z, r)$ [148] does not yield fractal ray trajectories. It explicitly ensues from the first equation of (79) which describes differentiable trajectories.

Wave diffusion also occurs in the general case of distribution in randomly nonuniform media with small-scale inhomogeneities. A diffusive nature is reported to be inherent in both the shift and the widening of a wave beam in such a medium, with inhomogeneities smoothly changing longitudinally and short-range correlated transversally relative to the direction of wave propagation. In this case, a parabolic equation may be used to describe the wave field. A numerical study of transverse displacements and widening of a wave beam propagating in such a medium has been reported in Ref. [44]. The authors analysed the following model equation for changes of wave amplitude ψ along the discrete longitudinal coordinate t:

$$\psi_{t+1}(x) = -i\left[\frac{1}{2}\Delta_x\psi_t(x) + r(x, t)v\psi_t(x)\right] + \psi_t(x)\ ,$$

where x are the transverse coordinates, $r(x, t)$ is a random quantity which adopts equiprobable values 1 and -1, v has the sense of inhomogeneity amplitude. The study evaluated the displacement of the centre of the transmitted beam x_c and beam widening Δx.

In the three-dimensional case at $v < 2$, dependencies $x_c \sim t^{\nu}$, $\Delta x \sim t^{\nu'}$ are fulfilled where $\nu = \nu' = 1/2$. At $v > 2$, there is a qualitative change in the behaviour of these variables. Specifically, a simple diffuse displacement of the beam is replaced by superdiffusion with exponent $\nu = 0.67$. Conversely, the beam widening becomes slower ($\nu' = 0.45$). In the two-dimensional case, superdiffusion occurs at any amplitude of inhomogeneities, with $\nu = 0.75$, $\nu' = 1/2$. ν values suggest the fractal character of the beam trajectory (see Section 2). However, to the best of our knowledge, there have been no studies in which wave propagation in a random medium was considered from this point of view. It is worthwhile to note that the fractal wave structure in a random medium may lead to fractal structures arising as a result of wave effects on the medium. Although the current theory of wave propagation in random media works well without fractal notions, the fractal analysis of resulting fields may be expected to provide novel information.

Another statistical wave problem which is likely to lead to fractal structure pertains to excitation transfer in a two-level resonant medium with a uniformly widened transition [42, 43]. Excitation of such medium from an external source $F(r)$ results in a distribution $n(r)$ of the excited level concentration which is induced due to excitation transfer by photons emitted during transition. The emitted photons are distributed in a certain frequency range as a consequence of level widening and have different distributions of free path times until they are captured by another resonance centre. It has been shown that the resulting distribution of the excitation transfer distance has no finite dispersion, which accounts for its Levy-type stable distribution in the limit of large distances [43]. In this work, the process of excitation transfer is described by the following equation:

$$n(r) = F(r) + \int K(r - r')\, n(r')\, \mathrm{d}V' ,$$

where the kernel K has, at large distances, asymptotics

$$K(r) \sim \frac{1}{r^{-3-2\gamma}} .$$

The probabilistic interpretation of the transfer equation gives an asymptotic for the probability distribution of excitation transfer distances in the form of $1/r^{-1-2\gamma}$ corresponding to the stable distribution with exponent $\alpha = 2\gamma$ (see Section 2.3). Intrinsic trajectory fractal properties of the 'Levy flight' must be equally apparent in the described process.

There are far more examples of statistical wave problems with a possibility of fractal structure manifestation, besides the two above, and further studies in this field are certain to provide new and interesting results.

5.4 Dynamic chaos in nonlinear wave fields

The examples of fractal structure formation in wave fields examined in the two previous sections illustrate linear wave processes in inhomogeneous media. Nonlinear wave interactions may equally result in the appearance of fractal structures in a homogeneous medium. Here, the most extensive studies were carried out to investigate dynamic chaos and the associated fractal structure of phase trajectories. Detailed reviews of these problems may be found in Refs [17, 149, 150]. Some processes leading to dynamic chaos in nonlinear wave fields are examined below.

Infinite-dimensional wave systems may be reduced to finite-dimensional dynamic systems by introducing envelope amplitudes of a small number of interacting quasi-monochromatic waves. A rather general mechanism underlying the dynamic chaotic behaviour of the amplitudes of interacting waves is related to decay instability. It includes parametric excitation of low-frequency waves in the field of a high-frequency wave. One of the signs of such instability appears to be directly related to turbulent transition in the boundary layer [151–153]. It is known that turbulent transition in the boundary layer originates as the formation of Tolmin–Schlichting (TS) waves. As soon as the Reynolds number exceeds a critical excitation level of the flow (TS wave), wave numbers within a certain range start increasing downstream. This process involves wave numbers larger than a certain fixed value. An experimental study of the nonlinear evolution of an artificially excited increasing TS wave [151] revealed early excitation of subharmonics followed by the induction of a wide spectrum of low-frequency perturbation components showing stability in a linear approximation. These events precede turbulent transition.

Calculations reported in Ref. [152] confirmed the feasibility of subharmonic instability. A later study [153] demonstrated the possibility of cascade excitation of subharmonics. This indicates that the process of laminar–turbulent transition in the boundary layer may be analogous to a transition to chaos through doubling the period.

Experimental measurements of trajectory dimension for the motion in the boundary layer using the Takens algorithm [154] showed that at the early stochastic stages, the motion may be described by the finite-dimensional dynamic system.

Certain phenomena associated with interaction between waves and parametric excitation of subharmonics are described by equations for slow amplitudes reminiscent of the well-known Lorentz model [149]. These phenomena include, among others, the effect of second harmonic generation in a disequilibrated medium which amplifies the harmonic and the interaction between ion sound and plasma waves following parametric excitation.

Chaotic behaviour is also manifested in the case of forced high-frequency wave scattering on a low-frequency wave (Mandelstamm–Brillouin scattering) [155]. Here, the chaotic regime is due to the nonlocal interaction at weak attenuation of the acoustic wave when its amplitude may be so large that the sound self-effect causes phase disturbance of resonance.

The general approach to distributed systems with chaotic dynamics is based on equations for perturbation amplitudes in the medium resembling the Ginzburg–Landau equation and may be applied to a broad class of wave and nonwave problems [17, 150]. This approach is based on the possibility of identifying rather weakly interacting nonlinear structures distributed in space or their defects. Their collective dynamics are described by a discrete analogue of the Ginzburg–Landau equation and result in finite-dimensional spatial chaos.

An example of such behaviour of the wave field is examined both experimentally and theoretically in Refs [156, 157]. These studies made use of the Faraday ripple, i.e. the system of parametrically excited capillary waves generated on the water surface in a vessel with an oscillating bottom. When the vibration amplitude of the bottom was small, it was possible to observe generation of a regular wave structure with square cells formed by pairs of waves propagating in opposite directions. An increase in the vibration amplitude resulted in modulatory instability and formation of the regular periodic structure of a modulation wave of the primary lattice. Further growth of the vibration amplitude caused defects in the modulation structure and chaotic patterns in its motion.

5.5 Fractal structures in wind waves on the sea surface

Wind waves in the sea provide additional examples of fractal structures in wave fields. They may also be associated with ray chaos [158]. Fractal characteristics are intrinsic in the shape of the rough sea surface with both directed [159] and random [45] waves. The latter work studied power-law flow spectra of wind waves with exponents $\beta = 11/3$ and 4 for gravity waves and

$\beta = 17/6$ for capillary ones. The authors evaluated fractal dimensions of the curves describing the change with time of elevations in a point and the curves that describe rises along the surface section by a vertical plane. The curve that described the time-course of elevations for gravity waves was not fractal in itself, but its derivative possessed the property of fractality and had dimensions 5/3 and 3/2 for exponents $\beta = 11/3$ and $\beta = 4$ respectively. The curve with respect to time for capillary waves turned out to be fractal and had dimension 13/12. The surface sectioned by the vertical plane was represented by a fractal curve for both exponents in the gravity wave spectrum, the respective dimensions being 4/3 and 5/4. The spatial curve for capillary waves was lacking in fractality while its derivative (surface slope) was a fractal with dimension 13/8. The range of fractal behaviour scales was naturally restricted by the correlation radius of the troubled surface. It should be noted in this context that wave dispersion over the sea surface is actually scattering on a fractal.

Another approach to the analysis of fractal properties of sea-surface elevation has been reported in Ref. [160]. Using the Takens algorithm, the authors measured the attractor dimension in phase space. The dimension of the attractor showed a tendency towards a decreased growth rate with increasing space dimension. However, the numerical model of random signal with the spectrum derived from measured values exhibited similar behaviour. It was concluded that the sea surface elevation was not controlled by a finite-dimensional dynamic system with a strange attractor.

Fractal properties of the sea surface on scales exceeding the ripple correlation radius have been examined in Refs [46, 47]. Analysis of aerial photographs in Ref. [46] revealed a fractal distribution of wave collapse zones over the surface with fractal dimension 1/2. Studies using a scanning laser locator [47] demonstrated fractality of a mirror-point distribution along the time–space line produced by the ship when underway. The fractal dimension was found to be 0.8. Both papers report manifestation of fractal properties on scales of at least up to ten times the correlation radius of the troubled surface. Measurements were made in the tropical areas of the open ocean in the Atlantic where the trade-wind maintained stationary agitation during a few successive days. Capillary ripple intensity was recorded for many hours along the vessel's course using a scanning laser locator.

Fig. 18 demonstrates the sampled spatial spectrum of the parameter measured in the above study. The analysis was performed by averaging over frequency bands as described in Ref. [134] (see Section 4.2). The results obtained in different study areas and under different wind conditions are shown in Fig. 19. All the records revealed power-law averaged spectra with practically the same exponent in the range of scales from 40 m to 1.6 km which lay beyond the limits of ripple correlation scales. Such universal behaviour suggests that large-scale fractal variability of the ripple is characteristic of weak wave turbulence for waves with a nondecaying spectrum, a model describing the growth and the stationary spectra of wind agitation.

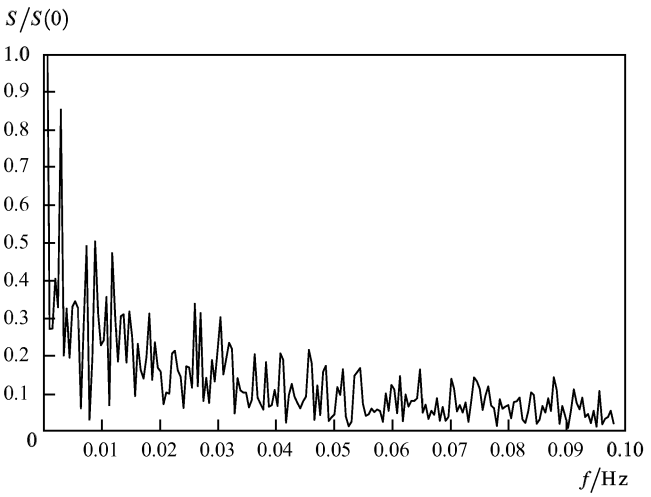

Figure 18. Sampled spectrum of large-scale variability of the intensity of a capillary-gravity ripple obtained by laser scanning [47]. The number of reflections was measured by surface scanning with a thin laser beam. Spectra were measured on board a ship underway at 8 m s^{-1}, frequency of 1 Hz corresponds to the spatial scale of 8 m.

5.6 Fractal analysis of signals in seismology

A variety of similarity laws in seismology are known to be fulfilled in a wide range of scales. They include the Gutenberg–Richter law [161] for the scaling dependence of recurrence frequency on the earthquake energy class and the Knopoff–Kagan law [162] for the distribution of time intervals between events. These laws are reported to be fulfilled for disintegration processes even if their scale is smaller than that of earthquakes. A recent work [163] investigated acoustic emission during breakdown of a hydrogen-saturated metal sample. The sample was saturated at high temperature and destroyed (microcracking) after cooling. The study produced information about the distribution of the amplitudes of acoustic emission impulses in the form of $N(A' > A) = A^{-0.9}$ and showed that this dependence was fulfilled on the interval of amplitudes over two orders of magnitude. This is one of the ways to represent the Gutenberg–Richter law.

The Gutenberg–Richter law may be explained in terms of lattice models for elastic bodies [103, 164]. Such models make use of an expression for elastic forces in a lattice [e.g. Eqns (32), (38)] and introduce the rule to select and destroy lattice sites when their deformation exceeds a certain critical level. Also, these models simulate fractal distribution of the damaged parts.

Distribution analysis of earthquake hypocentres† based on the results of a field study [156] revealed fractal patterns, with fractal dimension of −1.9. Similar results were obtained by simulation on a lattice using the elasticity model (38) [165] in which values of elastic constants were random and exhibited a power-law distribution.

Fractal properties are also inherent in signals of seismoacoustic emission during periods between earthquakes. Such signals were examined in detail in Refs [40, 52]. Fig. 20 shows results of fractal analysis of envelopes of seismoacoustic emission signals in different frequency bands. It illustrates the dependence of the Hurst exponent H and fractal dimension of the curve D_- on interval lengths being examined (expressed through the number of readings k). The relation between the Hurst exponent and the fractal

†Earthquake epicentres are distributed over the surface while hypocentres are located in the crust. Hypocentres lie at some depth beneath epicentres.

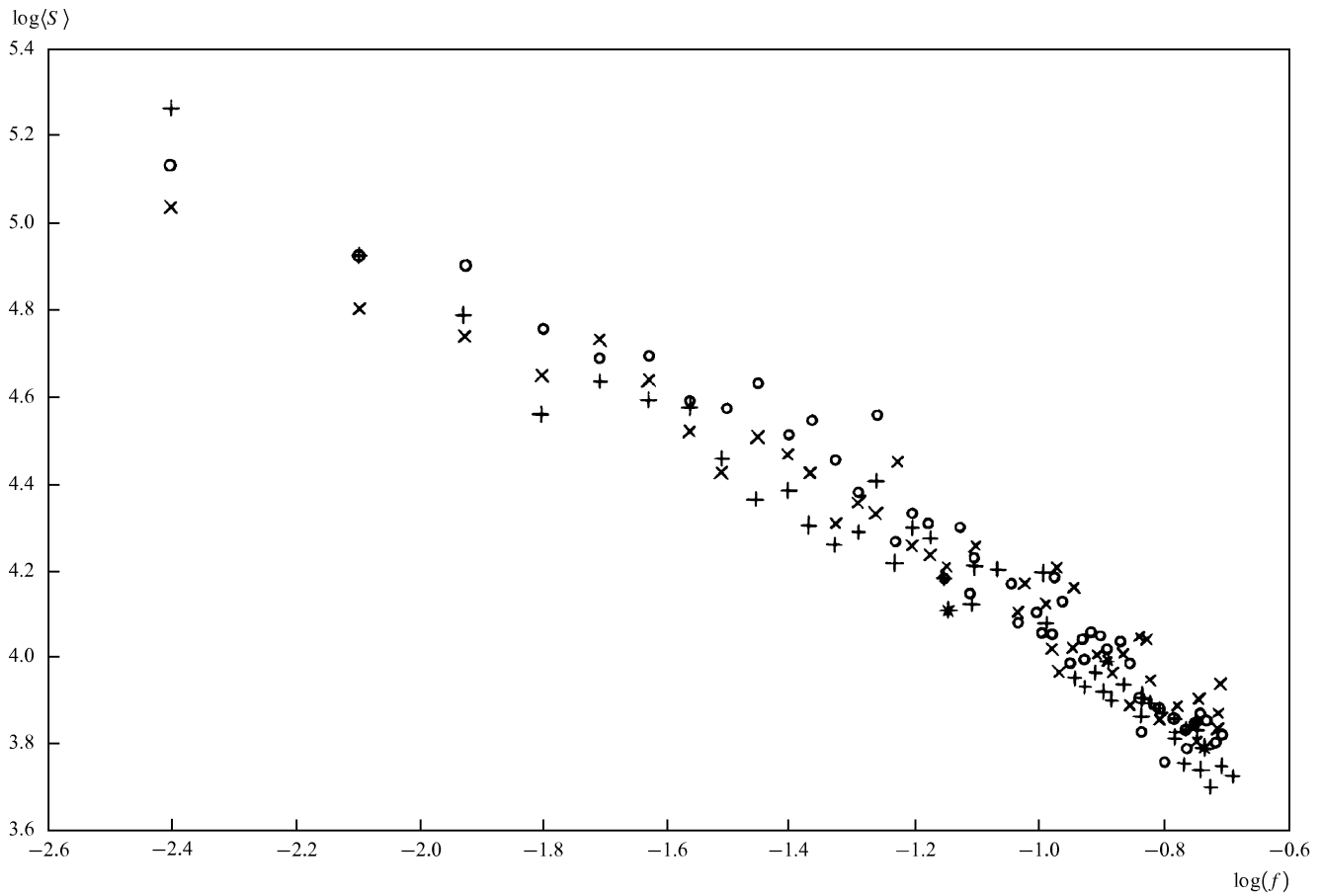

Figure 19. Spectra of ripple variability averaged over frequency bands 4×10^{-3} Hz. Labels denote different experiments. Scaling takes place on the spatial interval 40–400 m (0.2–0.02 Hz).

dimension is fulfilled, that is the process may be simulated by generalised Brownian motion. The measurements indicate the occurrence of crossover from the behaviour with the Hurst exponent $H = 0.4-0.6$, at a certain interval length. Refs [40, 52] offer the following interpretation of this phenomenon. Sources of seismoacoustic emission are supposed to be rock repacking fronts, i.e. sites where transition from the loose rock structure to the compact one occurs under the effect of strain. The pore concentration in such sites undergoes spatial alteration until it reaches the percolation threshold in a certain place. Therefore, the repacking front structure may be described by the model of percolation in a concentration gradient [83]. In this model, clusters of different size are formed at those sites of the front where concentration is close to the critical level such that the number of particles in the front is subject to fluctuations as a result of cluster attachment and detachment. For this reason, fluctuations on a certain time interval behave like a Brownian process with the Hurst exponent 1/2; the Hurst exponent vanishes at larger intervals.

For the purpose of comparison with Fig. 20, Fig. 21 presents the results of numerical evaluation of the structure function for particle number fluctuations in the diffusion front for different concentration gradients [83]. Evidently, plots in Figs 20 and 21 qualitatively coincide.

Rock restructuring is completed with the approaching earthquake which must result in qualitative changes in the structure of signals of seismoacoustic emission. These changes can be identified by measuring the fractal dimension. Dramatic changes in signal fractal dimension with the approach of an earthquake were confirmed by experiment [52].

6. Conclusions

There is hardly a field in physics where wave theory is not exploited for one or another purpose. This statement refers to basic and even more so to applied physical research. Physics owes to wave theory many important results and advanced methodology. However, basic concepts of the wave theory are based on the models for continuous media and use the mathematical apparatus largely intended for operations with smooth functions of time and space. This explains why fractal models introduce qualitative changes in the methods employed in wave studies. The use of fractal models in this area is by no means confined to exposition of known facts in a new fashion.

The theory of fractons on which the present review has largely focused has actually been designed to solve the problem of wave propagation in inhomogeneous and disordered media which cannot be described by models for continuous media. The concepts of effective refractive index and effective compression make no sense if applied to such media. In principle, the notion of fractons ensures an identical approach to the problem of elastic wave propagation in the fractal lattice and that of multiple scattering on fractal aggregates. Both problems deal with the scale-

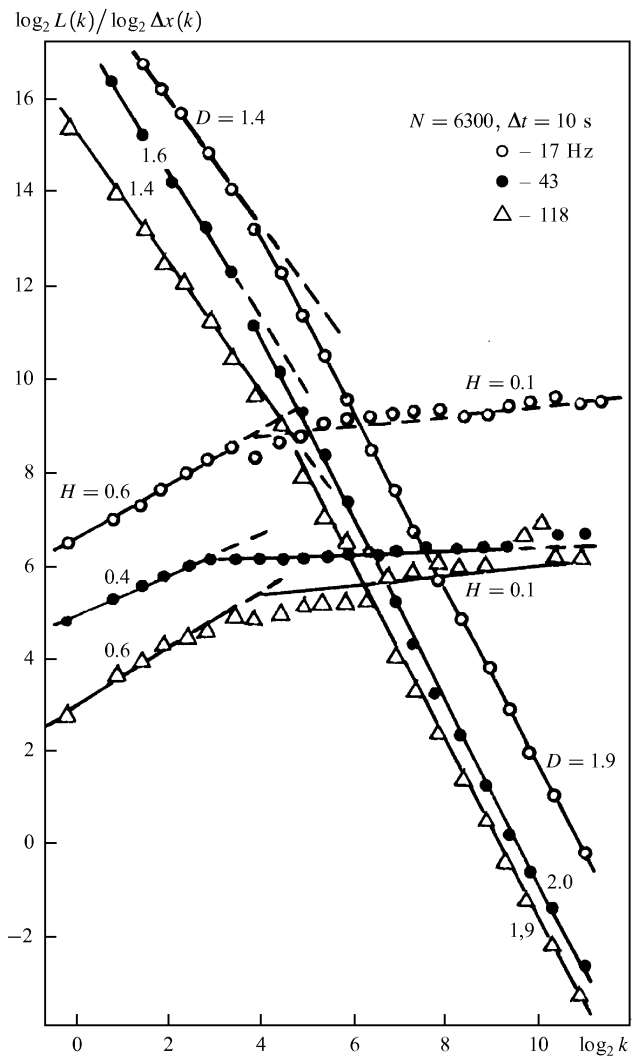

Figure 20. Structure function and envelope plot length of the signal of seismoacoustic emission in different frequency bands depending on the interval length [40, 52]. The plot length is assessed by measuring the length of the broken line with different link lengths. Dependence of the measured line length on the length of links suggests fractality of the plot while the slope of this dependence gives the fractal dimension.

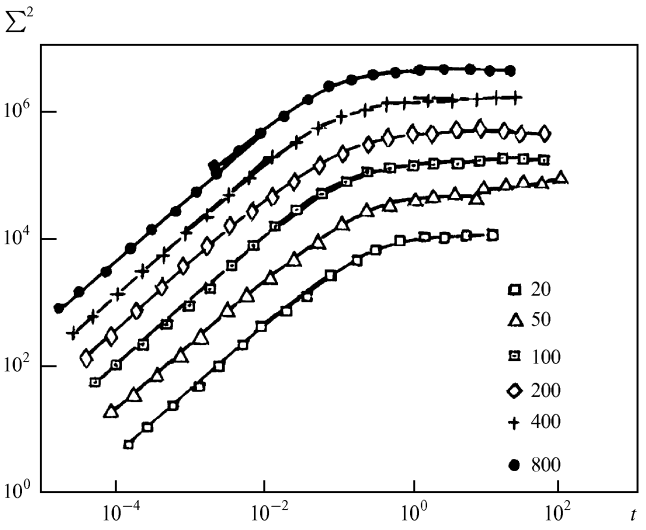

Figure 21. Structure functions $\Sigma^2 = \langle [N(t) - N(0)]^2 \rangle$ for fluctuations of the particle number in the diffusion front for different values of the inverted concentration gradient. Results of numerical calculations reported in Ref. [83].

invariant spectrum of excitations of a medium which is believed to be responsible for wave processes.

A more specific problem of concrete spectral dimension values has not until now been completely solved. In the first place, there is a discrepancy between experimental data on neutron scattering and values predicted by elastic fractal models which are fairly well confirmed in experiments with larger-scale objects.

An important aspect of findings available in the framework of the theory of fractons concerns prospects of their practical application, primarily the development of materials with unusual wave characteristics. The intuitive approach evolved in traditional wave theory sometimes fails to serve the purpose, and applied studies using it may bring about quite unexpected results.

Studies of fractal structures in wave fields do not always yield such new results as the theory of fractons. Nevertheless, considerable progress has been made in this field. In the first place, multifractal analysis allows for the description of intermittent field structures. Unlike the power spectrum or correl-ation function of the process, the singularity spectrum bears information about the local structure of the process which facilitates differentiation between signals of different origin. Also, multifractal analysis provides concise meaningful characteristics of moments of different order for the two-point distributions of process probabilities. Fractal properties of ray dynamics are equally important for the understanding of wave distribution in natural media. Fractals are believed to allow the most natural approach to the description of such a variable and intriguing phenomenon as wind-generated waves. Moreover, the application of fractal analysis to seismoacoustics may prove useful for the development of new methods for earthquake prognostication.

Acknowledgement. This work was supported by the Russian Fund for Basic Research, Grant 93-02-16204.

References

1. Uhlenbeck G *Usp. Fiz. Nauk* **103** 275 (1971) (translated into Russian)
2. Malinovsii V K, Novikov V N, Sokolov A P *Usp. Fiz. Nauk* **163** (5) 119 (1993)
3. Wilson K G *Usp. Fiz. Nauk* **141** 193 (1983); "The renormalization group and critical phenomena", Nobel Lecture, 8 December 1982
4. Mandelbrot B B *Les Objets Fractals: Forme, Hasard et Dimension* (Paris: Flammarion, 1975)
5. Mandelbrot B B *Fractals: Form, Chance and Dimension* (San- Francisco: Freeman, 1977)
6. Mandelbrot B B *The Fractal Geometry of Nature* (New York: Freeman, 1983)
7. Mandelbrot B B, in Ref. [21] p. 9
8. Zel'dovich Ya B, Sokolov D D *Usp. Fiz. Nauk* **143** 493 (1985) [*Sov. Phys. Usp.* **27** 546 (1984)]
9. Feder E *Fractals* (translated into Russian) (Moscow: Nauka, 1991)]
10. Sokolov I M *Usp. Fiz. Nauk* **150** 221 (1986) [*Sov. Phys. Usp.* **29** 924 (1986)]
11. Smirnov B M *Fizika Fraktal'nykh Klasterov* (Physics of Fractal Clusters) (Moscow: Nauka, 1991)

12. Kaplan J C, Yorke J A, in *Functional Differential Equations and Approximations of Fixed Points* (Ed. H-O Peirgen) Walther Lecture Notes in Mathematics (Berlin: Springer, 1979) Vol. 750
13. Russel D A, Hanson J D, Ott E *Phys. Rev. Lett.* **45** 1175 (1980)
14. Schroeder M *Fractals, Chaos, Power Laws* (New York: Freeman, 1991)
15. Gould H, Tobochnik J *Introduction to Computer Simulation. Applications to Physical Systems* (Reading, MA: Addison-Wesley, 1988)
16. Schuster H G *Deterministic Chaos. An Introduction* (Cambridge, England: VCH Publishers, 1987)
17. Rabinovich M I, Sushchik M M *Usp. Fiz. Nauk* **160** (1) 3 (1990) [*Sov. Phys. Usp.* **33** 1 (1990)]
18. Bershadsky A G *Usp. Fiz. Nauk* **160** (12) 189 (1990) [*Sov. Phys. Usp.* **33** 1073 (1990)]
19. Dinariev O Yu *Izv. Ross. Akad. Nauk, Mekh. Zhidk. Gaza* **5** 101 (1992)
20. Moon F C *Chaotic and Fractal Dynamics* (New York: John Wiley and Sons Inc., 1992)
21. *Fractals in Physics* (Proceedings of Sixth International Symposium, Trieste, 1985) Eds L Pietronero, E Tosatti (Amsterdam: North-Holland, 1986)
22. Olemskoi A I, Flat A Ya *Usp. Fiz. Nauk* **163** (12) 1 (1993) [*Phys. Usp.* **36** 1087 (1993)]
23. Zosimov V V, Lyamshev L M *Akust. Zh.* **40** 709 (1994) [*Acoust. Phys.* **40** 627 (1994)]
24. Alexander S, Laerman C, Orbach R, Rosenberg H M *Phys. Rev. B* **28** 4615 (1983)
25. Alexander S, Orbach R *J. Phys. Lett.* **43** L625 (1982)
26. Alexander S, Entin-Wholman O, Orbach R *Phys. Rev. B* **34** 2726 (1986)
27. Jagannatham A, Orbach R, Eutin-Wohlman O *Phys. Rev. B* **39** 13465 (1989)
28. Jagannatham A, Orbach R *Phys. Rev. B* **41** 3153 (1990)
29. Allen W P et al. *Phys. Rev. B* **49** 257 (1994)
30. Klinger M I *Usp. Fiz. Nauk* **152** 623 (1987) [*Sov. Phys. Usp.* **30** 699 (1987)]
31. Sheka E F *Usp. Fiz. Nauk* **160** (2) 263 (1990) [*Sov. Phys. Usp.* **33** 147 (1990)]
32. Klinger M I *Usp. Fiz. Nauk* **160** (1) 159 (1990) [*Sov. Phys. Usp.* **33** 88 (1990)]
33. Berry M V *J. Phys. A* **12** 781 (1979)
34. Bale H D, Schmidt P W *Phys. Rev. Lett.* **53** 596 (1984)
35. Schaefer D W et al. *Phys. Rev. Lett.* **52** 2371 (1984)
36. Markel V A, Muratov L C, Shtokman M N *Zh. Eksp. Teor. Fiz.* **98** 819 (1990) [*Sov. Phys. JETP* **71** 455 (1990)]
37. Maksimenko V V, Lushnikov A A *Pis'ma Zh. Eksp. Teor. Fiz.* **57** (4) 204 (1993) [*JETP Lett.* **57** 212 (1993)]
38. Szekely G J *Paradoxes in Probability: Theory and Mathematical Statistics* (Dordrecht, Holland: Reidel, 1987)
39. Smirnov B M *Usp. Fiz. Nauk* **163** 51 (1993) [*Phys. Usp.* **36** (7) 592 (1993)]
40. Mukhamedov V A *Izv. Ross. Akad. Nauk, Fiz. Zemli* (3) 39 (1992)
41. Abdullaev S S, Zaslavskii G M *Usp. Fiz. Nauk* **161** (8) 1 (1991) [*Sov. Phys. Usp.* **34** 645 (1991)]
42. Biberman L M *Zh. Eksp. Teor. Fiz.* **17** 416 (1947)
43. Abramov Yu Yu, Dikhne A M, Naportovich A P *Zh. Eksp. Teor. Fiz.* **56** 654 (1969) [*Sov. Phys. JETP* **29** 358 (1969)]
44. Feng S, Golubovie L, Zhang J-C *Phys. Rev. Lett.* **65** 1028 (1990)
45. Stiassnie M, Agnon J, Shemer L *Physica D* **47** (3) 341 (1991)
46. Zaslavskii M M, Sharkov E A *Dokl. Akad. Nauk SSSR* **294** 1362 (1987) [*Sov. Phys. Dokl.* **32** 499 (1987)]
47. Naugol'nyh K A, Zosimov V V *Chaos: An Interdisciplinary Journal of Nonlinear Science* **4** (1) 21 (1994)
48. Paladin G, Vulpiani A *Phys. Rep.* **156** (4) 147 (1987)
49. De Wolf E A, Dremin I M, Kittel W *Usp. Fiz. Nauk* **163** (1) 3 (1993)
50. Akimov V G, Zosimov V V, Sushkov A L *Akust. Zh.* **38** 375 (1992) [*Sov. Phys. Acoust.* **38** 205 (1992)]
51. Petri A, Pietronero L *Phys. Rev. B* **45** 12864 (1992)
52. Mukhamedov V A *Akusticheskaya Emissiya Diskretnoi Geofizicheskoi Sredy.* Avtoreferat Diss. Dok. Fiz.-Mat. Nauk (Acoustic Emission of Discrete Geophysical Medium, Dissert. Dr Phys. Math. Sci.) (Ashkhabad, 1993)
53. *Physica D* **38** (1) 3 (1989)
54. D'Antonio P *Sound Vibr.* **26** (10) 24 (1992)
55. Loong Ch, in Ref. [21] p. 260
56. Forrest S, Witten T *J. Phys. A* **12** L109 (1979)
57. Schaefer D W, Keefer K D *Phys. Rev. Lett.* **53** 1383 (1984)
58. Bale H D, Schmidt P W *Phys. Rev. Lett.* **53** 596 (1984)
59. Witten T A, Sander L M *Phys. Rev. Lett.* **47** 1400 (1981)
60. Smirnov B M *Usp. Fiz. Nauk* **160** (4) 1 (1990) [*Sov. Phys. Usp.* **33** 261 (1990)]
61. Corum K L, Corum J F, "High-voltage RF ball lightning experiments and electro-chemical fractal clusters", Paper presented at Third All-Union Seminar on Ball Lightning, Moscow, 1989
62. Smirnov B M *Usp. Fiz. Nauk* **161** (8) 141 (1991) [*Sov. Phys. Usp.* **34** 711 (1991)]
63. Smirnov B M *Usp. Fiz. Nauk* **161** (6) 171 (1991) [*Sov. Phys. Usp.* **34** 526 (1991)]
64. Ozhovan M I *Zh. Eksp. Teor. Fiz.* **104** 4021 (1993) [*J. Exp. Theor. Phys.* **77** 939 (1993)]
65. Devyatko Yu N, Rogozhkin S V, Fedotov B A *Zh. Eksp. Teor. Fiz.* **104** 2556 (1993) [*J. Exp. Theor. Phys.* **77** 159 (1993)]
66. Takens F *Dynamical Systems and Turbulence* (Berlin: Springer, 1981)
67. Lautenborn W, Cramer E *Phys. Rev. Lett.* **47** 1145 (1981)
68. Lautenborn W, Parlitz U, in *Problemy Nelineinoi Akustiki*. Sb. Tr. Simp. po Nelineinoi Akustike (Problems of Nonlinear Acoustics, Trans. Symp. on Nonlinear Acoustics) (Novosibirsk: Nauka, 1987)
69. Tao Q, Ni W, Miao G, Wei R in Ref. [68], p. 242
70. Osborne A R, Provenzale A *Physica D* **35** 357 (1989)
71. Novikov E A, Stewart R U *Izv. Akad. Nauk SSSR, Ser. Geofiz.* (3) 408 (1964)
72. Pond S, Stewart R U *Izv. Akad. Nauk SSSR, Ser. Fiz. Atmos. Okeana* **1** 914 (1965)
73. Mandelbrot B B *J. Fluid Mech.* **62** 331 (1974)
74. Prasad P R, Sreenivasan K R *J. Fluid Mech.* **216** 1 (1990)
75. Meneveau C, Sreenivasan K R *Phys. Rev. A* **41** 2246 (1990)
76. Osborne A R, Caponio R *Phys. Rev. Lett.* **64** 1733 (1990)
77. Bassingthwaite J B, Beyer R P *Physica D* **53** (1) 71 (1991)
78. Shlesinger M F, West B J, Klafter J *Phys. Rev. Lett.* **58** 1100 (1987)
79. Feller W *An Introduction to Probability Theory and Its Applications,* Vol. 2 (New York: Wiley, 1971)
80. Shlesinger M F, Zaslavsky G M, Klafter J *Monthly Nature* **1** (5) 45 (1993)
81. Shklovskii B I, Efros A L *Usp. Fiz. Nauk* **117** (3) 401 (1975) [*Sov. Phys. Usp.* **18** 845 (1975)]
82. De Gennes P G *Scaling Concepts in Polymer Physics* (Cornell University Press, 1979)
83. Gouyet J F, Sapoval B, Boughaleb Y, Rosso M *Physica A* **157** 620 (1989)
84. Meakin P, Matsushita M, Hagakava Y *Physica A* **151** (3) 457 (1989)
85. Katz M A *A Few Probabilistic Problems of Physics and Mathematics* [translated into Russian (Moscow: Nauka, 1967)]
86. Slator T, Bernasconi A, Posselt D et al. *Phys. Rev. Lett.* **66** 1070 (1991)
87. Domany E, Alexander S, Bensimon D, Kadanoff L P *Phys. Rev. B* **28** 3110 (1983)
88. Rammal R *Phys. Rev. B* **28** 4871 (1983)
89. de Vries P, de Raedt H, Lagendijk A *Phys. Rev. Lett.* **62** 2515 (1989)
90. Laces R *Monthly Nature* **1** (2) 54 (1993)
91. Panyukov S V *Zh. Eksp. Teor. Fiz.* **98** 668 (1990) [*Sov. Phys. JETP* **71** 372 (1990)]
92. Panyukov S V *Pis'ma Zh. Eksp. Teor. Fiz.* **58** 750 (1993) [*JETP Lett.* **58** 726 (1993)]
93. Feng S, Sen P N *Phys. Rev. Lett.* **52** (5) 216 (1984)
94. Webman I, Kantor Y *Phys. Rev. Lett.* **52** 1891 (1984)

95. Deptuck D, Harrison J P, Zawadzky A *Phys. Rev. Lett.* **54** 913 (1985)
96. Benguigui L *Phys. Rev. B* **34** 8176 (1986)
97. Lobb C J, Forrester M G *Phys. Rev. B* **35** 1899 (1987)
98. Halperin I, Feng S, Sen P N *Phys. Rev. Lett.* **54** 2391 (1985)
99. Allen L C, Golding B, Haemmerle W H *Phys. Rev. B* **37** 3710 (1988)
100. Smirnov B M *Usp. Fiz. Nauk* **152** (1) 133 (1987) [*Sov. Phys. Usp.* **30** 420 (1987)]
101. Gross J, Fricke J, Pekala R W, Hrubesh L W *Phys. Rev. B* **45** 12774 (1992)
102. Arbabi S, Sahimi M *Phys. Rev. B* **47** 695 (1993)
103. Luis E, Guinea F, Flores F, in Ref. [21], p. 244
104. Balankin A S *Dokl. Ross. Akad. Nauk* **322** 5 869 (1992)
105. Mosolov A B *Zh. Tekh. Fiz.* **62** (6) 23 (1992) [*Sov. Phys. Tech. Phys.* **37** 594 (1992)]
106. Naugol'nykh K A, Ostrovskii L A *Nelineinye Volnovye Protsessy v Akustike* (Nonlinear Wave Processes in Acoustics) (Moscow: Nauka, 1990)
107. Skvortsov A T, Bogdanov A N *Trans. of 13 ISA* (Bergen, Norway, 1993) (Singapore: World Scientific, 1993) p. 659
108. Webman I, in Ref. [21], p. 488
109. Korzhenevskii A L, Luzhkov A A *Zh. Eksp. Teor. Fiz.* **99** 530 (1991) [*Sov. Phys. JETP* **72** 295 (1992)]
110. Craciun F, Bettucci A, Molinari E et al. *Phys. Rev. Lett.* **68** 1555 (1992)
111. Alexander S *Phys. Rev. B* **40** 7953 (1989)
112. *Fizicheskie Velichiny. Spravochnik* (Physical Values. A Reference Book) (Moscow: Energoatomizdat, 1991)
113. Sokolov A P, Kislink A, Soltwich M, Quitman D *Phys. Rev. Lett.* **62** 1540 (1992)
114. Page J N, McCalloch R D *Phys. Rev. Lett.* **57** (11) 1324 (1986)
115. Alexander S, Courtens E, Vacher R *Physica A* **195** (3&4) 286 (1993)
116. Buchenau U, Nucker N, Dianox A J *Phys. Rev. Lett.* **53** 2316 (1984)
117. Fontana A, Rocca F, Fontana M P *Phys. Rev. Lett.* **58** 503 (1987)
118. Boukenter A, Quinson J F, Serughetti J et al. *Phys. Rev. Lett.* **57** 2391 (1986)
119. Courtens E, Pelous J, Phalippon J, Vacher R, Woignier T *Phys. Rev. Lett.* **58** 128 (1987)
120. Zemlyanov M G, Malinovskii V K, Novikov V N et al. *Zh. Eksp. Teor. Fiz.* **101** (1) 284 (1992) [*Sov. Phys. JETP* **74** 151 (1992)]
121. Dianoux A J, Page J N, Rosenberg H M *Phys. Rev. Lett.* **58** 886 (1987)
122. Freltoft T, Kjems J, Richter D *Phys. Rev. Lett.* **59** 1212 (1987)
123. Tsujimi Y, Courtens E, Pelous J, Vacher R *Phys. Rev. Lett.* **60** 2757 (1988)
124. Vacher R, Courtens E, Goddens G *Phys. Rev. Lett.* **65** 1008 (1990)
125. Schaefer D W, Brinker C J, Richter D et al. *Phys. Rev. Lett.* **64** 2316 (1990)
126. Conrad H et al. *Phys. Rev. B* **41** 2573 (1990)
127. Yakubo K, Nakayama T *Phys. Rev. B* **40** 517 (1989)
128. Li Q, Sokoloulis C M *Phys. Rev. B* **41** 11713 (1990)
129. Montagna M, Pilla O, Vilrani G et al. *Phys. Rev. Lett.* **65** (9) 1136 (1990)
130. Lambert G J, Huges G D *Phys. Rev. Lett.* **66** (8) 1074 (1991)
131. Alippi A, Shkerdin G, Bettucci A et al. *Phys. Rev. Lett.* **69** 3318 (1992)
132. Berdiev A A, Mukhamedov V A, in *Problemy Nelineinoi Akustiki.* Sb. Tr. Simp. po Nelineinoi Akustike (Problems of Nonlinear Acoustics, Trans. Symp. on Nonlinear Acoustics) (Novosibirsk: Nauka, 1987)
133. Kuzmin V N *Izv. Akad. Nauk SSSR, Ser. Fiz. Atmos. Okeana* **28** (9) 953 (1992)
134. Allen A, Cloitre M, in Ref. [21], p. 91
135. Gurbatov S N, Malakhov A N, Saichev A I *Nelineinye Sluchainye Volny v Sredakh bez Dispersii* (Nonlinear Random Waves in Disperseless Media (Moscow: Nauka, 1990)
136. Schaefer D, Kefer K, in Ref. [21], p. 62
137. Maksimenko V V, Krikunov V A, Lushnikov A A *Zh. Eksp. Teor. Fiz.* **102** 1571 (1992) [*Sov. Phys. JETP* **75** 848 (1992)]
138. Lukkin F, in Ref. [21], p. 446
139. Gouyet J F *Physica A* **168** 581 (1990)
140. Chhabra A B, Meneveau C, Jensen R V, Sreenivasan K R *Phys. Rev. A* **40** 5284 (1989)
141. Turigin A Yu, Chechetkin V R *Zh. Eksp. Teor. Fiz.* **98** 146 (1990) [*Sov. Phys. JETP* **71** 80 (1990)]
142. Meneveau C, Sreenivasan K R *Phys. Rev. Lett.* **59** 1424 (1987)
143. Abdullaev S S, Zaslavskii G M *Zh. Eksp. Teor. Fiz.* **80** 524 (1981) [*Sov. Phys. JETP* **53** 265 (1981)]
144. Abdullaev S S, Zaslavskii G M *Akust. Zh.* **34** 578 (1988) [*Sov. Phys. Acoust.* **34** 334 (1988)]
145. Palmer D C et al. *Geophys. Res. Lett.* **15** (6) 569 (1988)
146. Yan J *JASA* **94** 2739 (1993)
147. Abdullaev S S *Chaos: An Interdisciplinary Journal of Nonlinear Science* **4** (1) 63 (1994)
148. Klyatskin V I, Tatarskii V I *Usp. Fiz. Nauk* **110** 499 (1973) [*Sov. Phys. Usp.* **16** 494 (1974)]
149. Rabinovich M I *Usp. Fiz. Nauk* **125** (1) 123 (1978) [*Sov. Phys. Usp.* **21** 443 (1978)]
150. Rabinovich M I, Fabrikant A L, Tsimring L Sh *Usp. Fiz. Nauk* **162** (8) 1 (1992) [*Sov. Phys. Usp.* **35** 629 (1992)]
151. Kachanov Yu S, Kozlov V V, Levchenko V Ya *Izv. Akad. Nauk SSSR, Mekh. Zhidk. Gaza* (3) 49 (1977)
152. Volodin A G, Zel'man M B *Izv. Akad. Nauk SSSR, Mekh. Zhidk. Gaza* (5) 78 (1978)
153. Zelman M B, Maslennikova I I *Zh. Prikl. Mekh. Tekh. Fiz.* **33** (2) 58 (1992) [*J. Appl. Mech. Tech. Pys.* **33** 197 (1992)]
154. Kozlov V V, Rabinovich M I, Ramazanov M P et al. *Pis'ma Zh. Tekh. Fiz.* **13** 986 (1987) [*Sov. Tech. Phys. Lett.* **13** 411 (1987)]
155. Kurin V V, Permitin G V, in *Nelineinye Volny. Struktury i Bifurkatsii* (Nonlinear Waves. Structures and Bifurcations) (Moscow: Nauka, 1987), p. 227
156. Ezersky A B, Korotin N I, Rabinovich M I *Pis'ma Zh. Eksp. Teor. Fiz.* **41** 129 (1985) [*JETP Lett.* **41** 157 (1985)]
157. Ezersky A B, Rabinovich M I, Reutov V P, Starobinets I M *Zh. Eksp. Teor. Fiz.* **91** 2070 (1986) [*Sov. Phys. JETP* **64** 1228 (1986)]
158. Brown M C, Tappert F D, Sundaram S E R B *J. Fluid Mech.* **227** 35 (1991)
159. Stiassnie M *Proc. Int. Sch. Phys. "Enrico Fermi" Varenna 25 Jul–5 Aug. 1988*, course 109 (Amsterdam–Bologna, 1991) p. 633
160. Elgar S, Mayer-Kress G *Physica D* **37** (1) 104 (1989)
161. Gutenberg B, Richter C F *Seismicity of the Earth and Associated Phenomena* (Princeton: Princeton Univ. Press, 1949)
162. Kagan Y Y, Knopoff L *J. Geophys. Res. B* **86** (4) 2853 (1981)
163. Cannelli G, Cantelli R, Corsero A *Phys. Rev. Lett.* **70** 3923 (1993)
164. Chen K, Bak P, Obuchov S P *Phys. Rev. A* **43** 625 (1991)
165. Salimi M, Robertson M C, Sammis C G *Phys. Rev. Lett.* **70** 2186 (1993)